ANA FILIPA DOS REIS MENDES

The synthesis and *in vitro* toxicological evaluation of the mitoxantrone naphthoquinoxaline metabolite: a comparative study with the parent drug

Dissertação do 2º Ciclo de Estudos Conducente ao Grau de Mestre em Toxicologia Analítica, Clínica e Forense, Faculdade de Farmácia, Universidade do Porto

Trabalho realizado sob a orientação de:

Professora Doutora Vera Marisa Costa

Professora Doutora Emília Sousa

Setembro de 2014

Aos meus pais, Isaura e Paulino,
Às minhas irmãs, Susana e Fátima,
E ao Miguel.

ACKNOWLEDGMENTS

Esta dissertação não poderia ter sido escrita sem a ajuda e a supervisão científica da Professora Doutora Vera Costa e Professora Doutora Emília Sousa, que não só me incentivaram como orientadoras como também me desafiaram para aumentar o meu conhecimento nestas duas grandes áreas. Ajudaram-me com o material de pesquisa, guiaram-me no laboratório e na dissertação, nunca aceitando menos do que os meus melhores esforços. Agradeço a ambas.

À professora Doutora Vera Costa, minha orientadora neste trabalho, pelo tempo despendido, pela disponibilidade e paciência revelada, pelo espírito crítico, pela supervisão e orientação desta dissertação. Muito obrigada pelo profissionalismo, pela sincera amizade e pela total disponibilidade que sempre revelou para comigo. O seu apoio foi determinante na elaboração desta dissertação.

À professora Doutora Emília Sousa, minha co-orientadora, pelo acompanhamento de todo o processo de síntese dos compostos e pelo apoio prestado. Agradeço também pela boa disposição em todos os momentos. A sua sabedoria foi essencial para que chegasse ao fim deste trabalho com um enorme sentimento de satisfação.

À Mestre Ana Sara Gomes, pela sua colaboração ao longo de todo o trabalho realizado no laboratório de Química. Obrigada pela amizade, companheirismo e ajuda, factores muito importantes na realização desta dissertação, que permitiu que cada dia fosse encarado com motivação.

À Doutora Sara, pelos conhecimentos transmitidos de cromatografia e pela prontidão com que esclareceu todas as minhas dúvidas.

À Faculdade de Farmácia da Universidade do Porto, ao Laboratório de Química Orgânica e Farmacêutica (departamento de Ciências Químicas), e ao Laboratório de Toxicologia (departamento de Ciências Biológicas) por me terem proporcionado as condições necessárias à realização desta dissertação.

À professora Doutora Maria Lourdes Bastos, coordenadora do mestrado em Toxicologia Analítica Clínica e Forense, e aos restantes professores que lecionaram neste mestrado, e que me incutiram um interesse cada vez maior na área da toxicologia. Agradeço a oportunidade e o privilégio que tive em frequentar este Mestrado que muito contribuiu para o enriquecimento da minha formação académica e científica.

À professora Doutora Madalena Pinto, responsável do Laboratório de Química Orgânica e Farmacêutica por toda a simpatia e disponibilidade.

Aos meus colegas e a todos os colaboradores destes laboratórios, por toda a ajuda prestada.

Aos meus familiares e aos meus amigos, pelo incentivo prestado ao longo desta dissertação.

Um agradecimento especial, ao Miguel por todo apoio e ajuda demonstrada, pela transmissão de confiança e de força, em todos os momentos.

A todos, o meu sincero obrigado.

This work was developed in REQUIMTE, Departamento de Toxicologia (Rede de Química e Tecnologia) and in Centro de Química Medicinal of University of Porto (CEQUIMED-UP) and CIIMAR – Interdisciplinary Centre of Marine and Environmental Research, Departamento de Ciências Químicas (Laboratório de Química Orgânica e Farmacêutica) both laboratories of the Faculty of Pharmacy, University of Porto. The work was funded through national funds from FCT – Fundação para a Ciência e a Tecnologia and also funded by EU/FEDER funds through the COMPETE program under the project FCT [EXPL/DTP-FTO/0290/2012]. The author of this thesis acknowledges all the participating laboratories and funding's.

The results presented in this thesis led to the following works:

Panel communications

- A. Reis-Mendes, E. Sousa, F. Remião, F. Carvalho, M.L. Bastos, and V.M. Costa, "Mitoxantrone causes time- and concentration-dependent toxicity in H9c2 differentiated cells at pharmacological relevant concentrations", 7th Meeting of young researches of U. Porto (**IJUP '14)**, Porto, Portugal, February 2014.

- A. Reis-Mendes, E. Sousa, F. Remião, F. Carvalho, M.L. Bastos, and V.M. Costa, "At pharmacology relevant concentrations, mitoxantrone causes time- and concentration-dependent toxicity in H9c2 differentiated cells with autophagy involvement" 50th Congress of the European Societies of **Toxicology,** Edinburgh (**Eurotox 2014)**, September 2014.

Abstract in international journals:

A. Reis-Mendes, E. Sousa, F. Remião, F. Carvalho, M.L. Bastos, and V.M. Costa, "At pharmacology relevant concentrations, mitoxantrone causes time- and concentration-dependent toxicity in H9c2 differentiated cells with autophagy involvement" Toxicol Lett 229, Supplement: S246.

ABSTRACT

As anticancer treatment becomes more effective, a larger number of patients survive to cancer and the long-term side effects of anticancer therapy become an increasingly important issue. The ideal anticancer drug with maximal activity and neglectful toxicity to non-cancer cells is not yet found. Thus, anticancer treatment side effects still affect healthy organs. Mitoxantrone (MTX) has been used in patients with advanced breast cancer, prostate cancer, acute leukaemia, lymphoma and in multiple sclerosis. Cardiotoxicity leading to heart failure is a serious side effect that can affect up to 18% of MTX-treated patients, although its' cardiotoxicity mechanisms are poorly known. The toxicity of the metabolites of anticancer drugs has been proved to be, at least, partially responsible for their reported cardiotoxicity. Regarding MTX, data regarding the synthesis and toxicological evaluation of its metabolites are scarcely available. Therefore, this work aims to synthetize MTX naphthoquinoxaline metabolite and to assess the toxicity of MTX and of the synthetized metabolite of MTX in an *in vitro* model.

The synthesis of MTX naphthoquinoxaline metabolite was accomplished by the horseradish peroxidase (HRP) catalyzed H_2O_2 oxidation. With the enzymatic oxidation of MTX, several derivatives could be observed by chromatographic analysis, and two purified derivatives were isolated and identified as naphthoquinoxaline (NAPHT), a well-known metabolite of MTX, and naphthoquinoxaline dicarboxylic acid (NAPHTdi). In this study, several spectroscopic methods for the identification of the metabolites obtained in the synthesis were performed, namely infrared, high performance liquid chromatography- with diode array detector, proton nuclear magnetic resonance, and high resolution mass spectrometry. The purity obtained was 97% for NAPHT and 75% for NAPHTdi. Moreover, the toxicological evaluation of MTX and of the synthetized metabolite, NAPHT, was performed in differentiated H9c2 myocytes. The effects toward energetics, mitochondria, nuclei and lysosomes, and cell death mechanisms were primarily focused. H9c2 cells were differentiated using Dulbecco's Modified Eagle Medium supplemented with 10 nM retinoic acid (RA) and 1% foetal bovine serum (FBS) for 7 days (medium changed every two-days). After the differentiation protocol, cells were incubated with MTX (0.01 µM to 5 µM) or NAPHT (1 to 5 µM) for two time-points (24 and 48h), and cytotoxicity tests [lactate dehydrogenase leakage (LDH) assay, the 3-(4, 5-dimethylthiazol-2-yl)-2, 5-diphenyl tetrazolium bromide (MTT) assay and the neutral red (NR) uptake assay] were performed. Phase contrast microscopy and several staining's were also used to evaluate cytotoxicity. Moreover, adenosine triphosphate (ATP) levels were assessed after MTX or NAPHT

exposure. For the higher concentrations of MTX (1, 2, and 5 µM), cytotoxicity was time- and concentration-dependent in all assays, being the NR assay more sensitive for the MTX toxic effects in H9c2 differentiated cells. On the other hand, for NAPHT (1, 2, and 5 µM), cytotoxicity was time- and concentration-dependent in all assays, being the LDH leakage assay the most sensitive test. Phase microscopy allowed observing that MTX and NAPHT caused cell damage, being more evident in the MTX incubation and in the longer time-point. Neither MTX nor NAPHT incubation resulted in evident signs of apoptosis after 24 or 48h incubation. Several pharmacological active molecules were used in an attempt to elucidate the mechanisms involved in MTX- and/or NAPHT-induced cardiotoxicity. N-acetyl cysteine (antioxidant), buthionine sulphoximine (inhibitor of gamma-glutamylcysteine synthetase), cycloheximide (protein synthesis inhibitor), L-carnitine (mitochondrial enhancer) and Ac-LETD-CHO (a broad caspase inhibitor) did not revert any of the MTX-induced cytotoxicity. Cytochrome P450 (CYP450) inhibitors, namely metyrapone and 1-aminobenzotriazole, were also used to evaluate the role of CYP450 towards MTX cytotoxicity. None of the compounds altered the cytotoxicity caused by MTX in H9c2 cells. Nevertheless, 3-methyladenine (an autophagy inhibitor) gave a partial protection against the MTX and NAPHT observed cytotoxicity in the NR cell assay. Assessment of mitochondrial transmembrane potential in differentiated H9c2 cells incubated with 2 and 5 µM of MTX or NAPHT (2 and 5 µM) for 12h showed significant effects: there was an evident decrease in mitochondrial potential observed by fluorescent microscopy in both drugs. To understand if MTX and NAPHT had any effects on cellular energetics, intracellular ATP levels were measured in H9c2 cells exposed to MTX and NAPHT for 24h. In the NAPHT tested concentrations (2 and 5 µM), no significance changes were detected. In the cells incubated with the MTX (2 and 5 µM), a significant increase of ATP levels was observed, suggesting an adaptive response of H9c2 cells towards MTX.

In conclusion, the isolation and structure characterization of NAPHT was accomplished and additionally, the isolation of a possible oxidation product of MTX, NAPHTdi, was isolated and characterized for the first time. Both MTX and NAPHT caused cardiotoxicity in micromolar concentrations in H9c2 cells, being autophagy involved. The cytotoxicity assays used show different sensitivities for both drugs. MTX and NAPHT caused a significant decrease of mitochondrial membrane potential in differentiated H9c2 cells. Moreover, ATP levels were affected in a different manner after MTX and NAPHT incubation, revealing that these two drugs may impair cellular pathways in a dissimilar manner.

Keywords: Mitoxantrone; Naphthoquinoxaline; Cardiotoxicity; H9c2 differentiated cells; Autophagy.

RESUMO

Atualmente, o tratamento anticancerígeno tem-se tornado mais eficaz, registando-se maiores taxas de sobrevivência. Desta forma, os efeitos adversos a longo prazo da terapêutica anticancerígena apresentam cada vez maior impacto. A terapêutica anticancerígena ideal com a máxima atividade e poucos ou nenhuns efeitos adversos ainda não foi encontrada, pelo que a terapêutica anticancerígena ainda hoje afeta os tecidos saudáveis. A mitoxantrona (MTX) tem sido usada em pacientes com cancro da mama avançado, cancro da próstata, leucemia aguda, linfoma e na esclerose múltipla. A MTX apresenta como efeito secundário a cardiotoxicidade, sendo que a insuficiência cardíaca é um dos efeitos mais graves que pode afectar até 18% dos pacientes tratados com MTX. Os mecanismos de cardiotoxicidade causada pela MTX são ainda hoje pouco conhecidos. A metabolização dos fármacos anticancerígenos tem sido demonstrada como parcialmente responsável pela cardiotoxicidade causada por estes fármacos. Relativamente à MTX, os dados são escassos, quer relativamente à síntese, quer à avaliação toxicológica dos seus metabolitos. Este trabalho teve como objetivos sintetizar o metabolito naftoquinoxalina da MTX e avaliar a toxicidade da MTX e deste metabolito *in vitro*. A síntese do metabolito naftoquinoxalina da MTX foi concretizada através da oxidação catalisada pela peroxidase de rábano na presença de H_2O_2. A oxidação enzimática da MTX permitiu obter vários derivados, como confirmado por análise cromatográfica. Desses derivados, dois compostos foram isolados, purificados e identificados como sendo a naftoquinoxalina (NAPHT) e o ácido dicarboxílico da naftoquinoxalina (NAPHTdi). Vários métodos espetroscópicos foram usados para a identificação dos derivados obtidos, nomeadamente infravermelho, cromatografia líquida de alta eficiência com detector de sistema de díodos, ressonância magnética nuclear protónica e espetrometria de massa de alta resolução. A pureza obtida foi de 97% para NAPHT e 75% para o NAPHTdi. Posteriormente, a MTX e a NAPHT foram avaliados toxicologicamente. Esta avaliação foi feita em células H9c2 diferenciadas. Os ensaios realizados focaram principalmente os efeitos nas mitocôndrias, núcleo e lisossomas, assim como nos mecanismos de morte celular. As células H9c2 foram diferenciadas com meio de cultura *Dulbecco Modified Eagle Medium* suplementado com 10 nM de ácido retinóico e 1% de soro fetal bovino, durante 7 dias (meio mudado a cada dois dias). Após o protocolo de diferenciação, as células foram incubadas com a MTX (0,01 μM até 5 μM) e NAPHT (de 1 a 5 μM) durante 24 ou 48 horas. Após a incubação com as moléculas, foram realizados os seguintes testes de citotoxicidade: ensaio da libertação da lactato desidrogenase, da redução do brometo de 3-[4,5-dimetil-tiazol-2-il]-2,5-

difeniltetrazólio a formazano (ensaio de redução do MTT) e o ensaio da incorporação do vermelho neutro. A microscopia de contraste de fase, assim como várias colorações, foram também usadas para avaliar a citotoxicidade. Além disso, os níveis de trifosfato de adenosina foram determinados após exposição a MTX ou NAPHT.

Para as concentrações mais elevadas de MTX (1, 2 e 5 μM), a citotoxicidade, em todos os ensaios, foi dependente da concentração e do tempo. O ensaio da incorporação do vermelho neutro foi o mais sensível para os efeitos tóxicos da MTX em células H9c2 diferenciadas. Por outro lado, a citotoxicidade causada pela NAPHT (1, 2 e 5 μM) foi também dependente da concentração e do tempo, em todos os ensaios realizados, sendo o ensaio da libertação da lactato desidrogenase o mais sensível aos efeitos tóxicos da NAPHT. Nem a incubação com a MTX nem com a NAPHT levaram a sinais evidentes de apoptose após 24 ou 48 horas. Várias moléculas farmacologicamente ativas foram utilizadas, numa tentativa de elucidar os mecanismos envolvidos na cardiotoxicidade induzida pela MTX e/ou da NAPHT. A *N*-acetilcisteína (antioxidante), a sulfoximina de butionina (inibidor de gama-glutamilcisteína sintetase), a ciclo-heximida (inibidor de síntese proteica), a L-carnitina (protector mitocondrial) e o Ac-LETD-CHO (um inibidor das caspases) foram usados e nenhum conseguiu reverter a citotoxicidade causada pela MTX. Os inibidores do citocromo P450, nomeadamente, a metirapona e o 1-aminobenzotriazol, foram também utilizados para avaliar o papel do metabolismo via citocromo P450 na citotoxicidade da MTX. Nenhum dos compostos mencionados foi capaz de alterar a citotoxicidade induzida pela MTX. No entanto, o inibidor de autofagia, 3-metiladenina, levou a uma protecção parcial contra a citotoxicidade causada pela MTX e pela NAPHT, no ensaio do vermelho neutro. A avaliação do potencial transmembranar mitocondrial nas células H9c2 diferenciadas incubadas com 2 e 5 μM de MTX e NAPHT durante 12 horas demonstrou que ambos os compostos causaram um decréscimo evidente no potencial mitocondrial. Além disso, os níveis intracelulares de trifosfato de adenosina foram avaliados nas células H9c2 expostas a MTX e NAPHT durante 24 horas. Nas concentrações de NAPHT (2 e 5 μM) testadas não foram detetadas alterações significativas. Nas células incubadas com MTX (2 e 5 μM) houve um aumento significativo dos níveis intracelulares de trifosfato de adenosina, o que sugere uma resposta adaptativa das células após exposição à MTX.

Em conclusão, o isolamento e caraterização da NAPHT, assim como o isolamento pela primeira vez do NAPHTdi foram concretizados nesta tese. Além disso, verificou-se que tanto a MTX como a NAPHT causam cardiotoxicidade em concentrações micromolares estando a autofagia envolvida. Os ensaios de citotoxicidade usados apresentaram diferentes sensibilidades para ambos os compostos. A MTX e a NAPHT causaram uma redução significativa do potencial de membrana mitocondrial nas células H9c2

diferenciadas. Os níveis de trifosfato de adenosina foram afectados de forma diferente nas células H9c2 incubadas com MTX e NAPHT, revelando que o fármaco e o seu metabolito podem alterar as vias celulares de forma distinta.

Palavras-chave: Mitoxantrona; Naftoquinoxalina; Cardiotoxicidade; Células H9c2 diferenciadas; Autofagia.

INDEX

INDEX OF FIGURES

INDEX OF TABLES

ABBREVIATIONS

ATP	Adenosine triphosphate
brs	Broad singlet
CYP450	Cytochrome P450
DAD	Diode array detector
DiO^6	3, 3'- Dihexyloxacarbocyanine iodide
DOX	Doxorubicin
DMEM	Dulbecco's modified eagle medium
DMSO	Dimethyl sulfoxide
DNA	Deoxyribonucleic acid
DNR	Daunorubicin
ECG	Electrocardiogram
EDTA	Ethylenediamine tetraacetic acid
FBS	Foetal bovine serum
h	Hours
HER2	Human epidermal growth factor receptor 2
HPLC	High performance liquid chromatography
HRMS	High resolution mass spectrometry
HRP	Horseradish peroxidase
IC_{50}	Concentrations that cause 50% inhibitory effect
IR	Infrared spectroscopy
J	Coupling constant
k	Retention factor
LVEF	Left ventricular ejection fraction
LDH	Lactate dehydrogenase
m	Multiplet

MeOH	Methanol
min	Minutes
mp	Melting point
MTT	3-(4, 5-Dimethylthiazol-2-yl)-2, 5- diphenyl tetrazolium bromide
MTX	Mitoxantrone
NADH	Nicotinamide adenine dinucleotide reduced form
NADPH	Nicotinamide adenine dinucleotide phosphate
NAPHT	Naphthoquinoxaline
NAPHTdi	Naphthoquinoxaline dicarboxylic acid
NOS	Nitric oxide synthase
NR	Neutral red
NMR	Nuclear magnetic resonance
PBS	Phosphate-buffered saline
RA	Retinoic acid
RP	Reverse phase
RNA	Ribonucleic acid
s	Singlet
SD	Standard deviation
SDS	Sodium dodecyl sulfate
SOD	Superoxide dismutase
t	Triplet
TLC	Thin layer chromatography
UV	Ultraviolet

OUTLINE OF THE THESIS

The present thesis consists of six sections. This thesis involves two main areas of research: the synthesis of a metabolite of mitoxantrone (MTX), the naphthoquinoxaline (NAPHT), and the evaluation of the toxicity of MTX and its metabolite.

1. INTRODUCTION

In this section, a review on the existing literature on the cardiotoxic effects of anticancer drugs and the possible influence of metabolism on that cardiotoxicity is presented.

2. AIMS

Herein the main objectives of the present thesis are described.

3. MATERIALS AND METHODS

In this chapter, the experimental procedures are described. The synthesis and the methods used for the structural characterization of the synthesized compounds are detailed. Also, the protocols used to evaluate the toxicological profile of MTX and NAPHT are described.

4. RESULTS

Results were subdivided in two subsections. In the first part, the synthesis and structural determination of the two synthesized derivatives of MTX are presented. In the second part, the results of the *in vitro* toxicological evaluation of MTX and NAPHT are described.

5. DISCUSSION AND CONCLUSIONS

This chapter includes the discussion and the general conclusions of the developed work.

6. REFERENCES

In this final part, the scientific literature used in the remaining sections is listed.

1.
INTRODUCTION

1. Introduction

1.1. The problem of cardiotoxicity caused by anticancer drugs

Presently, cancer is one of the most concerning health issues worldwide. Over 3.45 million new cases of cancer (excluding non-melanoma skin cancers) and 1.75 million deaths were registered in Europe in 2012, with breast and prostate cancers counting for more than 800.000 new cases (Ferlay et al., 2013). Cancer is currently the second leading cause of death in Portugal, after cardiovascular diseases. The colorectal cancer is the leading cause of cancer-related mortality in Portugal (Adão et al., 2013).

Briefly, cancer is a disequilibrium between cell division and cell death, accompanied with dysregulation of cell differentiation, which results in a limitless replicative potential and uncontrolled multiplication (Almeida et al., 2005, Ruddon, 2007). Most drugs used in cancer chemotherapy affect neoplastic transformation, cell proliferation, invasion and metastasis, and/or tumour-related angiogenesis. Ideally, targeted therapy spares normal cells and, therefore, would be better tolerated. The higher selectivity should translate into a wider therapeutic window that better enables the use of sufficient drug dosages to accomplish the therapeutic goals of tumour eradication or control, while minimizing the risk of resistance or toxicity (Bruce and Lin, 1969, Faivre et al., 2006). From the pharmacological point of view, agents used in anticancer therapy can be divided in chemotherapeutic agents (with several subgroups), biological or immunological agents. Radiation can also be used against cancer (Ewer and Suter, 2010). Chemotherapy is still the most frequent currently used therapy and it has largely contributed to the significant decrease of morbidity and mortality in several types of cancer. Even so, chemotherapy has general disadvantages, namely the potential development of cancer resistance and adverse effects due to the lack of selectivity of the drugs used (Espinosa and Raposo, 2010). Presently, the increase on the number of cancer survivors has led to the increase in toxic effects in non-target organs, especially long-term toxic effects. Several antineoplastic agents, namely cytotoxic antimetabolites, topoisomerase II inhibitors, alkylating and agents that interfere with tubulin, tyrosine kinase inhibitors, hormonal agents, and biological agents, among others, are widely reported to cause cardiac toxicity (Sá et al., 2009, Costa et al., 2013). The heart is an organ with limited potential for regeneration and, therefore, its damage may have long-term importance (Ewer and Suter, 2010).

The cardiotoxicity resulting from antineoplastic therapy is a growing concern for oncologists and cardiologists. The cardiotoxicity resulting from the administration of anticancer drugs is multifactorial and complex, as it is influenced by factors as dose, possible drug interactions, potential synergism by co-administration or sequential

administration of chemotherapeutic cardiotoxic drugs or the application of other therapeutics with potential cardiac toxicity (for example: radiotherapy in the mediastinum or immunotherapy) (Table 1) (Ewer and Suter, 2010, Senkus and Jassem, 2011, Octavia et al., 2012). Moreover, the biological variability of the patient and its health in the moment of treatment and thereafter has also a significant impact on the cardiovascular effects of the chemotherapeutic agent/combination of agents to be used. Therefore, when an attempt is made to diagnose or predict future cardiovascular effects after chemotherapy or radiation therapy, a large number of variables must be taken into account (Colombo and Cardinale, 2013).

Several cardiotoxic manifestations can arise from xenobiotic exposure, namely damage in electrophysiology mechanisms, in the cardiac muscle and/or changes in the lumen diameter of coronary arteries. From the clinical perspective, the cardiotoxicity caused by anticancer agents is associated with temporary functional impairment, permanent loss of contractile elements, abnormalities of rhythm formation and/or conduction, as well as vascular effects that include vasospasms, alterations of blood pressure and thromboembolic *sequelea* (Senkus and Jassem, 2011). One of the most common cardiotoxic manifestations associated with the antineoplastic agents is the development of left ventricular dysfunction, namely decreased left ventricular ejection fraction (LVEF), which can progress to congestive heart failure. Heart failure is a severely debilitating disease that results, in a few years, on the death of the majority of the patients diagnosed (Colombo and Cardinale, 2013).

The cardiac adverse effects of anticancer drugs may or may not be permanent. According to damage caused chemotherapy agents are divided in two groups: type I and type II (Table 1).

The type I agents show cardiotoxicity associated with the total cumulative dose of the drug administered and a high propensity for cardiac cell death occurs after exposure (Ewer and Suter, 2010). Type I chemotherapy-related cardiac dysfunction, typically anthracycline-induced, is irreversible and typically associated with significant ultrastructural changes at biopsy (Todaro et al., 2013). Type II agents can cause a reversible cardiac dysfunction (Ewer and Suter, 2010). In fact, type II chemotherapy-related cardiac dysfunction (often termed trastuzumab-induced) is associated with reversible myocardial dysfunction rather than structural damage, it is highly reversible (up to 79%) and generally is not dose-related. However, a synergistic cardiotoxic effect between anthracyclines and trastuzumab has been demonstrated, especially when the two compounds are administered over a short period of time. Type II agents are not described as causing cell death; however, when used in combination with anthracyclines or other type I agents or in high-risk cardiac patients, some degree of cell death can actually occur (Todaro et al., 2013).

Table 1. Comparison of cardiotoxicity caused by agents of type I and type II. Table adapted from Ewer and Suter, 2010, Senkus and Jassem, 2011, and Adão *et al.,* 2013.

Type I (myocardial damage) example: Doxorubicin	**Type II (myocardial dysfunction)** example: Trastuzumab
Predominantly cell death	Cellular dysfunction
Biopsy changes: vacuoles, sarcomere/ myofibrillar disruption, apoptosis and necrosis	No typical anthracycline-like biopsy changes: benign ultrastructure appearance
Cumulative dose-related	Not cumulative dose-related
Permanent (myocyte death, bad prognosis) and irreversible cell damage; may stabilize, but subclinical damage persists	Predominantly reversible (myocyte dysfunction, good prognosis), high probability of recovery after therapy interruption
Risk factors: • Chemotherapy of combination prior or concomitant • Age • Previous cardiac disease • Hypertension	**Risk factors:** • Chemotherapy prior or concomitant with anthracyclines or taxanes • Age • Previous cardiac disease • Obesity
Mechanisms of cardiotoxicity: • Reactive oxygen species formation, oxidative stress/damage, energy collapse, and calcium and iron dysregulation	**Mechanisms of cardiotoxicity:** • Block the human epidermal growth factor receptor 2 (HER2) signalling pathway, elimination of HER2/HER4-related survival factors (gene expression, growth, glucose uptake, sarcomere turnover)
Cardiovascular effects: • May result in heart failure and death	**Cardiovascular effects:** • Low probability of cardiovascular mortality

The best well-characterized cardiotoxic agents are the anthracyclines, namely doxorubicin (DOX), but other oncology drugs can also cause serious cardiovascular complications (Colombo and Cardinale, 2013). The anticancer drugs that adversely affect the cardiovascular system are systematized in Table 2.

Table 2. Agents used in anticancer therapy associated with cardiovascular toxicity. Table adapted from Ewer and Suter, 2010.

(I)	**<u>Agents associated with impaired left ventricular contractility</u>**	
(a)	Agents associated with type I related cardiac dysfunctions	
(i)	Anthracyclines:	Doxorubicin, daunorubicin, epirubicin, idarubicin
(ii)	Anthraquinones:	Mitoxantrone
(b)	Agents associated with type II related cardiac dysfunction (agents associated with potentially reversible dysfunction of the myocyte contractile elements)	
(i)	Trastuzumab, lapatinib, sunitinib and others monoclonal antibodies/ tyrosine kinase inhibitors	
(c)	Other cardiodepressant agents	
(i)	Cyclophosphamide (especially high dose)	
(ii)	α-Interferon	
(II)	**<u>Agents associated with ischemia</u>**	
(a)	5-Fluorouracil	
(b)	Capecitabine	
(c)	Vinblastine	
(d)	Vincristine	
(e)	Bleomycin	
(f)	Cisplatin	
(g)	Biological response modifiers	
(III)	**<u>Agents associated with hypertension or hypotension</u>**	
(a)	Bevacizumab	
(b)	Sunitinib	
(c)	Sorafenib	
(d)	Homoharringtonine	
(e)	Interleukin-2	
(IV)	**<u>Miscellaneous cardiotoxic agents</u>**	
(a)	Paclitaxel (bradycardia)	
(b)	Arsenic trioxide (QT prolongation and *torsades de points*)	
(c)	Radiation (pericardial damage, but may damage all cardiac structures)	

Several drugs have shown to cause toxicity towards the heart. Anthracyclines and mitoxantrone (MTX) have been widely described as cardiotoxic (Seiter, 2005, Menna et al., 2008, Adão et al., 2013, Todaro et al., 2013). In the introduction of this thesis, anthracyclines [DOX and daunorubicin (DNR)], cyclophosphamide and MTX will be addressed for their cardiotoxicity in independent sections: anthracyclines for their frequent clinical use and the

wide literature available; cyclophosphamide whose cardiotoxicity and antineoplastic effects strongly relates to its metabolism; and MTX as it is the drug of study in the present dissertation.

1.2. Anticancer drugs that lead to cardiotoxicity

1.2.1. Anthracyclines

Anthracyclines and related compounds are intercalating agents that are effective in treating many malignant diseases. DOX and DNR belong to the anthracyclines group. This family of compounds share a similar chemical structure (Figure 1) (Monsuez et al., 2010, Menna et al., 2012). According to the World Health Organization, to the group of anthracyclines belong 17 essential drugs that are used to treat cancers (Sikora et al., 1999). The skeleton of anthracyclines is composed by a tetracyclic system with quinone and hydroquinone moieties (often named anthraquinone skeleton), an amino sugar (daunosamine) attached by a glycosidic bond to C-7, and a side chain with a carbonyl group at C-13 (Figure 1) (Menna et al., 2012).

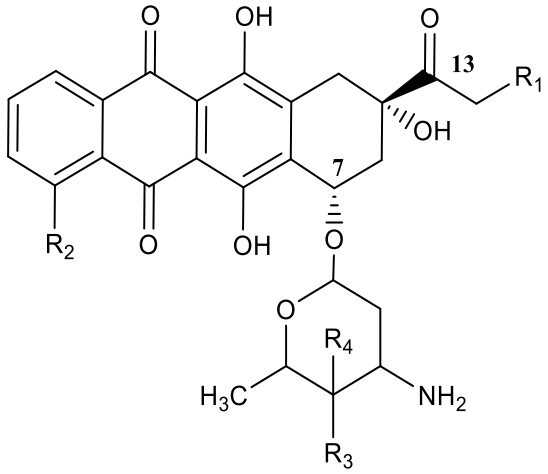

Compounds	R_1	R_2	R_3	R_4
DOX	OH	OCH_3	OH	H
DNR	H	OCH_3	OH	H

Figure 1. Chemical structure of DOX and DNR.

The anthracyclines were first isolated in the early 1950s from *Streptomyces peucetius* (Minotti et al., 2004a). During the decade of 1960, DNR was found to be very effective in treating leukaemia's and lymphomas (Tan et al., 1967). Also in the sixties, a resembled molecule of DNR, the 14-hydroxydaunomycin or adriamycin (later named as DOX) was isolated and shown to be a more effective anticancer agent than DNR in solid tumours (Arcamone et al., 1969, Di Marco et al., 1969). Anthracyclines are shown to have a high therapeutic efficacy towards several types of cancers, although cardiotoxicity is one of their most significant adverse effects (Bonadonna et al., 1970). Over the years, the search for new compounds produced by the same bacteria led to the discovery of five new anthracyclines, however all still cardiotoxic (Takemura and Fujiwara, 2007).

Anthracyclines are often used in combination with other antineoplastic agents, in the treatment of Hodgkin's disease, non-Hodgkin's lymphomas, acute leukaemia's, bone and soft-tissue sarcoma, neuroblastoma, Wilm's tumour, and malignant neoplasms of the bladder, breast, lung, ovary, and stomach (Gewirtz, 1999, Minotti et al., 2004a).

1.2.1.1. Pharmacological mechanisms and general adverse effects of anthracyclines

Several mechanisms for the anticancer proprieties of anthracyclines have been suggested: they are deoxyribonucleic acid (DNA) intercalating agents and disruptors of topoisomerase II, they cause oxidative stress, show alkylating properties and/or cause direct effects on the cell membrane. Anthracyclines have also been reported as inhibitors of the helicase, DNA polymerase, besides topoisomerase II. They induce apoptosis as a result of topoisomerase II inhibition (Uchegbu et al., 1995, Gewirtz, 1999, Minotti et al., 2004a, Takemura and Fujiwara, 2007, Ewer and Suter, 2010). Topoisomerase II is generally recognized to be the cellular main target of DOX. Anthracyclines act by stabilizing a reaction intermediate in which DNA strands are cut and covalently linked to this enzyme, therefore disrupting the DNA from returning to its natural structure (Simunek et al., 2009).

Anthracyclines administration is accompanied by adverse drug reactions arising from their limited selectivity towards cancer cells (Aronson, 2006). Particularly common are bone marrow depression, which is dose-limiting, and gastrointestinal problems. Alopecia occurs in the majority of patients. Occasional hypersensitivity reactions may also occur. However, a cumulative-dose dependent cardiac toxicity has been the major limitation of DOX usage (Aronson, 2006).

1.2.1.2. Cardiotoxicity of anthracyclines

Anthracyclines cardiotoxicity was not detected during the preclinical animal testing; however, it was described during the initial clinical trials with DNR and DOX (Bonadonna et al., 1970). Since then, the cardiotoxicity associated with anthracyclines has been intensively studied. Anthracyclines can cause acute, subacute and late cardiac damage. Acute morbidity occurs during or shortly after drug infusion and includes arrhythmias (supraventricular tachycardia, ventricular ectopy) accompanied in some patients by heart failure, pericarditis-myocarditis syndrome, as well as non-specific ST–T changes and QT prolongation (Senkus and Jassem, 2011). This acute toxicity is usually reversible and not dose-dependent. Acute cardiotoxicity occurs in 1% of patients and no development of chronic heart failure occurs later in life (Todaro et al., 2013). The subacute cardiac toxicity occurs within a few weeks, clinically resembles myocarditis (with oedema and thickening of the left ventricle walls), and is accompanied by diastolic dysfunction with a 60% mortality rate. These acute and subacute forms of cardiac morbidity are, however, rare (1-4%) (Senkus and Jassem, 2011). Anthracyclines can cause short-term adverse effects that may occur up to one year after the start of therapy, while the adverse long-term effects can be diagnosed years or decades after the end of anticancer therapy. In fact, clinically the most relevant side effect of anthracyclines is chronic cardiac toxicity leading to left ventricular dysfunction and most importantly congestive heart failure (Senkus and Jassem, 2011). Late-onset chronic left ventricular dysfunction occurs in 1.6–5% of patients at least 1 year to 10 to 30 years after completion of therapy. A study documented chronic left ventricular dysfunction later in life in 23% of children treated with anthracyclines (Todaro et al., 2013). A strong correlation between chronic left ventricular dysfunction and the cumulative dose of anthracyclines is widely demonstrated (Todaro et al., 2013). The prognosis in anthracycline-related heart failure is poor, with 50% 2-year mortality in untreated established left ventricular dysfunction (Senkus and Jassem, 2011, Colombo and Cardinale, 2013). However, early diagnosis and appropriate management can significantly improve the outcome and the quality of life of the patients (Colombo and Cardinale, 2013).

The risk factors for cardiac toxicity of anthracyclines are: the cumulative dose of the anthracycline administered, age, prior radiation therapy, concomitant (or previous) administration of other cardiotoxic anticancer agents and heart disease or pre-existing factors of cardiac risk (de Graaf et al., 1997, Pai and Nahata, 2000, Octavia et al., 2012, Adão et al., 2013) (Table 3). Clinical cases and pharmacovigilance data already obtained suggest that the most important risk factor for the development of delayed cardiotoxicity by anthracyclines is the maximum cumulative dose taken during all lifespan. After the absolute maximum cumulative dose threshold, the cardiotoxicity increases exponentially. This absolute cumulative dose varies according to the different anthracyclines (de Graaf et al.,

1997, Pai and Nahata, 2000, Menna et al., 2008, Volkova et al., 2011, Geisberg et al., 2012, Adão et al., 2013) (Table 3).

Table 3. Risk factors associated with the cardiotoxicity of anthracyclines. Table adapted from Ehninger *et al*., 1990, Mortensen *et al*., 1992, Singal and Iliskovic, 1998, Menna *et al*., 2008, Octavia et al., 2012, and Adão *et al*., 2013.

Risk factors associated with cardiotoxicity of anthracyclines	
Risk factor	**Increased risk**
Age	Paediatric patients or elderly to whom is administered the same cumulative dose
Gender	Female
Method of administration	Rapid intravenous injection
Cumulative dose	Most important predictor of cardiac dysfunction. Exceeding the cumulative dose of: Daunorubicin 550-800 mg/m^2 Doxorubicin 400-550 mg/m^2 Epirubicin 900-1000 mg/m^2 Idarubicin 150 - 225 mg/m^2 Mitoxantrone >100 - 140 mg/m^2
Chemotherapeutic combination	Therapy with cyclophosphamide, 5-fluorouracil, taxanes or trastuzumab
Mediastinal irradiation	Previous or concurrent
Previous cardiovascular disease	Hypertension, coronary heart disease
Electrolyte disturbances	Hypocalcemia, hypomagnesemia

The extremes of age, female gender, concomitant use of cyclophosphamide, 5-fluorouracil, taxanes or trastuzumab, previous mediastinal irradiation, cardiovascular comorbidities and their predisposing factors (hypertension, coronary disease, and smoking), *diabetes mellitus*, liver disease and hyperthermia also increase the incidence of anthracyclines' cardiotoxicity. The inter-individual variability regarding the susceptibility to cardiotoxicity observed after anthracyclines treatment is also attributed to genetic heritage

(de Graaf et al., 1997, Pai and Nahata, 2000, Octavia et al., 2012, Adão et al., 2013). Genetic factors possibly associated with sensitivity to anthracycline-induced cardiac damage include polymorphisms of multidrug resistance proteins 1 and 2, carbonyl reductase, 3 subunits of nicotinamide adenine dinucleotide phosphate (NADPH) oxidase and phase II detoxification enzymes such as glutathione-S-transferase of the P family (Senkus and Jassem, 2011).

Since this thesis main focus is cardiotoxicity and metabolism, the cardiotoxicity and pharmacokinetic aspects of anthracyclines will be briefly referred in the next sections. DOX will be detailed as the reference drug. Most of the general mechanisms of anthracyclines' toxicity are similar to those of DOX in this group and will not be the primary objective of this thesis. For systematization purposes, DNR will only be addressed regarding metabolism and its effect on cardiotoxicity.

1.2.1.3. General data on the pharmacokinetics of anthracyclines

In general, DNR and DOX are administered intravenously and they suffer hepatic metabolism and biliary excretion. The clearance plasma curve of DOX and DNR is multiphasic, with a 30 hours (h) half-life. The anthracyclines quickly reach the heart, the kidneys, the lungs, the liver and the spleen (Twelves et al., 1998). The distribution of a drug within the body is governed by factors such as blood flow to different organs, diffusion, protein and tissue binding, and lipid solubility. In general, drugs with extensive binding to tissues (e.g., DOX) or with high lipid solubility tend to exhibit prolonged elimination phases because there is a slow release from the tissues (Patel et al., 2013).

The metabolism of anthracyclines consists in several biochemical processes that vary according to the molecule. In general, the metabolic processes such as reduction of the C-13 carbonyl group (process more relevant in humans, accomplished by reductases of the aldo/ketoses or carbonyl reductases that gives rise to alcohols), the reductive cleavage of glycosidic C-7 and the hydrolytic cleavage of glycosidic ring are the most relevant (Menna et al., 2012). In Figure 2, the general metabolism of anthracyclines is presented.

Anthracyclines can be reduced at C-13. In the reduction of the C-13 carbonyl, the NADPH-dependent aldo/ketoses reductases enzymes add two electrons to the C-13 side chain of the anthracycline. The metabolites formed are designated doxorubicinol in the case of DOX and daunorubicinol in the case of DNR (Bachur and Gee, 1971, Minotti et al., 1995). Doxorubicinol is more hydrophilic than DOX and accumulates within the cardiomyocytes (Costa et al., 2013). Another metabolic process very relevant to the anthracyclines cardiotoxicity occurs after the reduction processes of the quinone ring (Serrano et al., 1999). Other metabolic routes include glycosidic breakage bond therefore producing aglycones,

which may be demethylated and conjugated via sulfate or glucuronide routes (Di Marco et al., 1967, Alberts et al., 1971, Takanashi and Bachur, 1976, Uchegbu et al., 1995, Minotti et al., 2004a).

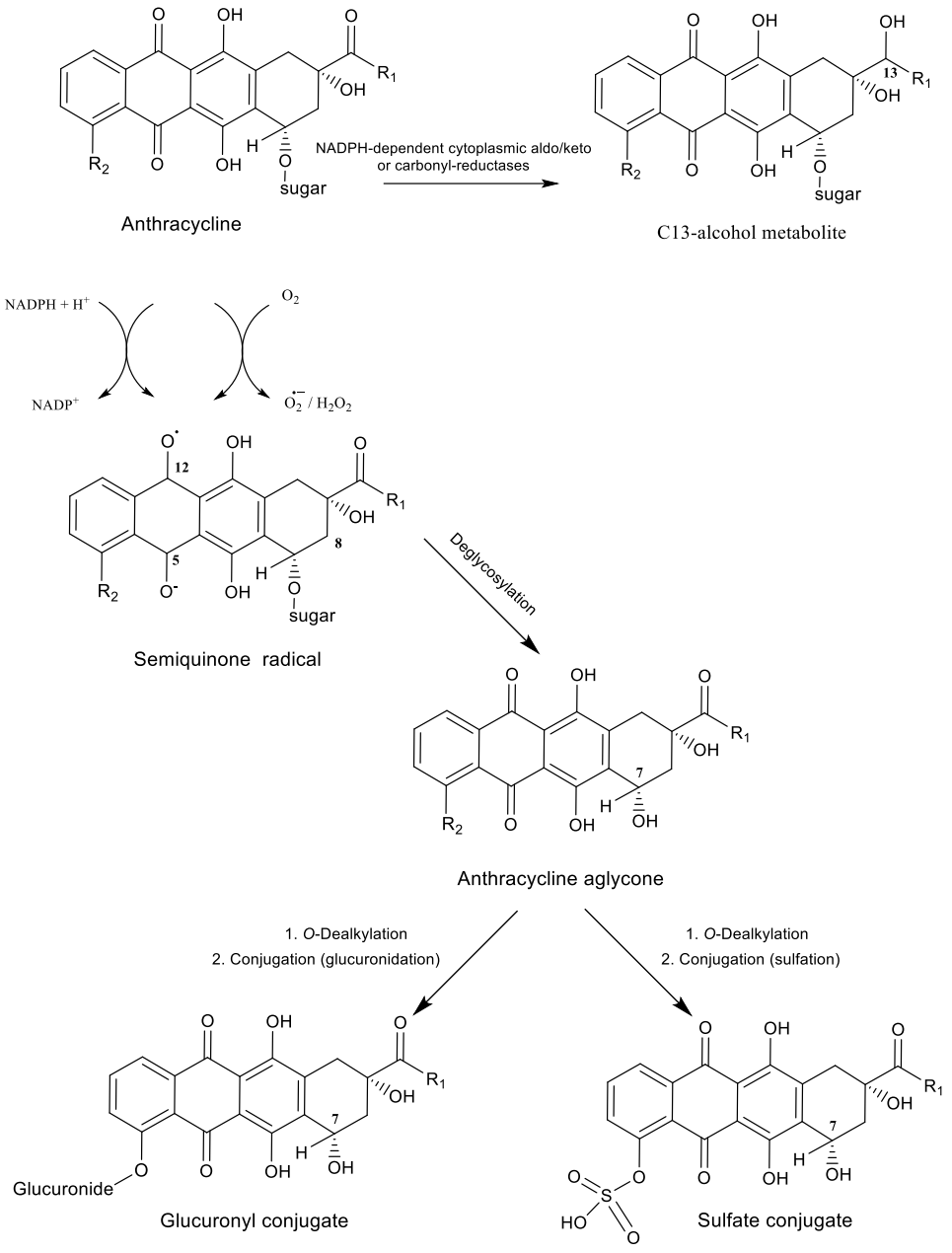

Figure 2. The general metabolism of anthracyclines.

1.2.2. Doxorubicin

DOX is the most widely used anticancer drug and the drug with the largest spectrum of anticancer action (Seiter, 2005). DOX is a cytotoxic antibiotic whose planar core intercalates with the DNA double helix and forms a ternary complex with topoisomerase II

and DNA. DOX also inhibits topoisomerase II directly, interacts with cellular and mitochondrial membranes, disturbs the transmission of intracellular signals and leads to the formation of reactive oxygen species (Gewirtz, 1999, Patel et al., 2013). Injectable DOX use is indicated for the treatment of various types of cancers and the doses used vary depending on the type of tumour. The most commonly used schedule is 60 to 75 mg/m^2 every three weeks (Seiter, 2005).

1.2.2.1. Cardiotoxicity of doxorubicin: human studies

The most common side effects of DOX are bone marrow suppression, cardiomyopathy, electrocardiogram (ECG) changes, nausea, vomiting, diarrhoea, and alopecia (Eksborg et al., 1985, Octavia et al., 2012). In fact, despite the clinical usefulness of this drug, its use is limited due to its acute and chronic cardiotoxic effects (Volkova et al., 2011). The primary factor limiting the use of DOX is the prolonged and cumulative exposure that typically results in the development of cardiomyopathies and, in more severe cases, congestive heart failure (Xu et al., 2005, Senkus and Jassem, 2011). In order to decrease the probability of cardiomyopathy development, it is recommended that the total cumulative dose of DOX should not exceed 450 mg/m^2 to 550 mg/m^2 of body surface area (Eksborg et al., 1985, Minotti et al., 1995, Singal and Iliskovic, 1998, Menna et al., 2008). Other risk factors for cardiotoxicity may lead to the recommendation to decrease its total cumulative dose (Table 3).

One of the first studies performed on DOX cardiotoxicity was a retrospective analysis of over 4000 patients who received DOX done by Von Hoff *et al*. (Von Hoff et al., 1979). More than two per cent (2.2%) of patients developed clinical signs and symptoms of congestive heart failure (Von Hoff et al., 1979). This study was performed to demonstrate that a major determinant for the development of heart failure is the cumulative dose of DOX and that there was a marked increase in the prevalence of heart failure after a total cumulative dose of 550 mg/m^2 (Von Hoff et al., 1979). However, the total dose of only 240 or 250 mg/m^2 of DOX can already cause pathological changes in the myocardium, as shown in subendocardial biopsies of DOX-treated patients (Billingham et al., 1978, Von Hoff et al., 1979). Others studies focusing on LVEF determined that decreased LVEF is dependent on the cumulative dose, particularly in cumulative doses of DOX higher than 350 mg/m^2 (Alexander et al., 1979, Buzdar et al., 1985).

In a more recent retrospective analysis of treatment with DOX for breast cancer or small cell lung cancer, LVEF was also measured (Swain et al., 2003). Swain *et al.* showed that 5.1% of patients had evidence of congestive heart failure or significant decrease in left ventricular function (Swain et al., 2003). This study also demonstrated an increased cardiotoxicity risk at a cumulative dose of DOX below 300 mg/m^2 (Swain et al., 2003). Other

studies demonstrated nonspecific changes in electron microscopy, including decrease in myocardial myofibrils, mitochondrial defects, and cell degeneration caused by DOX (Chabner et al., 2012). Sequential echocardiograms detected structural abnormalities in 25% of children who received up to 300 mg/m^2 of DOX, although less than 10% showed clinical manifestations of cardiomyopathy on long-term monitoring (Chabner et al., 2012).

Clinical incidence of apparent cardiomyopathy after DOX administration ranges from 1 to 10% in total doses lower than 450 mg/m^2. The risk rises sharply with dose and it is estimated heart failure in up to 20% in a cumulative dose of 550 mg/m^2 (Table 3) (Chabner et al., 2012). As stated, the cardiotoxicity risk increases in the presence of other risk factors (Table 3) (Volkova et al., 2011, Geisberg et al., 2012, Octavia et al., 2012).

1.2.2.2. Mechanisms involved in the cardiac toxicity of doxorubicin

Cardiovascular diseases, and specifically heart failure, can occur as a consequence of cancer therapy. Despite decades of basic and clinical research, anthracyclines and radiation therapy continue to cause clinically significant heart failure (Geisberg et al., 2012).

Several mechanisms are suggested to explain the cardiac toxicity caused by anthracyclines. The hypotheses more accepted are: oxidative stress caused by the redox cycle of the parent drug, the presence of cardiotoxic metabolites and changes in homeostasis of calcium and iron. The immunological aspects are also considered co-responsible for the cardiac anthracyclines' toxicity (Uchegbu et al., 1995, Volkova et al., 2011, Octavia et al., 2012). Defects in mitochondrial integrity and subsequent deterioration of the energy cycle of the myocardium, changes in calcium currents in sarcoplasmic reticulum and mitochondria, changes in gene expression of myocytes, activation of the ubiquitin-proteasome system and induction of apoptosis, as well as innate immunity activation are also culprits of DOX-induced cardiotoxicity. However, so far there is no single mechanism that totally explains the cardiomyopathy caused by DOX (Shi et al., 2011b, Volkova et al., 2011, Octavia et al., 2012).

1.2.2.1.1. Hypothesis of oxidative stress

The DOX toxicity in cardiomyocytes is associated with the formation of reactive species, mainly as a result of the redox metabolism of the parent quinone (Figure 3). The level of DOX-induced oxidative stress is up to 10 times greater in the heart than in the other tissues (liver, kidney, spleen) (Lenzhofer et al., 1983, Doroshow and Davies, 1986, Siveski-Iliskovic et al., 1995, Mukherjee et al., 2003), and therefore oxidative injury of the heart is a widely accepted theory for the DOX-induced cardiotoxicity. Anthracycline-induced cell death can be inhibited by antioxidants, both *in vitro* and *in vivo* (Geisberg et al., 2012) although controversial data exist (Costa et al., 2013).

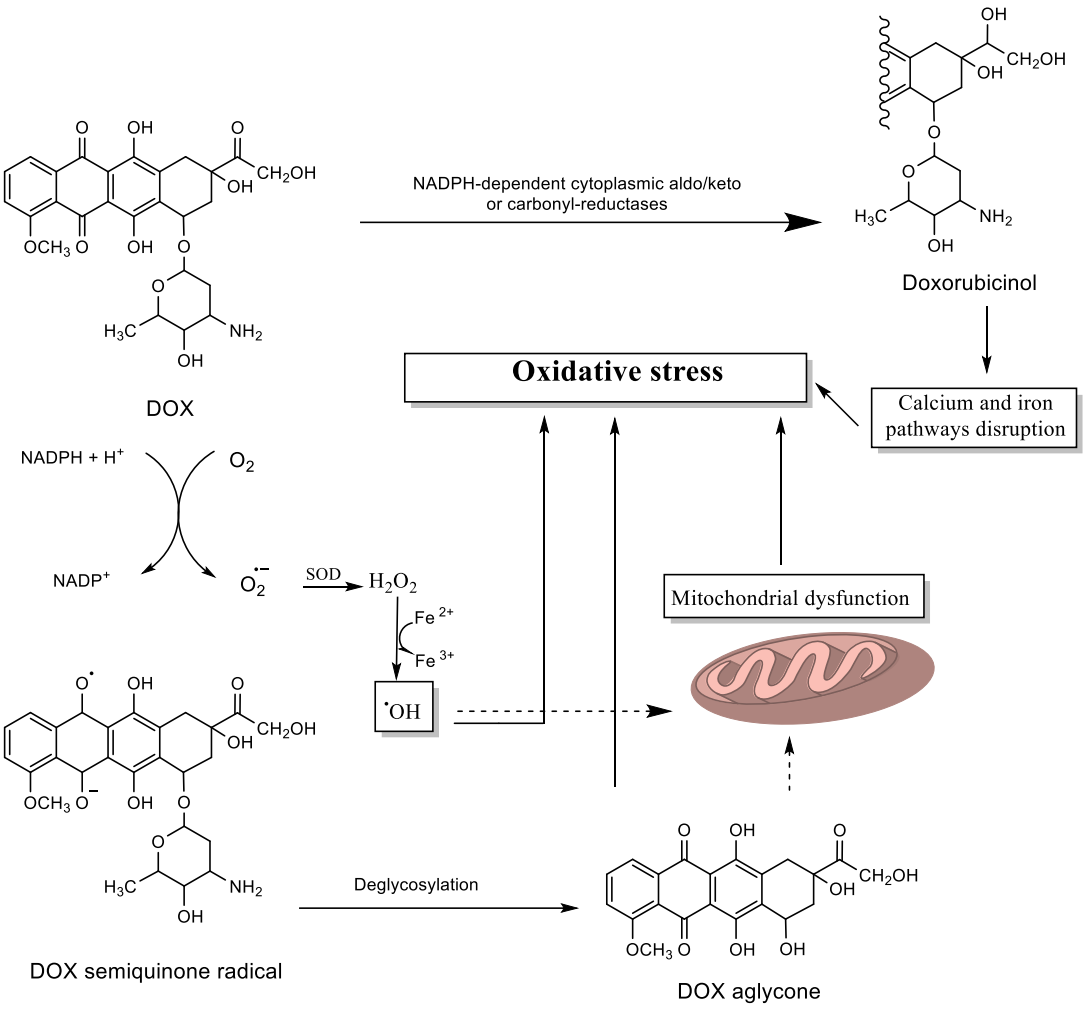

Figure 3. Oxidative stress related mechanisms for DOX-induced cardiotoxicity. Adapted from Costa *et al.,* 2013. (SOD: superoxide dismutase)

DOX easily enters cells through passive diffusion and accumulates in the cardiomyocytes. Intracellularly, DOX accumulates in the mitochondria due to DOX high affinity towards cardiolipin. This anthracycline may become cardiotoxic after one-electron reductive activation (Doroshow et al., 1980, Costa et al., 2013). One electron reduction of the quinone moiety of DOX results in the formation of a semiquinone free radical, which regenerates back to the parent quinone by reducing molecular oxygen to superoxide anion radical ($O_2^{\bullet -}$) (Doroshow and Davies, 1986, Serrano et al., 1999). The NADPH oxidoreductases [cytochrome P450 (CYP450) or -b5 reductases, mitochondrial nicotinamide adenine dinucleotide reduced form (NADH) dehydrogenase, xanthine dehydrogenase, and endothelial nitric oxide synthase (NOS) (reductase domain)] can be responsible for the reduction of DOX quinone in the heart (Costa et al., 2013). The $O_2^{\bullet -}$ is converted to hydrogen peroxide (H_2O_2) spontaneously or through the action of superoxide

dismutase (SOD). Hydrogen peroxide has a low toxic potential, being eliminated from the body by enzymatic antioxidant defence system (catalase and glutathione peroxidase). However, in the presence of the transition metals, especially iron, H_2O_2 and $O_2^{\bullet -}$ can generate the highly toxic $^{\bullet}OH$. This process occurs during the Haber-Weiss reaction, which is actually quite slow. The presence of iron strongly catalyses the formation of $^{\bullet}OH$, in a two-step process. In the first step, ferric ion (Fe^{3+}) is reduced in to ferrous ion (Fe^{2+}) by $O_2^{\bullet -}$. Ferrous ion then reacts with H_2O_2 (formed during DOX reduction) and results in in the formation of $^{\bullet}OH$ (Figure 4). Unlike H_2O_2 and superoxide anion radical, $^{\bullet}OH$ is extremely reactive and cannot be neutralized by antioxidant enzymes (Kotamraju et al., 2002, Minotti et al., 2004b, Halliwell and Gutteridge, 2007).

Moreover, DOX can directly bind to iron and, in the presence of oxygen, it can cycle between the Fe^{2+} and Fe^{3+} states (Figure 4). The DOX-Fe^{3+} complex can be reduced to the DOX-Fe^{2+} complex in the presence of NADPH CYP450 reductase, glutathione, or cysteine. These reactions are accompanied by the formation of $O_2^{\bullet -}$ and the conversion of the anthracycline quinone moieties to the semiquinone free radical (Doroshow et al., 1980, Rajagopalan et al., 1988, Vasquez-Vivar et al., 1997, Sawyer et al., 1999, Xu et al., 2005, Takemura and Fujiwara, 2007).

As stated, the oxidation of the semiquinone again to the quinone results in the formation of the superoxide radical anion. It is believed that this radical is the initiator of oxidative stress caused by DOX in the heart. The reactive oxygen species formed, in particular the $^{\bullet}OH$, can begin the peroxidation process of unsaturated membrane lipids and cause cellular damage in the myocardium (Kotamraju et al., 2002, Minotti et al., 2004b). In addition, reactive oxygen species can seriously affect nucleic acids and proteins, particularly ion channels and ion transporters (Halliwell and Gutteridge, 2007). It has been reported that DOX decreases the levels of enzymatic antioxidant defences (vitamin C, SOD, glutathione, catalase) making the heart more susceptible to oxidative stress (Costa et al., 2013).

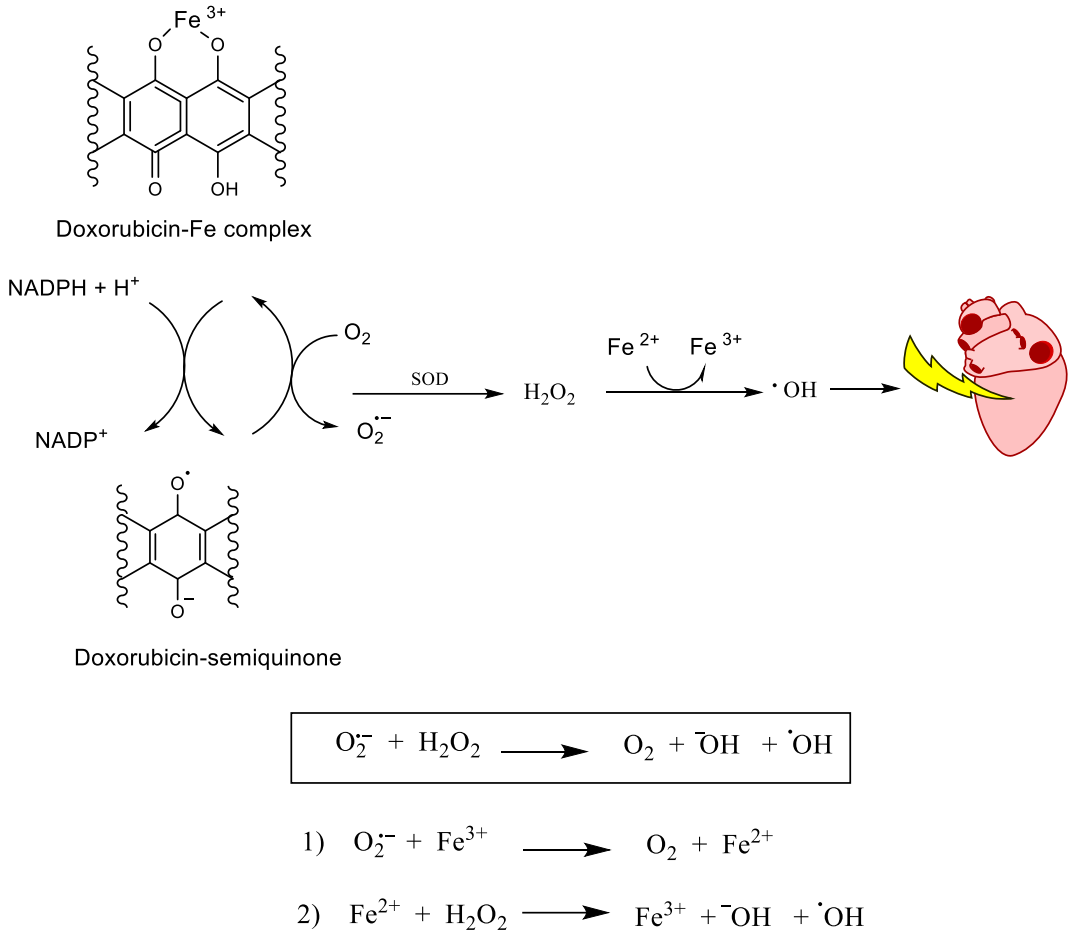

Figure 4. Iron involvement on DOX cardiotoxicity. Adapted from Torres and Simic, 2012.

Importantly, it was also found that NOS3 also contributes to cardiac dysfunction and injury observed after DOX administration of a single dose of 20 mg/kg, in a study using mice (Neilan et al., 2007). The results strongly suggest that DOX induces cardiac reactive species production via a NOS3-dependent mechanism. When NOS3 is deprived of L-arginine or cofactors, superoxide can be generated from the oxygenase domain instead of •NO, and this uncoupling may be associated with dissociation of NOS3 dimers. An alternative mechanism by which DOX can induce NOS3 to generate superoxide radical anion involves the conversion of DOX by the NOS3 reductase domain to an unstable semiquinone intermediate, which in turn produces superoxide radical anion in the presence of oxygen (Neilan et al., 2007).

1.2.2.3. Hypothesis of impairment of calcium homeostasis and cell death pathways by doxorubicin

An alternative hypothesis for the cardiotoxicity caused by DOX is the hypothesis of mitochondrial damage and changes on mitochondrial calcium concentration. The change in mitochondrial calcium is associated with reactive oxygen species production and dissipation of the mitochondrial membrane potential, which in turn may result in depletion of cellular adenosine triphosphate (ATP) (Zhou et al., 2001, Geisberg et al., 2012). This change in the transport of calcium leads to an irreversible decrease in storage ability and cell death, tissue damage, and consequently compromised cardiac contraction (Zhou et al., 2001). It is important to notice that the changes caused by the accumulation of reactive oxygen species, the alteration in calcium homeostasis and the mitochondrial damage observed are not isolated events, but can occur sequentially or simultaneously after DOX exposure (Kalyanaraman et al., 2002). Intracellular calcium is involved in the mechanisms of cell death. Usually, it is known that if exposed to low concentrations of anthracyclines, cardiomyocytes undergo apoptosis, whereas if exposed to high concentrations cardiomyocytes undergo necrosis (Doroshow et al., 1980, Rajagopalan et al., 1988, Vasquez-Vivar et al., 1997, Sawyer et al., 1999, Takemura and Fujiwara, 2007). When cell exposure to anthracyclines leads to apoptosis, one of the mediators of this process is the transcription factor and DNA damage sensor p53, accompanied with the activation of caspases (proteases) (Geisberg et al., 2012). However, ceramide, a lipid degradation product and the Fas receptor-ligand system have also been implicated in the damage caused by anthracyclines (Friesen et al., 1996).

1.2.2.4. Damage caused by metabolites of doxorubicin

There are reports that attribute anthracyclines cardiotoxicity not only to oxidative stress, but also to the damage caused by their metabolites, namely their secondary alcohols derivatives and aglycones.

DOX is metabolized by aldo/ketoses reductases that convert DOX to a secondary alcohol, the doxorubicinol (Figure 3). Those carbonyl reductases are present in the cytosol of cardiac cells (Boucek et al., 1987, Minotti et al., 1998). Cytosolic fractions from human myocardium have NADPH-dependent aldo/ketoses reductases capable of adding two electrons to the C-13 carbonyl group of DOX (Minotti et al., 1995). The doxorubicinol formed after enzymatic catalysis accumulates in the cardiac tissue and it is eliminated more slowly from the heart than the original drug, DOX (Gambliel et al., 2002). Stewart *et al*. demonstrated that doxorubicinol levels are higher (60%) than the levels of DOX in samples of heart tissue obtained from autopsies of patients treated with the parent compound (Stewart et al., 1993). Moreover, doxorubicinol levels are positively related to the cumulative administered dose of DOX (Stewart et al., 1993), which was identified as the main risk factor for the development of chronic cardiotoxicity since the early studies (Minow and Gottlieb,

1975). Autopsy tissues were collected from 35 patients who had received DOX at any time *ante-mortem* (Stewart et al., 1993). The major species found in human autopsy cardiac tissues were doxorubicinol (median concentration 92 ng/g, range 0 to 484 ng/g), and DOX (median 58 ng/g, range 0-1665 ng/g). Of the ten organs studied, heart ranked fifth regarding the median DOX concentration and ranked fourth regarding median doxorubicinol concentration. These results showed that heart accumulates large amounts of DOX and of its alcohol metabolite (Stewart et al., 1993).

Behnia and Boroujerdi used phenobarbital as an inhibitor of aldo/ketoses reductases after which they used DOX at 10 mg/kg, intravenously. They demonstrated a decrease of doxorubicinol levels *in vivo*, as well as a reduction in cardiac damage as assessed by serum levels of creatine kinase in the rat, when phenobarbital was administered (Behnia and Boroujerdi, 1999). The correlation between secondary alcohols and cardiotoxicity has also been clearly shown by the use of transgenic animals. Mice with only one functional copy of the gene carbonyl reductase are healthy and grossly normal despite having decreased levels of carbonyl reductase transcript and protein (Olson et al., 2003). To control wild-type animals and to carbonyl reductase transgenic mice were administered DOX at 20 mg/kg intraperitoneally. Within 2 weeks, 91% of wild-type mice were severely affected by DOX when compared to 18% of mice with only one functional copy of the gene carbonyl reductase. Transgenic mice showed decreased circulating levels of the metabolite, doxorubicinol, after administration. Echocardiography and histological analysis showed that those transgenic mice were protected from gross and cellular level pathologies associated with DOX treatment (Olson et al., 2003). Another study with transgenic mice that overexpressed a heart-specific human carbonyl reductase was performed (Forrest et al., 2000); it was found that the administration of a single injection of DOX (15 mg/kg) in these animals resulted in a higher cardiotoxicity than in control wild-type mice (Forrest et al., 2000). Moreover, levels of doxorubicinol were found to be four times higher in the human carbonyl reductase expresser hearts than in the nonexpressers. Acute cardiotoxicity was evident by a 60% increase in serum creatine kinase activity and a 5-fold increase in cardiac damage seen in the transgenic mice measured by electron microscopy. The human carbonyl reductase expressers survived for 5 weeks when compared with 12 weeks for the controls DOX-treated animals. Electrocardiograph profiles and necropsies showed the cause of death to be the development of cardiomyopathies leading to congestive heart failure. Electron microscopy data showed swelling and major structural damage of the mitochondria in the human carbonyl reductase expresser's mice that had DOX treatment (Forrest et al., 2000).

Doxorubicinol plays an important role in DOX cardiotoxicity, possibly by amplifying the damage induced by other species (e.g., reactive oxygen species). Thus, abnormal

increases of doxorubicinol formation in the heart can lead to an acceleration in the progression of cardiotoxicity and cause the development of heart failure at lower cumulative doses of DOX than predicted (Minotti et al., 2004a). Doxorubicinol is an inhibitor of cardiac contractility, acts on the calcium transport ATPase of the sarcoplasmic reticulum and in the calcium release promoted by the calcium channel of the sarcoplasmic reticulum (Olson et al., 1988). In preparations obtained from cardiac tissue, doxorubicinol is a negative inotropic agent even more potent than DOX (Olson et al., 1988). It should be added that doxorubicinol interferes with ferritin (Minotti et al., 1995). Doxorubicinol is able to release Fe^{2+} from ferritin, which is the major site of iron storage in cytosolic medium of human cardiomyocytes (Minotti et al., 1995, Minotti et al., 1996). Another work suggested that this secondary alcohol may also contribute to the cardiotoxicity through its ability to impair the iron regulatory protein/ aconitase system involved in the homeostasis of the intracellular iron (Minotti et al., 1998). Changes in iron homeostasis have been implicated in the cardiotoxicity induced by the DOX. Moreover, doxorubicinol or reactive oxygen species may contribute to cardiotoxicity by inactivating iron regulatory proteins that modulate the fate of the messenger ribonucleic acid (RNA) for the transferrin receptor and ferritin (Minotti et al., 2001). Doxorubicinol is also able to remove iron from the catalytic Fe-S cluster of cytoplasmic aconitase (Minotti et al., 2001).

The comparison between the properties of DOX and doxorubicinol has shown how a simple hydroxylation can strongly affect the toxic properties of those compounds (Heibein et al., 2012). Generally, doxorubicinol is less prone than DOX to cause oxidative stress. However, since it has a high cardiac accumulation (Stewart et al., 1993), doxorubicinol can lead to a large accumulation in the cardiac tissue when compared to the parent drug (Platel et al., 2000).

DOX and doxorubicinol may still undergo reduction via the reaction of glucosidase generating metabolites called aglycones (Boucek et al., 1987) (Figure 5). The deglycosylation of the daunosamine sugar at C-7 aglycone of DOX may lead to 7-hydroxydoxorubicin aglycone and 7-hydroxydoxorubicinol aglycone (Figure 5). The resulting hydroxyl group at C-7 can be metabolized to obtain 7-deoxydoxorubicin aglycone or 7-deoxydoxorubicinol aglycone (Takanashi and Bachur, 1976).

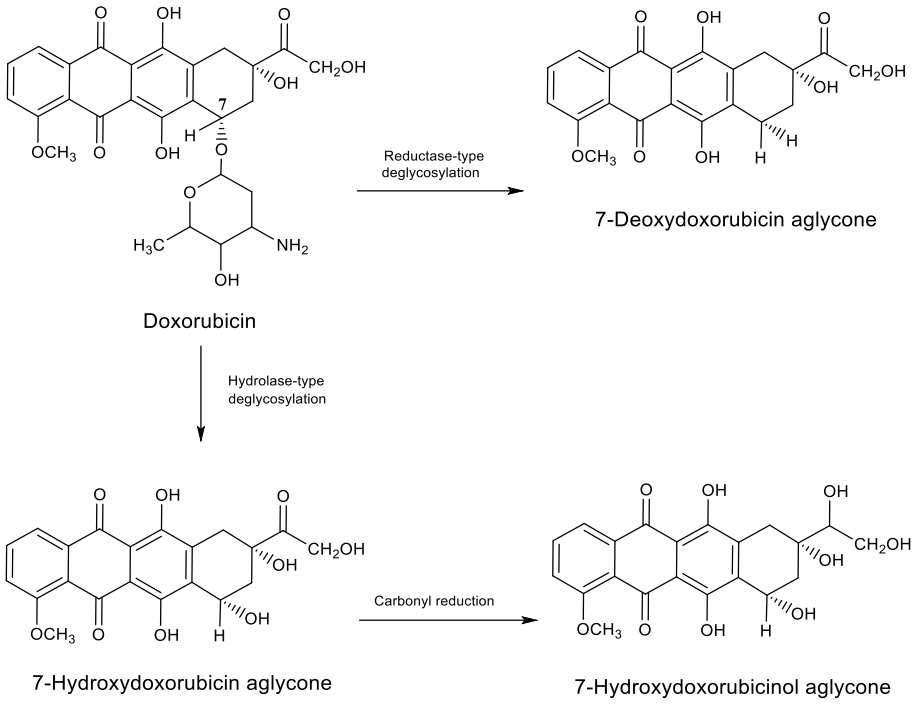

Figure 5. Doxorubicin formation of aglycones.

Aglycones are powerful mitochondrial toxins and mitochondrial dysfunction further amplifies oxidative stress (Costa et al., 2013). The aglycones formed lead to increased permeability of the inner membrane in the mitochondria of the heart, being this phenomenon accompanied by the release of mitochondrial calcium, by mitochondrial swelling, disfunction of the membrane potential, and mitochondrial oxidation of pyridine nucleotides (Sokolove, 1988). Aglycones can also modify mitochondrial sulfhydryl groups and induce a calcium independent oxidation of mitochondrial NADPH, which appears to redirect electron transport from NADH to oxygen and result in the production of superoxide radical anion (Sokolove, 1994). Calcium release and sulfhydryl modification are shown to depend similarly on aglycone concentration and on the C-7 substituent of the anthracycline ring (Sokolove, 1988). In particular, the 7-hydroxydoxorubicin aglycone decreased the amount of calcium required to trigger the mitochondrial permeability increase. 7-Deoxydoxorubicin aglycone, the most prominent aglycone metabolite of DOX, was similarly effective in inducing calcium release, and both aglycones were substantially more effective than the parent drug (Sokolove and Shinaberry, 1988). Sulfhydryl modification induced in mitochondria by 7-deoxydoxorubicin aglycone is more efficient than by 7-hydroxydoxorubicin aglycone. High potency of aglycones towards thiols may reflect increased access to key membrane thiols, due to their enhanced hydrophobicity (Sokolove, 1988). Moreover, Sokolove *et al*. examined the effects of DOX and its aglycone derivatives

on the pyridine nucleotide redox status of isolated, intact heart mitochondria. DOX aglycones induced the slow, calcium-independent oxidation of mitochondrial NADPH with 7-deoxydoxorubicin aglycone showing greater or equal potency than 7-hydroxydoxorubicin aglycone. That ability was much greater than DOX (Sokolove, 1991).

Studies on laboratory animals have limited value in the prediction of the structure and reactivity of toxic metabolites in humans. Therefore, some authors use ethically cytosolic fractions of myocardial samples obtained during surgery for coronary bypass grafting (Licata et al., 2000). After reconstitution with NADPH and incubation with DOX, these fractions generate the alcohol metabolite doxorubicinol as well as 7-deoxydoxorubicin aglycone and 7-hydroxydoxorubicinol aglycone. These data show that the reduction of the side chain carbonyl group, reductase-type deglycosylation of the anthracycline, and the hydrolase-type deglycosylation followed by carbonyl reduction, respectively, occurs in human samples. The authors have suggested through structure-activity considerations that aglycones and doxorubicinol may inflict cardiac damage by inducing oxidative stress and by perturbing iron homeostasis, respectively (Figure 5) (Licata et al., 2000).

1.2.2.5. Hypothesis associated with immune and genetic mechanisms

It was suggested by some authors that the cardiac damage caused by anthracyclines would increase due to their ability to activate the immune response. The damage caused by DOX in the cytoplasmic membrane of cardiomyocytes alone would compromise cardiac function, but the involvement of the immune system, with the consequent inflammatory response, exacerbates the cardiac dysfunction (Zhang et al., 1993). Zhang *et al.* showed that there was evidence of inflammatory responses in mice treated with DOX, since they exhibited increased dendritic antigen presenting cells. These results indicated that DOX treatment triggers immune reactions in which interstitial dendritic cells function as the antigen-presenting cells of the heart (Zhang et al., 1993). In addition to this inflammatory response, the release of vasoactive amines (histamine, catecholamines, prostaglandins, etc), after DOX administration, causes chemotaxis, further aggravating cardiac dysfunction (Huber, 1990, Zhang et al., 1993).

Another accepted mechanism for anthracyclines toxicity results from altered expression of cardiac proteins or the activation of some genetic programs. DOX negatively influences the expression of genes involved in the production of constitutive proteins of the cardiac muscle (cardiac troponin, myosin, etc) and mitochondrial proteins and other proteins (Takemura and Fujiwara, 2007), thus affecting the quality of cardiac work. Several transcription factors, including factor nuclear kappa B, are sensitive to the redox state of the myocyte (Valen et al., 2001) and redox mechanisms may explain, at least in part, the effect on the expression of this gene induced by DOX.

1.2.3. Daunorubicin and its' general pharmacokinetic data

DNR was the first discovered active substance in the anthracyclines group (Iwamoto et al., 1968). This drug is for injectable use and has significant activity on acute myelogenous leukaemia, being rarely used in other types of tumours. DNR is also used in the treatment of neuroblastomas (Infarmed, 2011). DNR and DOX differ only in a hydroxyl group (Figure 1); however, their activity spectrum greatly differs (Infarmed, 2011).

The recommended administration schedule for DNR is 25 to 45 mg/m^2 for three days. Total doses higher than 550 mg/m^2 are associated with a high cardiotoxicity risk (Table 3) (Chabner et al., 2012). DNR is widely distributed among tissues, mainly spleen, kidneys, liver, lungs, and heart (Trillet et al., 1985).

DNR undergoes rapid and extensive metabolism in the liver and other tissues, mainly through cytoplasmic aldo/ketoses reductases. One hour after its administration, the predominant metabolite in the plasma is the metabolite daunorubicinol (Bachur and Gee, 1971) that has a plasma half-life of 26.7h and has antineoplasic activity (Takanashi and Bachur, 1975, Roche, 2002).

Other metabolic routes for DNR include the glycosidic bond breakdown resulting in the production of aglycones, which have little or no antiproliferative activity and are further demethylated and conjugated via sulfate or glucuronide (Figure 6) (Di Marco et al., 1967, Alberts et al., 1971). In mouse and rabbit hepatocytes in suspension, DNR was shown to be metabolized mainly into daunorubicinol and deoxydaunorubicinol aglycones. The deoxydaunorubicin aglycone was rarely observed in both species. The anthracyclines conjugates were not observed in hepatocytes of any species (Gewirtz and Yanovich, 1986).

The overall metabolites of DNR were identified as: daunorubicinol, daunorubicinol aglycone, deoxydaunorubicin aglycone, deoxydaunorubicinol aglycone, demethyl deoxydaunorubicinol aglycone, deoxydaunorubicinol aglycone 13-*O*-β-glucuronide, demethyl deoxydaunorubicinol aglycone 4-*O*-sulfate and demethyl deoxydaunorubicinol aglycone 4-*O*-β-glucuronide. The human DNR metabolism involves mainly reduction of the carbonyl, reductive glycosidic cleavage, *O*-demethylation, *O*-sulfation and *O*-glucuronidation (Figure 6) (Takanashi and Bachur, 1975).

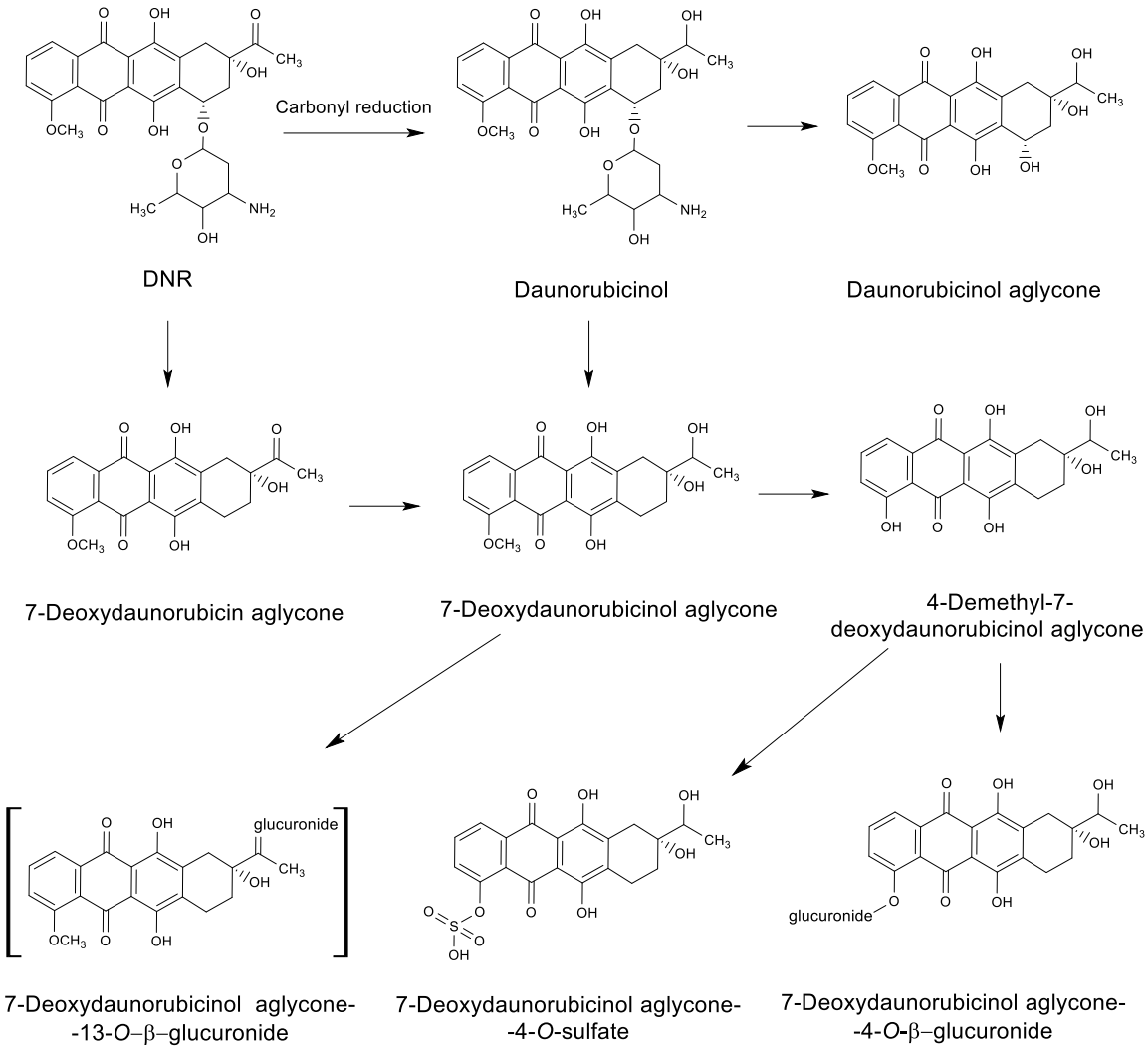

Figure 6. Main metabolites of DNR.

DNR and its metabolites are excreted in urine and bile (approximately 40% of the administered dose) (Rusconi et al., 1968, Alberts et al., 1971).

1.2.3.1. Cardiotoxicity of daunorubicin and daunorubicinol

The risk of developing congestive heart failure increases even in the absence of other cardiac risk factors when the total cumulative dose of DNR exceeds 550-800 mg/m^2 in adults (Adão et al., 2013), 300 mg/m^2 in children over two years of age, or 10 mg/kg in children under two years of age (Mortensen et al., 1992). These cardiotoxicity effects are long known (Bonadonna and Monfardini, 1969, Marmont et al., 1969) and the risk factors for cardiotoxicity resemble other anthracyclines (Table 3).

Several studies were performed in animal models to better highlight the cardiotoxicity of DNR and its main metabolite, daunorubicinol. In a rat model, and after

treatment with 6 doses 3 mg/kg intraperitoneally, DNR showed a strong ability of decreasing functional cardiac parameters, while daunorubicinol administered in the same dose and administration route did not cause any observed cardiotoxicity (Platel et al., 2001). Both treatments led to a similar accumulation of daunorubicinol in the myocardium while DNR was found only in the hearts of rats treated with this drug and not with daunorubicinol (Platel et al., 2001). Direct infusion to isolated rat hearts of the same dose (10 μM) of DNR or daunorubicinol induced a depression of heart function in both groups; however, only DNR induced a progressive increase in diastolic pressure. On the other hand, in cardiac sarcoplasmic reticulum vesicles, daunorubicinol at a concentration of 5.5 μ/g tissue or 10 μM inhibited calcium uptake by 39 ± 3%, whereas 10 μM of DNR did not cause any detectable inhibition (Cusack et al., 1993). Another study, however, demonstrated that both DNR and daunorubicinol were several fold more potent at inhibiting than they were at stimulating sarcoplasmic reticulum calcium release in canine heart vesicles (Olson et al., 2000). Concentrations that cause 50% inhibitory effect (IC_{50}) on caffeine-induced calcium release of DNR and daunorubicinol were 1.2 and 0.6 μM, respectively, and for spontaneous calcium release were 3 and 1 μM, respectively (Olson et al., 2000). The model used and the amounts of calcium used for loading may explain these dissimilar results. After DNR or daunorubicinol administration with 6 doses of 3 mg/kg intraperitoneally on rat, DNR strongly decreased the cardiac functional parameters, while daunorubicinol did not induce cardiotoxicity (Platel et al., 2001).

In summary, DNR follows the same metabolic route of DOX, namely regarding the reduction to daunorubicinol (Loveless et al., 1978). However, in contrast to DOX, DNR administration leads to much higher concentrations of this metabolite in the plasma and tissues than the parent compound (Robert and Gianni, 1993, Platel et al., 2001), whereas the formed alcohol metabolite is less cardiotoxic than the initial drug (Platel et al., 2001).

1.3. Alkylating agents (i.e. cyclophosphamide) and their cardiotoxicity

Alkylating agents are highly reactive compounds that readily bind to phosphates, amines, imidazole and hydroxyl groups found in nucleic acids. The cytotoxic and mutagenic effects of alkylating agents are directly related to DNA alkylation, which can lead to the replacement of base pairs, breaks or the formation of covalent bonds between DNA strands, stopping the DNA replication and causing cell death (Chabner et al., 2012). The most important pharmacological actions of the alkylating agents affect DNA synthesis and cell division. Therefore, they are more cytotoxic in rapidly proliferating tissues. However, these agents affect both healthy and cancer cells and notwithstanding act on the cells at any stage of the cycle (Chabner et al., 2012). Cyclophosphamide is an alkylating agent used orally or

by intravenous administration. It prevents cell proliferation and acts mainly in malignant cells, therefore being used for treating various types of cancer, including colon-rectal, breast and their metastases, adenocarcinoma of the lung, testicle, prostate, endometrial, ovarian, bladder, or kidney cancers, soft tissue sarcoma, acute lymphocytic leukaemia, myelocytic and monocytic leukaemia, multiple myeloma, Wilms' tumour, Hodgkin's disease, non-Hodgkin's lymphoma, Burkitt's lymphoma, as well as disorders of the autoimmune system, Wegener's granulomatosis, *myasthenia gravis*, multiple sclerosis, hemolytic anaemia, and other conditions (Infarmed, 2004). It has been used as an immunosuppressant for the prevention of transplant rejection in kidney, liver, heart, bone marrow, but it has been also used in rheumatoid arthritis, systemic lupus erythematosus, and nephrotic syndrome (Goldberg et al., 1986, Infarmed, 2004). It is a prodrug, therefore it requires a process of metabolic activation, mainly by CYP450 (in the liver and tissues) before exercising its anticancer actions (Figure 7).

Regarding to pharmacokinetics, cyclophosphamide is well absorbed orally, with an oral bioavailability of 75%. The peak plasma level occurs one hour after oral administration. The protein binding rate is relatively low (10% to 56%), while the volume of distribution is 0.48 to 0.71 L/ kg. The elimination half-life is 1.3 to 16h (Infarmed, 2004). Cyclophosphamide is less than 10% excreted in the urine as an unchanged drug and is 85% to 90% excreted as metabolites (Infarmed, 2004).

High therapeutic doses of cyclophosphamide may cause lethal cardiotoxicity. A combination of symptoms and signs of myopericarditis can result in congestive heart failure, arrhythmias, cardiac tamponade, and myocardial depression (Gottdiener et al., 1981, Ayash et al., 1992). Severe cardiac haemorrhagic necrosis has been reported in the high doses of cyclophosphamide used prior to bone marrow transplantation. The pathological findings in autopsy of patients treated with high dose cyclophosphamide and heart problems include dilated heart, transmural irregular bleeding, focal areas of fibrous pericarditis, myocardial necrosis and interstitial lesions with signs of haemorrhage, oedema and fibrin deposition (Crossley, 1984). In bone marrow transplantation, cyclophosphamide dosing can reach 120-240 mg/kg provided for one to four days (O'Connell and Berenbaum, 1974, Appelbaum et al., 1976, Goldberg et al., 1986). The incidence of fatal cardiomyopathy varies from 2.0% to 17.0%, depending on the different regimens and populations. The large increases in plasma lactate dehydrogenase (LDH) and creatine phosphokinase suggest myocardial damage and their values are elevated in approximately half of the patients administered with high doses of this drug. Symptoms of cardiac necrosis may become apparent within two weeks after the administration, but are rapidly fatal when detected (Slavin et al., 1975).

In the work of Goldberg and co-workers with patients that had not received any previous cardiotoxic therapy, namely anthracycline or radiation, the incidence of congestive

heart failure was reported to be 0/32 in patients receiving doses lower than 1.55 g/m^2 and 6/52 in patients receiving higher than 1.55 g/m^2 cyclophosphamide (Goldberg et al., 1986). Reversible decreases in ECG voltage and increases in left ventricular mass, possibly reflecting myocardial oedema or haemorrhage were observed in the twice-daily, higher-dose (mean total 174 ± 34 mg/kg) of cyclophosphamide regimen (Goldberg et al., 1986). Another study reported an incidence of 9% fatal cardiomyopathy and/or pericarditis with combination therapy or high-dose cyclophosphamide and total body irradiation (Cazin et al., 1986). The majority of patients in these studies had previously received anthracyclines, which certainly increased the risk of cardiotoxicity. In another study, the cardiotoxicity of cyclophosphamide administered twice daily at a high dose (total of 174 average ± 34 mg/kg) was evaluated and compared with a lower daily dose schedule (87 ± 11 mg/kg) (Braverman et al., 1991). The LVEF did not change significantly in both groups, however, four of the five patients who developed clinical cardiotoxicity belonged to the group with the highest dose (Braverman et al., 1991).

Several therapeutic and toxic effects of cyclophosphamide seem to require its metabolic activation by hepatic microsomal CYP450 mixed function oxidase system and those metabolites were shown *in vitro* and *in vivo* to cause cardiotoxicity (Levine et al., 1993, Dorr and Lagel, 1994, Ismahil et al., 2011). Cyclophosphamide is extensively metabolized in the liver by CYP450 enzymes to active/toxic metabolites (4-hydroxycyclophosphamide, aldophosphamide, phosphoramide mustard, and acrolein) and inactive metabolites (4-ketocyclophosphamide, carboxyphosphamide) (Figure 7) (Dorr and Lagel, 1994). The distribution of these metabolites can cause high cardiac concentrations of these metabolites, without need of *in loco* metabolization (Dorr and Lagel, 1994).

Nakamura *et al*. investigated the toxic effects of cyclophosphamide, acrolein, and DOX in H9c2 cell line and in isolated rat hearts. Cyclophosphamide itself had no toxic effect, while the toxicity of acrolein was 1000 times greater than of DOX in cell line H9c2 (Nakamura et al., 2010). In the isolated rat heart, acrolein, but not cyclophosphamide, reduced left ventricular pressure and heart rate and increased left ventricular end-diastolic pressure. These results suggest that the cardiac toxicity of cyclophosphamide may be caused by acrolein, one of its metabolites (Nakamura et al., 2010).

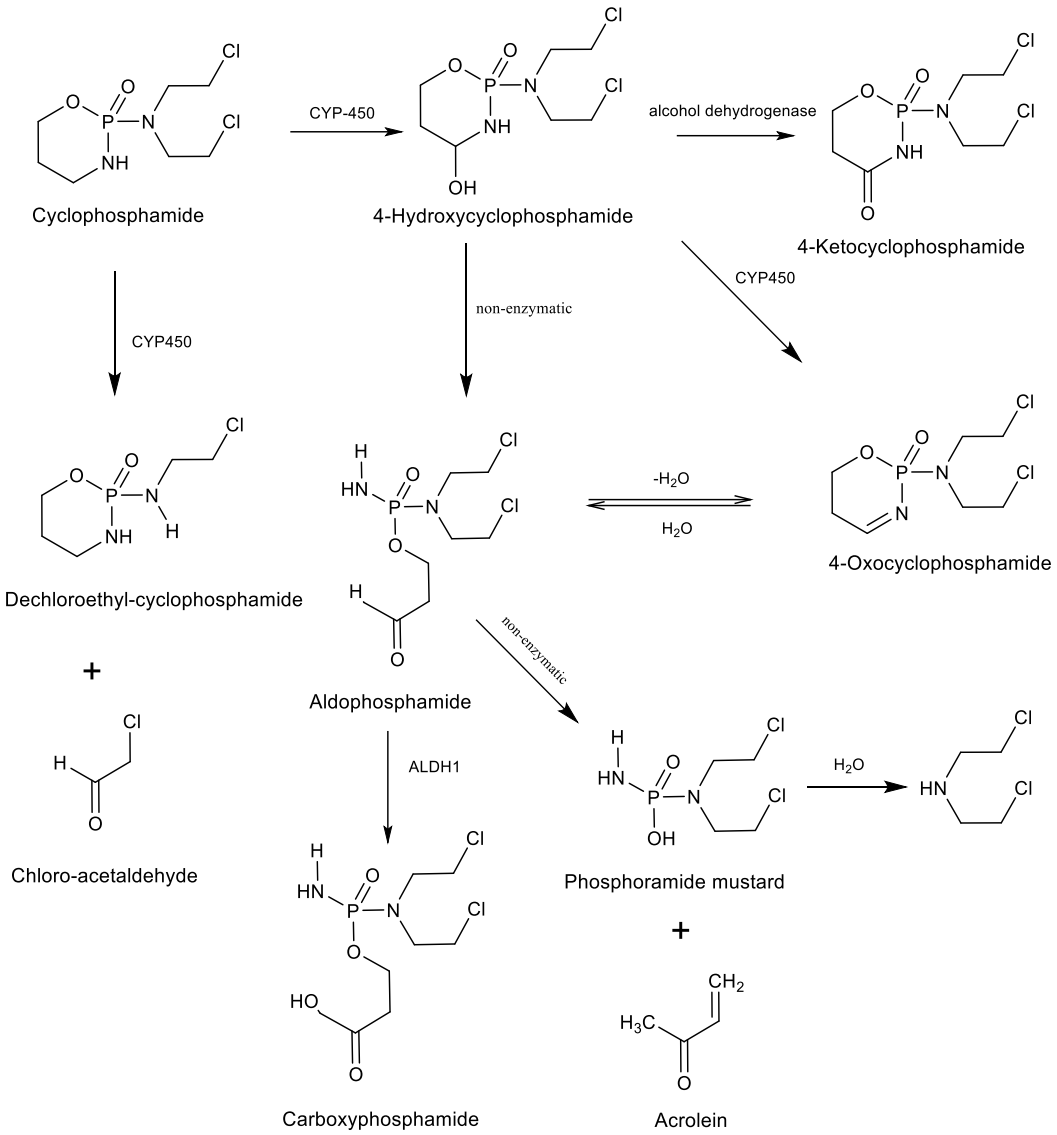

Figure 7. The main metabolites of cyclophosphamide (ALDH1: aldehyde dehydrogenase type 1).

The conversion of the synthetic probe 4-hydroperoxyclophosphamide to the metabolite 4-hydroxycyclophosphamide and then its transformation to acrolein is rapid *in vitro* (Dorr and Lagel, 1994). The 4-hydroperoxyclophosphamide causes changes in the contents of various ions (Na^+, K^+, and Ca^{2+}) and decreases the content of ATP in cardiac myocytes, all early indicators of cytotoxicity (Levine et al., 1993).

Neonatal rat heart myocytes were used to evaluate the acute cardiotoxic effects of cyclophosphamide metabolites (Dorr and Lagel, 1994). The decrease in ATP levels on the myocytes with 4-hydroperoxycyclophosphamide and acrolein had an IC_{50} value of 123 µM and 152 µM, respectively. The parent compound, cyclophosphamide, had no significant action on ATP levels. Glutathione levels were initially reduced and then transiently elevated

following exposure to 4-hydroperoxycyclophosphamide (Dorr and Lagel, 1994). With acrolein, glutathione levels were reduced to non-measurable levels at all-time points evaluated (up to 72h). Finally, two exogenous sulfhydryl-containing compounds (mesna and *N*-acetyl cysteine) were shown to block the toxic effects of both 4-hydroperoxycyclophosphamide and acrolein in that model. These results suggest that acrolein and 4-hydroperoxycyclophosphamide are equipotent cytotoxics and that a transient depletion in glutathione accompanies their toxic effects in cardiac myocytes (Dorr and Lagel, 1994, Nakamura et al., 2010).

The intracellular antioxidant, glutathione, is suggested to play an important role in the protection against heart damage caused by cyclophosphamide (Friedman et al., 1990, Todorova et al., 2009), suggesting that the cardiac toxicity of cyclophosphamide involves oxidative stress and reactive metabolites. In Fischer 344 rats, administration of cyclophosphamide at a dose that is lethal to 10% of control athymic nude mice resulted in sudden death within 3h of the all mice that had been pre-treated with the glutathione synthesis inhibitor, buthionine sulphoximine. Cardiac monitoring revealed ventricular fibrillation to be the cause of death of those animals (Friedman et al., 1990). Adult mice cardiomyocytes exposed to 1 μM of acrolein showed a marked increase in the intracellular reactive oxygen species and calcium concentration, by 12- and 2-fold, respectively, compared to control values, corroborating the involvement of oxidative stress (Wang et al., 2011). Acrolein (1 mg/kg daily) was administered orally to C57BL/6 mice by gavage-fed for 48 days (Ismahil et al., 2011). Acrolein-fed mice exhibited significant left ventricular dilatation, contractile dysfunction, and impaired relaxation. Histological and biochemical evaluation revealed myocardial oxidative stress (membrane-localized protein-4-hydroxy-*trans*-2-nonenal adducts), nitrative stress (increased protein-nitrotyrosine) and varying degrees of plasma and myocardial protein-acrolein adduct formation. These data showed physical translocation of the ingested acrolein to the heart. Acrolein also caused myocyte hypertrophy, increased apoptosis, and decreased cardiac activity of NOS3 (Ismahil et al., 2011).

Risk factors for the development of congestive heart failure caused by cyclophosphamide were already reported and include: cyclophosphamide doses of approximately 1.55 g/m^2/day (Goldberg et al., 1986), administration of doses over 6h, instead of 30 to 60 minutes (min) (Kushner and Cheung, 1991), activation of cyclophosphamide and increased formation of metabolites (Ayash et al., 1992) and low levels of cardiac glutathione (Friedman et al., 1990). In fact, cyclophosphamide's cardiac toxicity is undoubtedly related to levels of the antioxidant glutathione, and this antioxidant is present at low levels in the heart (Costa et al., 2013). The cyclophosphamide metabolites contribute to its cardiac toxicity, possibly through oxidative stress mechanisms.

1.4. Mitoxantrone

MTX, 11,4-dihydroxy-5,8-bis[(2-[(2-hydroxyethyl)amino]ethyl)amino]-9,10-anthracenedione (Figure 8) is an antineoplastic agent belonging to the family of the synthetic anthracenediones (Ehninger et al., 1990). MTX was originally synthesized in 1979 (Fox, 2004). The main chemical alteration of MTX comparing with anthracyclines was the replacement of the amino sugar on the anthracyclines for aminoalkylalcohol chains (Figure 8) (Pratt et al., 1986).

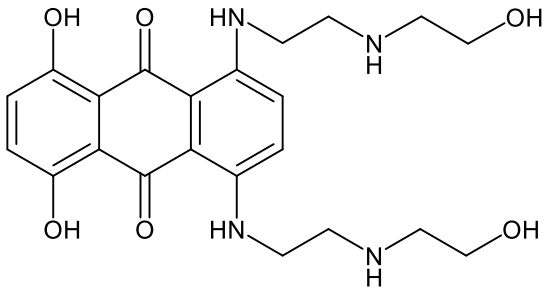

Figure 8. The chemical structure of MTX.

In 1979, Murdock published a work, which indicated that MTX had a potent anticancer activity (Murdock et al., 1979). MTX is the only compound in the series of anthracenediones that has undergone extensive clinical trials. MTX showed cytostatic effects both *in vitro* and in animal testing (Johnson et al., 1979, Schabel et al., 1983). In fact, in 1979, the phase I clinical trials with MTX were initiated to define the maximum tolerable doses with various administration regimens. MTX approval was aimed to maintain or improve the anthracyclines antitumor activity and reduce their cardiotoxic side effects (Fox, 2004, Ferlay et al., 2013).

1.4.1. Pharmacological mechanisms of mitoxantrone

In clinical studies, the anticancer activity of MTX has been demonstrated in patients with advanced breast cancer, acute leukaemia and lymphoma, solid tumours and prostate cancer (Coltman et al., 1983, Paciucci et al., 1983, Smith, 1983, Yap et al., 1983, Stuart-Harris et al., 1984, Seiter, 2005, Patel et al., 2013). In 2000, MTX was also approved by the U.S. Food and Drug Administration as an immunomodulation agent for reducing neurological disability of worsening relapsing-remitting or secondary progressive multiple sclerosis, an autoimmune disease characterized by the progressive destruction of the

myelin sheath surrounding axons in the central nervous system (Avasarala et al., 2003, Seiter, 2005, Neuhaus et al., 2006, Paul et al., 2009, Patel et al., 2013).

The known mechanism of action of MTX involves the intercalation of DNA and inhibition of topoisomerase II activity (Ehninger et al., 1990, Seiter, 2005, Patel et al., 2013). Although the MTX chemical core contains a planar structure that is usually associated with intercalation of DNA, the extensive amino alkyl side chains in positions one and four prevent the incorporation of the entire molecule in the DNA helix (Neidle, 1978) (Figure 8). MTX binds to DNA through a mechanism that involves both hydrogen interactions, as well as π-π stacking (Lown et al., 1985). Some authors have demonstrated that MTX inhibits the synthesis of DNA, RNA and protein *in vitro* (Durr et al., 1983, Johnson et al., 1983). It is believed that the anticancer activity of MTX is due to the stabilization of topoisomerase II with a DNA cleavable complex (Liu, 1989). Cells treated with MTX exhibit typical cellular effects of topoisomerase II inhibitors, including inhibition of DNA synthesis, cell cycle arrest in the G2 phase and the occurrence of various types of breaks in the DNA chain (Bowden et al., 1985, Fox and Smith, 1990). MTX, at high concentrations, inhibits the biosynthesis of prostaglandins and the release of calcium, a finding that may have an additional meaning given the role of prostaglandins in metastatic spread of tumours and the hypercalcemia that occurs in cancers (Novak et al., 1988, Ehninger et al., 1990). Recently, the MTX potential epigenetic effects were demonstrated given its high affinity to bind to histone H1 and core histones *in vitro* (Hajihassan and Rabbani-Chadegani, 2011). Immunomodulatory effects of MTX may also contribute to its anticancer activity and its use in multiple sclerosis (Fidler et al., 1986).

There are many studies that evaluate the reductive bioactivation of anticancer drugs by cellular oxidoreductases, especially by NADPH cytochrome reductase. These bioactivations can result in covalent DNA-binding of the formed metabolites (Cummings et al., 1991, Skladanowski and Konopa, 1994, Bailey et al., 2001), leading to a significant increase cytotoxic activity of these compounds (Bartoszek and Wolf, 1992, Patterson et al., 1995, Cowen et al., 2003). The formation of reactive species is occasionally referred as a possible anticancer mechanism of MTX. However, while the reactive species can be generated in cells treated with MTX, a redox cycle quinone-dependent similar to DOX does not occur in biological conditions (Kharasch and Novak, 1983, Sinha et al., 1983, Duthie and Grant, 1989, Nguyen and Gutierrez, 1990). This subject will be addressed in the following sections.

1.4.2. Pharmacokinetics and metabolism of mitoxantrone

MTX is poorly absorbed orally, so it is administered intravenously, intraperitoneally, or via intra-arterial administration through a continuous infusion (Ehninger et al., 1990). In

clinical studies using a single intravenous infusion of MTX, the administered dose ranges between 5-14 mg/m^2, while the administration schedule can vary according to the disease and response to therapy, ranging from 4-6 weeks for the treatment of acute myeloid leukaemia, 3 weeks for the treatment of prostate cancer (Fox, 2004), and 3 months for multiple sclerosis (Scott and Figgitt, 2004).

The plasma concentration-time curve of MTX can be best fitted with three exponentials: a rapid half-life of 4.1 to 10.7 min, corresponding to the moment when MTX rapidly leaves the plasma and binds to the endothelial surface; an intermediate half-life of 0.3 to 3.1h, corresponding to the distribution phase; and a long terminal half-life of 8.9h to 9 days (Batra et al., 1986, Ehninger et al., 1990, Fox, 2004). Therefore, MTX exhibits a rapid initial distribution phase followed by a relatively slow elimination phase from the deep tissues (Fox, 2004). In summary, the pharmacokinetic characteristics of MTX are: rapid plasma clearance, long half-life elimination without the need for significant change in the case of kidney or liver dysfunctions and persistent tissue concentrations (Stewart et al., 1986). MTX has a very large volume of distribution, suggesting that most of the drug is accumulated in the tissues (Stewart et al., 1986). MTX is mostly bound to human plasma proteins (approximated 78%) (Batra et al., 1986). The elimination of the drug is slow, with a half-life of about 12 days (range 5-18 days) with persistent tissue concentrations in mice with tumour xenographs (Patel et al., 2013).

One study examined the concentrations of MTX in autopsy tissue samples from 11 patients who had received the drug 10 to 272 days before death (Stewart et al., 1986). The total cumulative lifetime dose of MTX for these patients ranged from 6 to 100 mg/m^2. MTX was detected in tissues from all patients, even 272 days after administration. The highest concentrations were found in the thyroid, liver, and heart. The lowest concentration was reported in the brain (Stewart et al., 1986). Also in humans, MTX was detected 35 days after a single dose of 12 mg/m^2 in the liver (1140 ng/g) and heart (716 ng/g) (Batra et al., 1986). These studies were conducted in cancer patients, and the results may therefore be different in patients with multiple sclerosis who are dosed differently than cancer patients (Fox, 2004).

The major route for the elimination of MTX from the body is biliary excretion, as renal clearance can account for only up to 10% of the total clearance of the drug (Fox, 2004). ^{14}C-labeled MTX was administered to eight patients who had advanced soft tissue cancers (Alberts et al., 1985) and only 6.5% of the total MTX dose administered was excreted in the urine as unchanged drug over the next 5 days. The mean recovery of ^{14}C-labeled material in faeces over 5 days was 18.3% of the administered dose. Thirty-five days after MTX administration, one of the patients died of progressive kidney cancer, and approximately 15% of the ^{14}C dose was found in seven major organs (Alberts et al., 1985).

Two of the MTX metabolites were isolated from the urine of patients and characterized as of mono- and dicarboxylic acids resulting from oxidation of the terminal methyl groups in the side chains (Figure 9) (Chiccarelli et al., 1986). Regarding the inter-species variability, the major metabolic difference between rat and humans relates to mono- and dicarboxylic acids that are the main products of human metabolism of MTX, whereas in rat, they are residual (Blanz et al., 1991b, Richard et al., 1991). Therefore, the metabolic differences between the species can determine that electrophilic metabolites can be formed in higher amounts in rats.

Controversial data still exists whether the MTX undergoes one electron reduction or reduction by two electrons (Wolf et al., 1986, Duthie and Grant, 1989, Fisher and Patterson, 1992). In fact, the reduction of MTX by flavin reductase is not facilitated, due to its low reduction potential (Fisher and Patterson, 1992). Thus, the preferred metabolism route of MTX seems to occur through two electron reduction as evidenced in studies where inhibition of CYP450-mediated metabolism is done (Duthie and Grant, 1989, Mewes et al., 1993, Li et al., 1995). It has been shown that a cyclic metabolite of MTX, the naphthoquinoxaline (NAPHT) (Figure 9) is a product of biotransformation of MTX *in vivo* in humans, pig, and rat (Blanz et al., 1991b, Bruck and Bruck, 2011). This metabolite has been described as the product of metabolism through systems containing CYP450 enzymes and peroxidases and it is found in urine (Blanz et al., 1991b, Bruck and Bruck, 2011). Other studies suggest that this metabolite has a significant role in the pharmacological anticancer activity of MTX (Mewes et al., 1993, Shipp et al., 1993, Feofanov et al., 1997, Panousis et al., 1997).

After incubation of urine from MTX-treated patients with β-glucuronidase or sulfatase, no differences between control and test samples were found (Smyth et al., 1986). Therefore, glucuronidation and conjugation with sulfate did not seem to be part of the biotransformation of MTX in humans in that study (Smyth et al., 1986). However, other works confirm that the glucuronides are also urinary metabolites of MTX in humans (Batra et al., 1986, Blanz et al., 1991a). The human urinary glucuronide metabolite was detected in 1991 (Blanz et al., 1991a), whereas the MTX glutathione metabolites were only detected in animals (Rossato et al., 2013a) or in *in vitro* models (Mewes et al., 1993). In rat liver hepatic microsomes or S9 fraction, MTX formed glucuronic and glutathione conjugates (Wolf et al., 1986, Rossato et al., 2013a). Incubation of MTX with peroxidase/H_2O_2, in the presence of glutathione, led to the formation of two MTX glutathione conjugates (Blanz et al., 1991b).

An *in vivo* study was performed to investigate whether the metabolites of MTX previously found *in vitro* were also present in liver and heart of rats, after one intraperitoneal administration of 7.5 mg/kg MTX 24h before (Rossato et al., 2013a). MTX and NAPHT metabolite were present in the heart and liver of male rats (Rossato et al., 2013a). Moreover,

in that study, an *in vitro* study was also performed using rat liver S9 fractions. In that system, MTX metabolism led to the formation of five metabolites all of them maintaining the chromophore group. Of those five metabolites, NAPHT and a new metabolite, an acetoxy ester derivative, were identified as resulting of MTX metabolism (Rossato et al., 2013a).

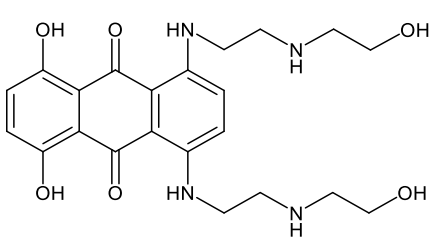

MTX

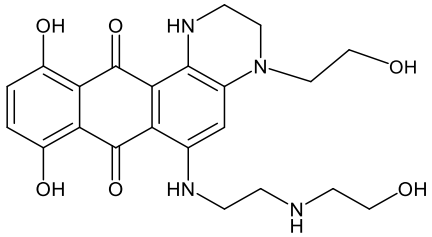

Naphthoquinoxaline metabolite

Other metabolites of MTX

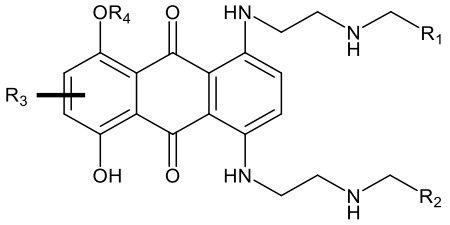

Compounds	R_1	R_2	R_3	R_4
Monocarboxylic acid of MTX	COOH-	CH_2OH-	H-	H-
Dicarboxylic acid of MTX	COOH-	COOH-	H-	H-
Glucuronide metabolites of MTX	CH_2OH-	CH_2OH-	H-	Glucuronide-

Figure 9. The major human metabolites of MTX.

1.4.3. The cardiotoxicity of mitoxantrone

Despite its initial objective, MTX is potentially cardiotoxic (Avasarala et al., 2003, Seiter, 2005). In 1993, Estorch *et al.* suggested that MTX was less cardiotoxic than anthracyclines (Estorch et al., 1993), but this conclusion has not been corroborated by other studies (Thomas et al., 2002, Avasarala et al., 2003). In fact, the cardiotoxicity of MTX remains a major concern for patients receiving intensive and/or prolonged therapy with MTX (Ehninger et al., 1990). Presently, the recommended maximum lifetime cumulative dose of MTX is 140 mg/m^2, with 2.6 to 13% of patients developing cardiac toxicity (Seiter, 2005). As early as 1984, the cardiotoxicity of MTX was detected in 34 patients with advanced breast cancer that had never received previous chemotherapy. They were treated with MTX

(14 mg/m^2 intravenous every 21 days) (Coleman et al., 1984). Before starting the MTX therapy, and every 3 months thereafter, radionuclide assessment of ventricular performance was obtained at rest and in response to stress. Ten patients showed a deterioration in ejection fraction and two of them developed congestive cardiac failure (Coleman et al., 1984). In another study, biopsies were examined in a small number of patients treated with MTX by Unverferth and colleagues. This study found cardiac histopathological changes similar to those found in treatment with anthracyclines. The nuclear chromatin changes included shrinkage, nucleolar agglutination and degeneration. They also observed mitochondrial swelling and tubular swelling in cardiomyocytes (Unverferth et al., 1983). In a study by Benjamin *et al.*, biopsies from patients treated with MTX revealed dilatation of sarcoplasmic reticulum with vacuoles and myofibrillar changes (Benjamin et al., 1985). Those histological changes were also found to be initial cardiac findings in DOX therapy (Benjamin et al., 1985). In addition, an increase in cell damage with a higher dose of MTX was observed. Thus, the cardiac histological data of MTX indicates that it produces adverse changes in the human heart, which are similar to those produced by DOX (Benjamin et al., 1985).

The clinical cardiotoxicity signs of MTX include decreased LVEF, congestive heart failure, ischemic chest pain, arrhythmias and conduction abnormalities on the ECG (Henderson et al., 1989, Estorch et al., 1993). Some predisposing factors for MTX cardiotoxicity include prior exposure to anthracyclines, thoracic radiation or pre-existing heart disease, although cardiotoxicity can occur in the absence of these risk factors (Benjamin et al., 1985) (Table 3).

1.4.4. Cardiotoxicity of mitoxantrone in experimental models

The chronic cardiotoxicity has been studied in animal models in an attempt to discover and counteract the cardiotoxic mechanisms associated (Zbinden and Beilstein, 1982, Perkins et al., 1984, Rossato et al., 2013a, Rossato et al., 2014). In a study by Zbinden and Beilstein with a twice a week administration of MTX, and then interrupted for 18 days and then resumed with four other injections, several evaluations were made (Zbinden and Beilstein, 1982). After about six weeks, the authors observed significant changes in the ECG, elevated serum marker enzymes of cardiac damage and marked changes in mitochondrial structure in heart tissue (Zbinden and Beilstein, 1982). In the same study the authors compared the mitochondrial alterations induced by DOX and MTX *in vivo* (Zbinden and Beilstein, 1982). In these experiments, MTX injections (1 mg/kg) and DOX (2 mg/kg) were administered twice *per* week for four weeks. Each week, a group of animals were sacrificed and mitochondria were isolated from the heart, being the oxygen uptake and oxidative phosphorylation activity measured. Under these conditions, the

mitochondrial function was inhibited in a time dependent manner, in both MTX and DOX. MTX caused a marked inhibition of the activity of the pump Na^+/K^+ ATPase (from 41% to 68% of the control) in the first week and that measurement remained unchanged thereafter (Zbinden and Beilstein, 1982). These results were in agreement with the findings of Neri and Cini-Neri (Neri and Cini-Neri, 1986); the later observed a progressive reduction in oxygen consumption and loss of ATP and phosphocreatine from rat heart samples incubated with DOX or MTX *in vitro* (Neri and Cini-Neri, 1986).

Chronic MTX cardiotoxicity was also studied in mice with a twice *per* week of MTX administration (2 mg/kg) at weeks 1, 2, 5, 6 and 7 (Perkins et al., 1984). The rats were sacrificed during week 11 and the hearts were evaluated by histology. Of the 14 mice treated with MTX, 12 exhibited myocardial injury. The Bertazzoli scale was used to quantify the degree of cardiac damage and the rate 0 degree indicating that there is no difference between the control animals, while grade 4 indicates the most marked damage of myocardial fibres (Bertazzoli et al., 1979). In the Perkins *et al.* study, twelve animals showed myocardial changes: five with grade 1, four with grade 2 and three with grade 3. Infiltration focal mononuclear cells also occurred in three hearts (Perkins et al., 1984).

In a more recent study, male Wistar rats were treated with 3 cycles of 2.5 mg/kg of MTX at day 0, 10, and 20 and then one treated group was euthanized on day 22 to evaluate the early MTX cardiac toxic effects, while the other group was euthanized on day 48, to allow the evaluation of MTX late cardiac effects (Rossato et al., 2014). Decreased levels of plasma total creatine kinase and creatine kinase-MB were detected in the early sacrificed animals while increased plasma levels of lactate were seen in the animals sacrificed later on. Increased cardiac relative mass and microscopic changes were evident in both treated groups, while activity of mitochondrial complexes was changed in both groups when compared to control. MTX induced an increase in the complex IV and complex V activities in early sacrificed treated group, while a decrease in the complex V activity was accompanied by the reduction in ATP content in the late-sacrificed rats (Rossato et al., 2014).

1.4.5. The role of metabolism in the mitoxantrone's toxicity

Most studies on MTX cardiotoxicity *in vitro* were performed in order to evaluate the MTX cardiotoxicity compared to DOX, instead of trying to explain the biochemical basis of cardiotoxicity that is observed in MTX. However, these studies have contributed immensely to the overall understanding of the biochemical activity and the toxicity of the drug. Metabolism is involved in MTX anticancer proprieties, however, little is known about the influence of metabolism on MTX cardiotoxicity.

The oxidoreductive metabolism of MTX has a significant role on its antitumour effects. MTX has particular effectiveness in tumours with high contents of peroxidases (Blanz et al., 1991b, Bruck and Bruck, 2011), and it was verified that the inhibitory effect of MTX on cell growth was prevented by inhibiting the activity of CYP450 mixed oxidase function in a human hepatoma-derived cell line (Duthie and Grant, 1989). Similar results were obtained with rat hepatocytes (Mewes et al., 1993) and with human breast cancer cells (Li et al., 1995) incubated with MTX. Moreover, phorbol ester-stimulated human neutrophils can bioactive MTX through myeloperoxidase metabolism and the generated metabolites can form adducts with DNA, although the chemical nature the metabolites is unknown (Panousis et al., 1997).

As stated, the role of MTX metabolism in its induced cardiotoxicity is poorly studied; however, two studies have been made that can give some hints on that subject (Shipp et al., 1993, Rossato et al., 2013a). In the work by Rossato *et al*., H9c2 cells were incubated with non-metabolized MTX or MTX after metabolization (Rossato et al., 2013a). It demonstrated that the cytotoxicity caused by MTX after metabolization was significantly higher than that observed in the H9c2 cells incubated with non-metabolized MTX. The co-incubation of MTX with CYP450 and CYP2E1 inhibitors partially prevented the cytotoxicity caused by the drug, thus highlighting that the metabolism of MTX is relevant for its undesirable effects (Rossato et al., 2013a).

The work by Shipp *et al.* demonstrates that the metabolite NAPHT has a higher potential on ATP depletion than MTX and, importantly, that the bioenergetics impairment hugely depends on iron availability (Shipp et al., 1993). Furthermore, the catechol ring of MTX and of the metabolite NAPHT seems to be relevant to the observed ATP decrease since ametantrone has no significant effect on ATP levels (Shipp et al., 1993). One can speculate by putting together all the scarce data available that MTX is not able *in vivo* to cause an initial redox cycle that is sufficient to cause an early and abrupt oxidative stress (as do the aglycones and semiquinones of DOX); however, MTX and its NAPHT metabolite rapidly accumulate in the heart (Ehninger et al., 1985, Rossato et al., 2013a) easily impairing ATP homeostasis in the heart, factors that seem to depend on iron (Shipp et al., 1993).

2.

AIMS

2. AIMS

The toxicity of anticancer drugs and particularly of MTX towards the cardiovascular system is well known. However, the mechanisms involved are largely unknown. Pharmacokinetic metabolism is involved in the cardiotoxicity of several anticancer drugs, whereas the data regarding to MTX metabolism and its relation to MTX-induced cardiotoxicity are scarce. The full understanding of the cardiotoxic effects induced by MTX and/or metabolites is important to reveal the underlying cardiac mechanisms, but also to pursue cardioprotective strategies when MTX is to be used.

The main aim of this dissertation was to clarify the underlying mechanisms by which MTX and, its metabolite NAPHT, elicit cardiotoxicity.

The following specific objectives were pursued:

- Synthesis of MTX-metabolite, NAPHT,
- Structure characterization of the obtained derivatives of MTX,
- Evaluation of the cytotoxicity caused by MTX in different time-points and concentrations,
- Evaluation of several pharmacological-active drugs towards MTX-elicited cytotoxicity in H9c2 differentiated cells,
- Evaluation of cytotoxicity caused by NAPHT in different time-points and concentrations,
- Evaluation of pharmacological-active drugs towards NAPHT-elicited cytotoxicity in H9c2 differentiated cells.

3.

MATERIALS AND METHODS

3. Materials and methods

3.1. Materials and chemicals

MTX dihydrochloride (MTX, ≥97% purity) and peroxidase, from horseradish (Type II) were purchased from Sigma-Aldrich (St. Louis, MO, USA), hydrogen peroxide (H_2O_2) 30% (Perhydrol®) and acetic acid glacial 100% were grade for analysis and were purchased from Merck (Germany), sodium acetate trihydrate for analysis was purchased from Panreac Quimica Sau (Barcelona, Spain). The solvents used were products pro analysis or high performance liquid chromatography (HPLC) grade of the firms Sigma-Aldrich, Chem-Lab NV, Merck, VWR Chemical and Panreac Quimica Sau. Purifications of compounds were performed by chromatography flash cartridge using silica gel reverse phase (RP)-18 (Grace Resolv®) and preparative thin layer chromatography (TLC) using Merck silica gel HPLC60 RP-18 (GF254) plates purchased from Merck (Germany).

The rat cardiomyocyte derived H9c2 cell line was obtained from European Collection of Cell Cultures [passage 8; H9c2 (2-1) cell line from rat (BDIX heart myoblast), from Sigma-Aldrich (St. Louis, MO, USA)]. The protein assay kit Bio-Rad RC DC was purchased to Bio-Rad Laboratories (California, USA). Sterile pipettes, 6-multiwell plates, 12-multiwell plates, 48-multiwell plates, 96-multiwell plates and 75 cm^2 flasks were obtained from Corning Costar (Corning, NY, USA). Phosphate-buffered saline (PBS) and penicillin/streptomycin 10.000 µg/mL were obtained from Biochrom (Berlin, Germany). Foetal bovine serum (FBS) was purchased to Gibco (Invitrogen, Paisley, UK). Hanks' balanced salt solution and Dulbecco's phosphate buffered saline with calcium and magnesium were purchased to Gibco (Invitrogen, Paisley, UK). Other reagents, namely, trypan blue solution (0.4%), pyruvate, potassium dihydrogen phosphate, dipotassium hydrogen phosphate, Triton X-100, Dulbecco's modified eagle medium (DMEM) – high glucose, sodium bicarbonate, dimethyl sulfoxide (DMSO), retinoic acid (RA), neutral red (NR) solution, ethanol, trypsin solution, 3-(4,5-dimethylthiazol-2-yl)-2,5-diphenyl tetrazolium bromide (MTT), hydrochloric acid, sodium dodecyl sulfate (SDS), buthionine sulphoximine, β-NADH, *N*-acetyl cysteine, Ac-Leu-Glu-Thr-Asp-al (Ac-LETD-CHO), caspase 8 and 9 inhibitor, L-carnitine, NaOH, 3-methyladenine, Hoechst 33258, paraformaldehyde, ethidium bromide, acridine orange, cycloheximide, 3,3'-dihexyloxacarbocyanine iodide (DiO^6), carbonyl cyanide 3-chlorophenylhydrazone, 1-aminobenzotriazole, 2-methyl-1,2-di-3-pyridyl-1-propanone (metyrapone), bovine serum albumin, luciferase from *Photinus pyralis* (firefly), D-luciferin sodium salt, glycine sodium salt, tris base, potassium hydrogen carbonate and ATP were obtained from Sigma-Aldrich (St. Louis, MO, USA). Ethylenediamine tetraacetic acid (EDTA), perchloric acid, and $MgSO_4$ were purchased from Merck (Germany).

3.2. Methods used in the synthesis of mitoxantrone metabolites

Melting points (mp) were obtained in a Köfler microscope and are uncorrected. Infrared (IR) spectra were measured in KBr microplate in a Fourier transform infrared spectroscopy spectrometer Nicolet iS10 from Thermo Scientific with Smart OMNI-Transmisson accessory (Software OMNIC 8.3) (cm^{-1}). ^{1}H nuclear magnetic resonance (NMR) spectra were taken in DMSO-d6 at room temperature, on Bruker Avance 300 instrument (300.13 MHz for ^{1}H). Chemical shifts are expressed in δ (ppm) values relative to tetramethylsilane as an internal reference. Coupling constants are reported in hertz (Hz). High resolution mass spectrometry (HRMS) mass spectra were measured on a APEX III mass spectrometer, recorded as Electrospray ionization mode in Centro de Apoio Científico e Tecnolóxico á Investigation (CACTI, University of Vigo, Spain).

3.3. Synthesis and purification of mitoxantrone metabolite naphthoquinoxaline

To a solution of MTX dihydrochloride (100 mg, 0.19 mmol) dissolved in 16 mL of sodium acetate buffer (pH 6), peroxidase horseradish and Perhydrol ® (1:1) were added and the solution was magnetically stirred 30 min at room temperature. The reaction was monitored by TLC [methanol (MeOH)/NH_3 0.25%]. The reaction was stopped by the addition of a diluted hydrochloride solution. After filtration (0.2 µm, Millipore), the solvent was evaporated under a stream of nitrogen.

The crude product was purified by preparative column chromatography with silica C18 (3 g), using a gradient of MeOH: aqueous solution of NH_3 1% (5:5) until 100% of MeOH basified with NH_3. The fractions eluted with MeOH: aqueous solution of NH_3 1% (5:5) were gathered and the solvent evaporated furnished a blue solid corresponding to compound naphthoquinoxaline dicarboxylic acid (NAPHTdi); the fractions eluted with MeOH: aqueous solution of NH_3 1% (7:3) were gathered and the solvent evaporated furnished a purple solid corresponding to compound NAPHT. The derivatives were further purified by the procedures described below.

Compound NAPHT was purified by solid phase extraction with a cation exchange cartridge Discovery® DSC-SCX, with a sulfonic acid moiety following the steps: condition with MeOH (5 mL), loading with a solution of NAPHTdi in MeOH: water/ formic acid 1% (5 mL); elution with MeOH (10 mL) followed by a solution of MeOH/NH_3 1% (10 mL); the basic fractions were collected and the solvent evaporated under reduced pressure to afford a

purple solid corresponding to 8,11-dihydroxy-4- (2-hydroxyethyl) -6-[[2-[(2-hydroxyethyl)-amino]- ethyl]- amino]- 1,2,3,4,7,12- hexahydronaphtho- [2,3-*f*]- quinoxaline- 7,12- dione [NAPHT, 97% purity by HPLC-diode array detector (DAD), 20 mg, 24% isolated yield]: mp 112-115ºC (MeOH); IR (KBr) υmax: see table 4. (DMSO-d6, 75.47 MHz) δ = see table 5. Anal. Calc. for $C_{22}H_{26}N_4O_6$: 442.1852, found: 442.18469. Compound NAPHTdi was purified by a C18 preparative column chromatography. Fractions eluted with MeOH: aqueous solution of NH_3 1% (7:3) were collected, reunited and the solvent evaporated to furnish a blue solid corresponding to 3-((2-((4-(2-carboxyethyl)-8,11-dihydroxy-7, 12-dioxo-1, 2, 3, 4, 7, 12- hexahydronaphtho- [2,3-*f*]-quinoxalin-6-yl)amino)ethyl) amino)propanoic acid (75% purity by HPLC-DAD, 1 mg, 1%): mp 65-70ºC (MeOH); IR (KBr) υmax: see table 4. ^{1}H NMR (DMSO-d6, 300.13 MHz) δ = see table 5. Anal. Calc. for $C_{22}H_{22}N_4O_8$: 470.1438, found: 470.17950.

3.4. High performance liquid chromatography analysis of mitoxantrone derivatives

HPLC analysis of the synthetic products was performed in a Spectrasystem P4000 Autosampler 3000, Thermo Fisher Scientific™ (USA), equipped with a DAD ultraviolet (UV) 8000, and using a C18 column (5 µm, 150 mm x 4.6 mm I.D.) from Fortis BIO Technologies (Cheshire, United Kingdom). The injected volume was 10 µL and the mobile phase was monitored at 254 nm. ChromQuest™ 5.0 software, Version 3.2.1, Thermo Fisher Scientific™ (USA) managed chromatographic data. HPLC ultrapure water was generated by a Milli-Q system (Millipore, Bedford, MA, USA). The mobile phase was degassed for 15 min in an ultrasonic bath before use. A linear gradient from 10 to 80% of eluent B within 30 min [eluent A: 0.1% aqueous solution of CF_3COOH; eluent B: 100% MeOH] was used at a constant flow rate of 0.5 mL/min. All samples were dissolved in MeOH and filtered through a hydrophilic Durapore-GV membrane of 0.45 mm pore size (Millipore) before injection. The retention factor (k) was determined as [$k= (t_R–t_0)/t_0$] and t_0 was considered to be equal to the peak of the solvent front.

3.5. Cell culture model used in the toxicological evaluation

The toxicological evaluation of MTX and of NAPHT was done *in vitro*, using H9c2 cells. The H9c2 cell line was isolated from the ventricular part of a thirteenth-day rat heart embryo and presents a myoblastic proliferative phenotype while maintained in normal 10% FBS-containing culture media (Kimes and Brandt, 1976). H9c2 is considered a valuable

model to assess *in vitro* cardiotoxicity (Kimes and Brandt, 1976), especially due to its metabolic features, which are comparable to those found in rat heart (Zordoky and El-Kadi, 2007).

3.5.1. Subculturing H9c2

H9c2 cells were maintained in the proliferative state in the presence of 10% FBS. H9c2 cell were grown in complete medium: DMEM with high glucose supplemented with 10% FBS and antibiotics (10 000 units/mL penicillin and 10 000 µg/mL streptomycin) at 37°C with 5% CO_2. Cell passaging was done by trypsinization. All experiments were carried out with cells before reaching 70–80 % confluence (Ruiz et al., 2012). The cell line was used between passage 15 and 30.

3.5.2. H9c2 cells differentiation

Differentiation into a "cardiac like" phenotype was induced with 1% FBS in culture medium supplemented with RA 10 nM (medium changed every two-days) (Pereira et al., 2011, Ruiz et al., 2012). The differentiation and decreased proliferation was assessed by contrast phase microscopy and the fluorescent nuclear dye Hoechst 33258 (Soares et al., 2013).

3.6. Cytotoxicity assays

After trypsinization, cells were placed in 48 well-plates, 12 well-plates, or 6 well-plates with the density of 24 000 cells/mL. After the 7-day differentiation protocol described, H9c2 cells were incubated with different chemicals. The first tests performed were the cytotoxicity curves of MTX and metabolite, combined with the morphological evaluation, using by phase contrast microscopy. After cell differentiation protocol, cells were incubated with MTX in concentrations that ranged from 0.01 to 5 µM and NAPHT in concentrations that ranged from 1 to 5 µM, and two time-points were selected (24 and 48h) for the cytotoxicity tests. The cytotoxicity tests used were: LDH leakage assay, the MTT assay and the NR uptake assay (Soares et al., 2013).

3.6.1. Morphological evaluation

3.6.1.1. Contrast phase microscopy

Cell cultures were assessed morphologically by phase contrast microscopy at the selected time-points in 6 or 12 well-plates. Cells were examined in a Nikon Eclipse TS100 equipped with a Nikon DS-Fi1 camera (Japan).

3.6.1.2. Hoescht nuclear staining

For Hoechst staining, H9c2 cells were seeded in 48 well-plates with 24 000 cells/mL and differentiated or not for 7 days. After reaching the end-point, cells were fixed in 4% paraformaldehyde (10 min, 4ºC) and washed with PBS (three times). Cells were then stained with the nuclear dye Hoechst 33258 for 10 min at 37°C (protected from light), after which they were washed with PBS (three times) at room temperature. Cells were examined in Nikon Eclipse TS100 equipped with a Nikon DS-Fi1 camera using a fluorescent filter ($\lambda_{excitation\ maximum}$ = 346 nm and $\lambda_{emission\ maximum}$ = 460 nm) (Soares et al., 2013).

3.6.1.3. Ethidium bromide and acridine orange staining

The fluorescent DNA-intercalating dyes ethidium bromide and acridine orange are suitable to distinguish live from dead cells. Also, the ethidium bromide and acridine orange staining allows the microscopic morphological discrimination between necrotic and apoptotic cell death and acridine largely accumulates in acidic vesicles. Ethidium homodimers do not penetrate intact cellular membranes. Therefore, ethidium bromide only intercalates with nucleic acids if the outer cellular membrane has disintegrated. In contrast, the fluorescent cationic dye acridine orange diffuses through intact membranes of live cells. When bound to DNA, it reaches an emission maximum at 525 nm (Capela et al., 2013). The staining of H9c2 was done after removing all the growth medium of the 48-wells after the incubation period with MTX or NAPHT. To the cells were added 200 µL of heated PBS with Ca^{2+}e Mg^{2+}, and then 8 µL of the stock solution ethidium bromide and acridine orange solution (0.5 mg/mL). A 5 min incubation in the dark was followed. After removing the ethidium bromide and acridine orange, cells were washed with warm PBS with Ca^{2+}e Mg^{2+} (200 µL/ well) and then new medium was added. Cells were examined in Nikon Eclipse TS100 equipped with a Nikon DS-Fi1 camera, using a standard fluorescein filter ($\lambda_{excitation}$ = 485 nm and $\lambda_{emission}$ = 525 nm).

3.7. Cytotoxicity tests

3.7.1. Lactate dehydrogenase kinetic leakage assay

H9c2 cells were seeded in 48-well plates. For MTX and NAPHT evaluation of induced cell death, cells were incubated for 24 or 48h with different drug concentrations. After cell treatment, cell death was evaluated as the measurement of membrane integrity seen by the percentage of LDH release over the total LDH. For experiments with caspase 8 and 9 inhibitor, Ac-LETD-CHO (200 µM and 100 µM) (Shi and Shen, 2008), the antioxidant N-acetyl cysteine, a glutathione precursor and reactive species scavenger (1 mM) (Martins

et al., 2013, Rossato et al., 2013b), the buthionine sulphoximine, an inhibitor of gamma-glutamylcysteine synthetase (50 µM) (Ferreira et al., 2013), L-carnitine, a mitochondrial enhancer (2mg/mL) (Rossato et al., 2013b), 3-methyladenine, an autophagy inhibitor (2.5 mM) (Soares et al., 2014), 1-aminobenzotriazole, a suicide substrate for CYP450 (0.5 mM) (Shi et al., 2011a), the addition of these compounds was done 1h prior to the addition of MTX 2 µM. In the case of NAPHT 2 µM incubation with N-acetyl cysteine (1 mM), this later molecule was added 1h prior to the addition of NAPHT.

The quantification of LDH activity was made using a colorimetric method, based on the reversible reduction of pyruvate to lactate (last step of anaerobic glycolysis) in the presence of β-NADH, as described below (Capela et al., 2006).

3.7.1.1. Extracellular lactate dehydrogenase activity

LDH can be found outside the cell only when there is cell death (apoptotic or necrotic type) or lysis of cytoplasmatic membrane. The extracellular activity of LDH was determined after the suitable amount of medium was added to β-NADH 0.15 mg/mL solution at room temperature, in 96-microplate wells. Finally, pyruvate 22.7 mM was added to start the reaction. NADH oxidation to NAD^+ was measured at 340 nm for 4 and a half min, using a 96-well plate reader (BioTek Instruments, Powerwave X, USA). The slope of the curve obtained was used for the calculation of the % LDH leakage (Capela et al., 2006).

3.7.1.2. Total lactate dehydrogenase activity

Total LDH activity was determined after adding 20 µL of Triton X-100 5% to each well and incubated at 37°C for 30 min. The cells were totally lysed by this procedure and then the activity of the LDH obtained was evaluated as described previously. Medium was added to 0.15mg/mL β-NADH solution at room temperature, in a 96-well microplate. Finally, pyruvate 22.7mM was added to start the reaction as described in the previous section (Capela et al., 2006). Cell death was quantified as a measurement of membrane integrity and evaluated by the percentage of LDH released over total LDH.

3.7.2. MTT reduction assay

The MTT assay was first done to evaluate the cytotoxicity of MTX and NAPHT in differentiated H9c2 cells. This colorimetric assay relies mostly on the ability of mitochondrial complexes (or other dehydrogenases) to convert the soluble yellow tetrazolium dye, MTT, into an insoluble blue formazan product that can be measured at 550 nm (Costa et al., 2009, Soares et al., 2013). After the removal of culture medium, to each well was added 200 µL of fresh medium (DMEM 1% FBS and 10 nM RA) and 20 µL of the MTT solution (final

concentration of MTT 500 µg/mL). Subsequently, cells were incubated at 37ºC for 4h. The reaction was stopped by adding 200 µL of 10% SDS in 0.01 M hydrochloric acid solution followed by an overnight incubation at 37ºC, to allow solubilization of the formed formazans. Finally, the formed formazans were measured at 550 nm using a 96-well plate reader (Capela et al., 2006). The percentage of MTT reduction of control/vehicle cells was set to 100%, and the effects resulting from the incubation with MTX or metabolite were expressed as the percentage to the respective controls or vehicle.

The MTT test was also done to evaluate the effects of cycloheximide, a glutarimide antibiotic (10 µg/mL) (Gupta et al., 2006), and metyrapone, CYP450 inhibitor (0.5 mM) (Rossato et al., 2013b), towards MTX cytotoxicity. Cycloheximide and metyrapone were added 1h before MTX.

3.7.3. Neutral Red lysossomal uptake assay

For this assay, H9c2 cells were seeded in 48-well plates. The amount of NR dye incorporated in the cells represents lysossomal functionality, as this dye easily penetrates viable cell membranes and accumulates intracellularly in lysosomes (Soares et al., 2013). At the end of the incubation time, the cellular medium was removed and 250 µL/well of NR solution (33 mg/mL of NR in DMEM 1% FBS) was added. Then, plates were incubated for 3h at 37ºC, protected from light. After this time, NR solution was removed and 200 µL/well of the solution formed by 50% ethanol/1% acetic acid was added to extract the NR dye meanwhile captured within the cells. The plates were then placed in a microplate shaker for 15 min, at room temperature and protected from light. Absorbance was measured at 540 nm, in a 48-well plate reader [Biotech Synergy HT (VT, USA)] and results were compared to control/ vehicle wells whose media of values was set to 100% (Soares et al., 2013).

The NR test was done to access the effects of 3-methyladenine (2.5 mM), 1-aminobenzotriazole (0.5 mM) and metyrapone (0.5 mM) following the exposure to MTX (and also 3-methyladenine in the case of NAPHT) in H9c2 differentiated cells. Those compounds were added 1h before MTX (or NAPHT).

3.8. Evaluation of mitochondrial potential

The evaluation of the mitochondrial potential was done according to Freitas *et al*., with some modifications (Freitas et al., 2013). Briefly, 7-days differentiated cells were incubated for 12h with MTX or NAPHT and then cells were incubated for 30 min at 37ºC with DiO^6 at the final concentration of 50 µM *per* well. In each condition and experiment, a well was placed with DiO^6 and the mitochondrial uncoupling agent, carbonyl cyanide 3-chloro-phenylhydrazone, at the final concentration 20 µM. Also, a well in each condition was

tested without any DiO[6] as to evaluate if any component of the medium or if MTX or NAPHT conditions had any residual fluorescence that interfered with the fluorescence readings. After the 30 min incubation time, the cells were then washed 2 times with warmed PBS with Ca^{2+}e Mg^{2+}. Photographs were taken in a fluorescent microscope (Nikon Eclipse TS100 equipped with a Nikon DS-Fi1 camera) with the standard fluorescein filter ($\lambda_{excitation}$ = 485 nm and $\lambda_{emission}$ = 520 nm).

3.9. Determination of cellular ATP levels

For this assay, H9c2 cells were seeded in 6-well plates. The ATP was evaluated in differentiated H9c2 cells incubated for 24h with 2 and 5 μM of MTX, and 2 and 5 μM NAPHT. After the incubation period, medium was discarded and cells were washed with cold PBS with Ca^{2+}e Mg^{2+} (750 μL/well). The PBS used for washing was discarded. Another 750 μL/well cold PBS with Ca^{2+}e Mg^{2+} was added and cells were scrapped. Two wells *per* each condition were collected and centrifuged at 5 000 rpm, 4°C, for 10 min. The supernatant was rejected and to the pellet was added 200 μL of cold 5% perchloric acid. Then, the obtained samples were vortexed and centrifuged at 13 000 rpm, for 10 min, at 4°C. The acidic supernatant was collected for ATP determination and placed at -80°C. The pellet was used for protein determination and stored at -20°C.

The ATP levels were determined by bioluminescence through the reaction with the firefly luciferin-luciferase system (Costa et al., 2007). D-Luciferin 90.9 mg/L stock reagent and luciferase from *Photinus pyralis* (firefly) (3 000 000 U/mL final concentration) were prepared in luciferin-luciferase buffer (50 mM glycine, 10 mM $MgSO_4$, 1 mM Tris, 0.55 mM EDTA, 0.1% bovine serum albumin, pH = 7.6) and light protected aliquots were stored at -20ºC until use. Before the assay, luciferin-luciferase reaction system was constituted by adding the two solutions and then kept at room temperature. Briefly, the assay consisted of neutralizing 150 μL of the acidic samples, standards or blank with 150 μL of 0.76 M of $KHCO_3$, followed by vortex, and centrifugation for 10 min at 13 000 rpm (4ºC). One hundred μL of neutralized supernatants was added to a 96-well white microtiter plate, followed by addition of 100 μL/well of the luciferin-luciferase reagent. The reading was immediately done in the plate reader [Biotech Synergy HT (VT, USA)]. Light output was given as the integral relative light units. The assay was made sequentially with few measurements in each reading in order to avoid loss of the bioluminescence signal (Costa et al., 2007). The levels of ATP were expressed as ATP levels *per* amount of protein.

3.10. Protein determination

The protein content assay was determined using the protein assay kit Bio-Rad RC DC, according to the manufacturer's instructions. Bovine serum albumin was used as protein standard and the calibration curve varied from 200 µg/mL to 1 200 µg/mL in 0.3 M NaOH. Five µL of samples, standards or blank was added in duplicated to a 96-well microtiter plate, followed by addition of 25 µL of Reagent A and 200 µL of Reagent B, light protected. The microtiter plate was kept protected from the light for 15 min, after which the absorbance was measured at 750 nm [BioTek Instruments, Powerwave X, (VT, USA)].

3.11. Statistical analysis

The data is presented as means ± standard deviation (SD) of different independent experiments. Statistical analysis was carried out by the non-parametric Anova (Kruskal-Wallis test) followed by a Dunn's *post hoc* test once a significant *p* was achieved. When the distribution was normal, one-way Anova was performed followed by Tukey's *post hoc* test. Statistical significance was considered with a *p* values < 0.05. All statistical analysis were assessed using the GraphPad Prism 6 software program (San Diego, CA, USA).

4.

RESULTS

4. Results

4.1. Synthesis of the mitoxantrone metabolite naphthoquinoxaline

The synthesis of the MTX metabolites was accomplished through the horseradish peroxidase (HRP)-catalysed H_2O_2 oxidation of MTX and the products isolated from this reaction are depicted in Figure 10.

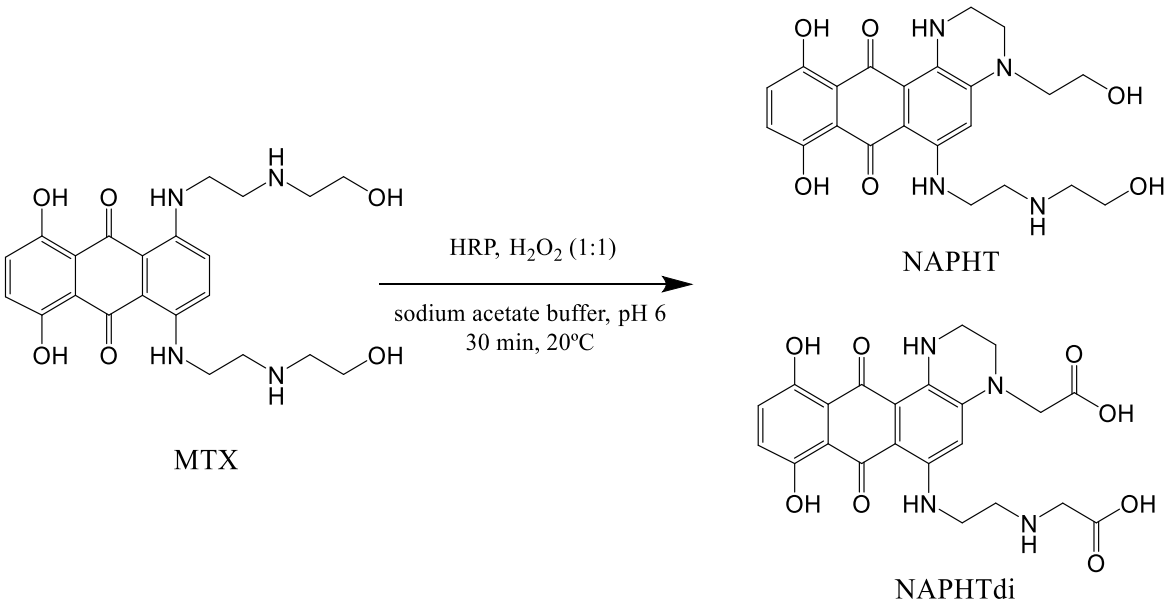

Figure 10. The isolated products of the incubation of MTX with HRP: NAPHT and NAPHTdi.

Although with the enzymatic oxidation of MTX, several derivatives could be observed by chromatographic analysis, only two purified derivatives were isolated and identified as NAPHT, corresponding to 8, 11-dihydroxy-4-(2-hydroxyethyl)-6-[[2-[(2-hydroxyethyl)-amino]ethyl]-amino]-1,2,3,4,7,12-hexahydronaphtho-[2,3-*f*]-quinoxaline-7,12-dione, and NAPHTdi, corresponding to 3-((2-((4-(2-carboxyethyl)-8,11-dihydroxy-7,12-dioxo-1,2,3,4,7,12-hexahydronaphtho-[2,3-f]-quinoxalin-6-yl)amino)ethyl)amino) propanoic acid, already proposed as a product of the peroxidase-catalyzed H_2O_2 oxidation of MTX by Bruck and colleagues (Bruck and Bruck, 2011). First attempts to purify the crude product using normal-phase chromatography were unsuccessful due to the retention of MTX derivatives in the stationary phase. Thus, procedures involving reverse-phase (for both) and/or ion exchange chromatography (for NAPHT) that have shown great versatility and capability for retaining and separating a variety of charged polar compounds, were used in the isolation of derivatives NAPHT and NAPHTdi (see Methods section).

The purity for the precursor MTX and of the isolated products NAPHT and NAPHTdi were determined by diode-array analysis performed in a HPLC-DAD (Figure 11) and were of 98%, 97%, and 75%, respectively.

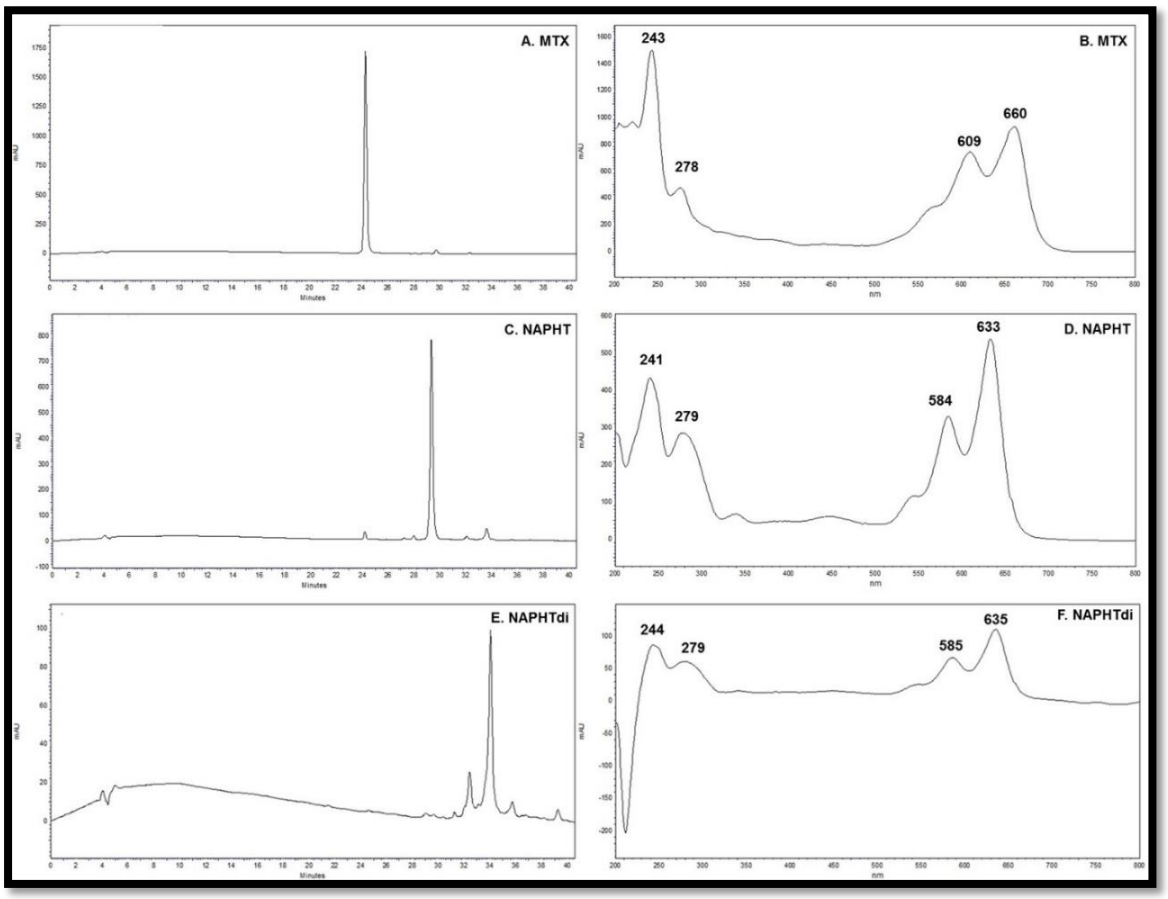

Figure 11. Representative HPLC chromatograms (left) [λ= 254 nm, C18, linear gradient from 10 to 80% of eluent B within 30 min (eluent A: 0.1% aqueous solution of CF_3COOH; eluent B: 100% MeOH)] and UV spectra (right) of MTX and isolated products NAPHT and NAPHTdi.

MTX and the derivatives NAPHT and NAPHTdi showed similar spectral features between 200 and 300 nm, but slight differences were observed in the visible range (Figure 11, left column). MTX shows absorbance maxima at 610 and 660 nm as previously reported (Bruck and Harvey, 2003); NAPHT revealed absorbance maxima at 584, 633 nm and a shoulder at 550 nm, which was previously described for this two-electron oxidized metabolite (Kolodziejczyk et al., 1988, Reszka and Chignell, 1996). For NAPHTdi a similar profile to NAPHT spectrum was observed but with reduced intensity.

The crude product from the peroxidase oxidation of MTX was also analysed by HPLC-DAD to determine the yields of the isolated derivatives NAPHT and NAPHTdi. A representative chromatogram is shown in Figure 12.

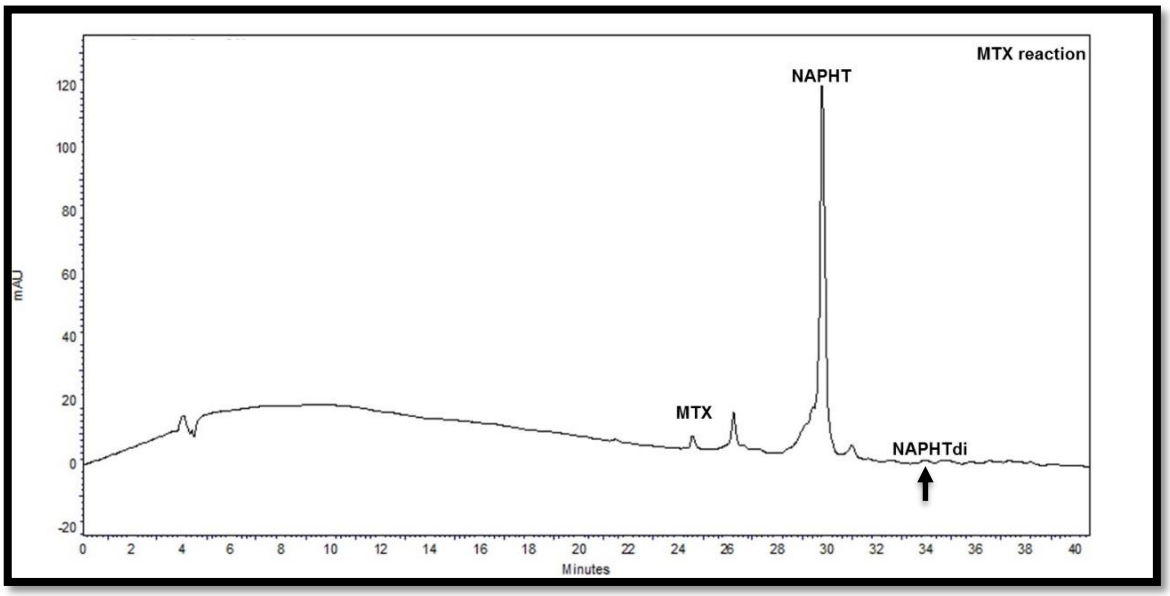

Figure 12. Representative HPLC chromatogram [λ= 244 nm, C18, linear gradient from 10 to 80% of eluent B within 30 min (eluent A: 0.1% aqueous solution of CF_3COOH; eluent B: 100% MeOH)] of 6.63 mg/mL solution of the crude product. MTX (k = 5.1), NAPHT (k = 6.3), NAPHTdi (k = 7.5).

Analysis of the reaction mixture by HPLC (Figure 12) indicated that the majority of MTX reacted after 30 min. The calculated HPLC yields for the products NAPHT and NAPHTdi (considering their areas as MTX) were 85% and 1.2%, respectively. The precursor MTX at that time point represented 2% of the total molecules.

4.2. Structure determination of naphthoquinoxaline and naphthoquinoxaline dicarboxylic acid

The structure elucidation of NAPHT and NAPHTdi was established by HRMS, IR, and by NMR techniques. The HRMS-ESI gave for NAPHT the accurate molecular mass of 442.18469 and the molecular formula $C_{22}H_{26}N_4O_6$ and for NAPHTdi the accurate molecular mass of 470.17950 and the molecular formula $C_{22}H_{22}N_4O_8$. These data allowed to suggest that the isolated compounds NAPHT and NAPHTdi, corresponded to 8,11-dihydroxy-4-(2-hydroxyethyl)-6-[[2-[(2-hydroxyethyl)-amino]-ethyl]-amino]-1,2,3,4,7,12-hexahydronaphtho-[2,3-*f*]-quinoxaline-7,12-dione and 3-((2-((4-(2-carboxyethyl)-8,11-dihydroxy-7,12-dioxo-1,2,3,4,7,12-hexahydronaphtho-[2,3-*f*]-quinoxalin-6-yl)amino)ethyl)amino) propanoic acid,

respectively. The IR data of MTX, NAPHT, and NAPHTdi are presented in Table 4 and Figures 13, 14, and 15, respectively.

Table 4. IR data for compounds MTX, NAPHT, and NAPHTdi.

Compound	Group	ν (cm^{-1})
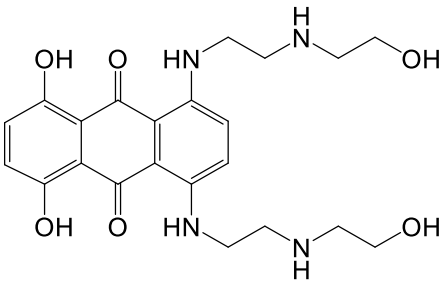 **MTX**	OH	3412, 3401
	N-H	3073, 3093
	C-H	2952, 2921, 2847, 2779
	N-H	1632
	C=O	1605, 1563
	C=C (Ar)	1546, 1528, 1510
	C-H	1486, 1450, 1392
	C-N, C-O	1208, 1222
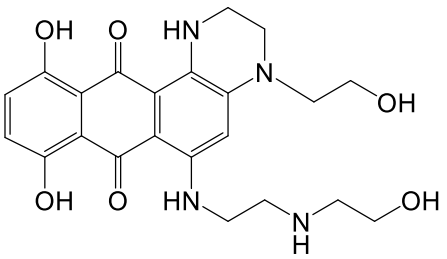 **NAPHT**	OH	3443
	C-H	2925
	N-H	1631
	C=O	1602
	C=C (Ar)	1560, 1541
	C-H	1458, 1385
	C-N, C-O	1340, 1248
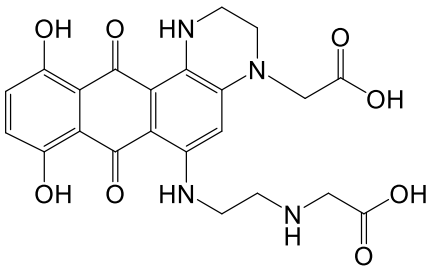 **NAPHTdi**	OH	3424
	C-H	2922, 2852
	N-H	1644
	C=O	1633, 1602
	C=C (Ar)	1567, 1501
	C-H	1384, 1340
	C-N, C-O	1247, 1213

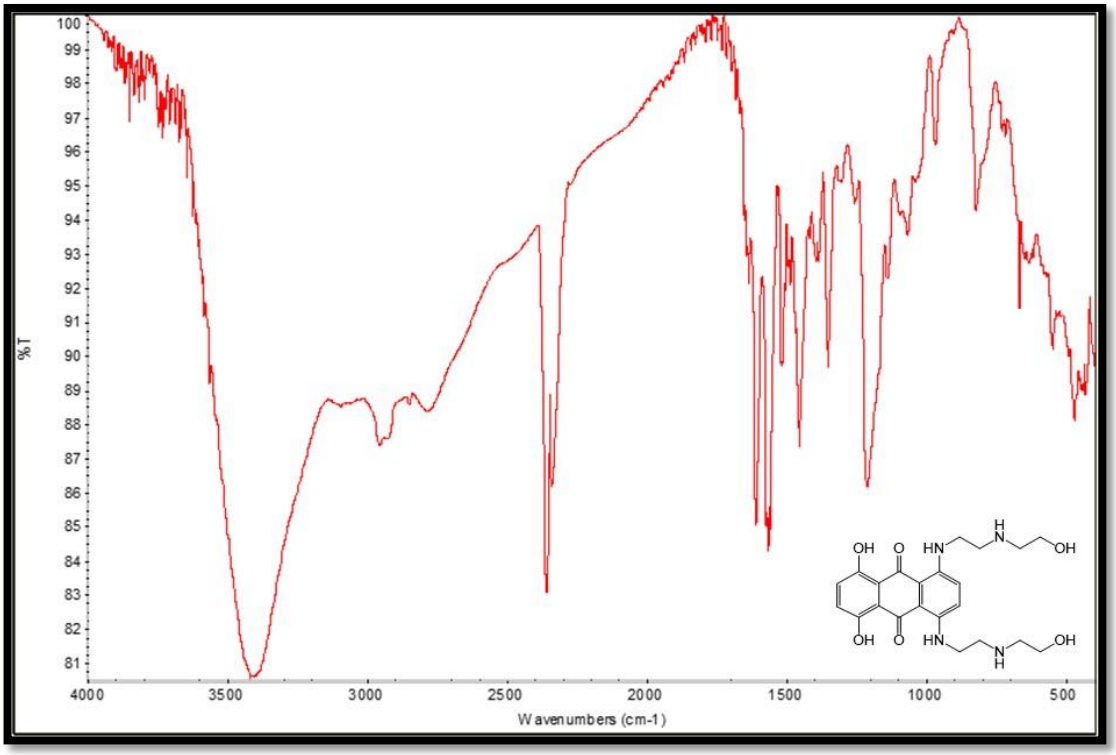

Figure 13. IR spectra of MTX.

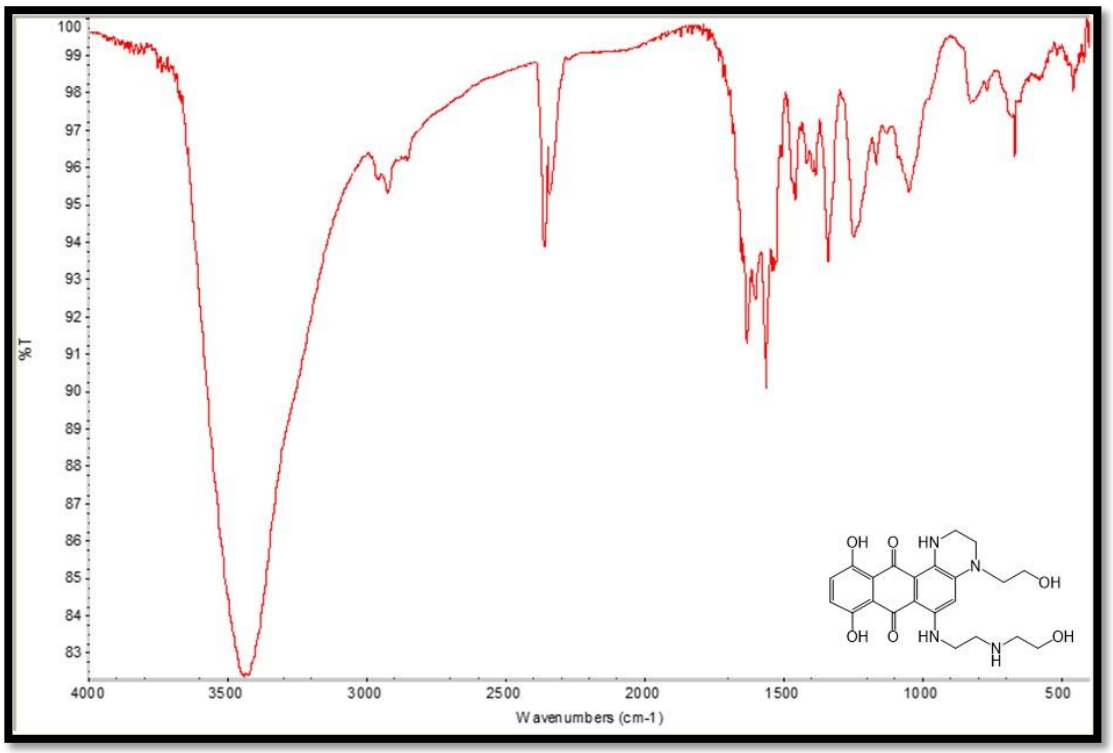

Figure 14. IR spectra of NAPHT.

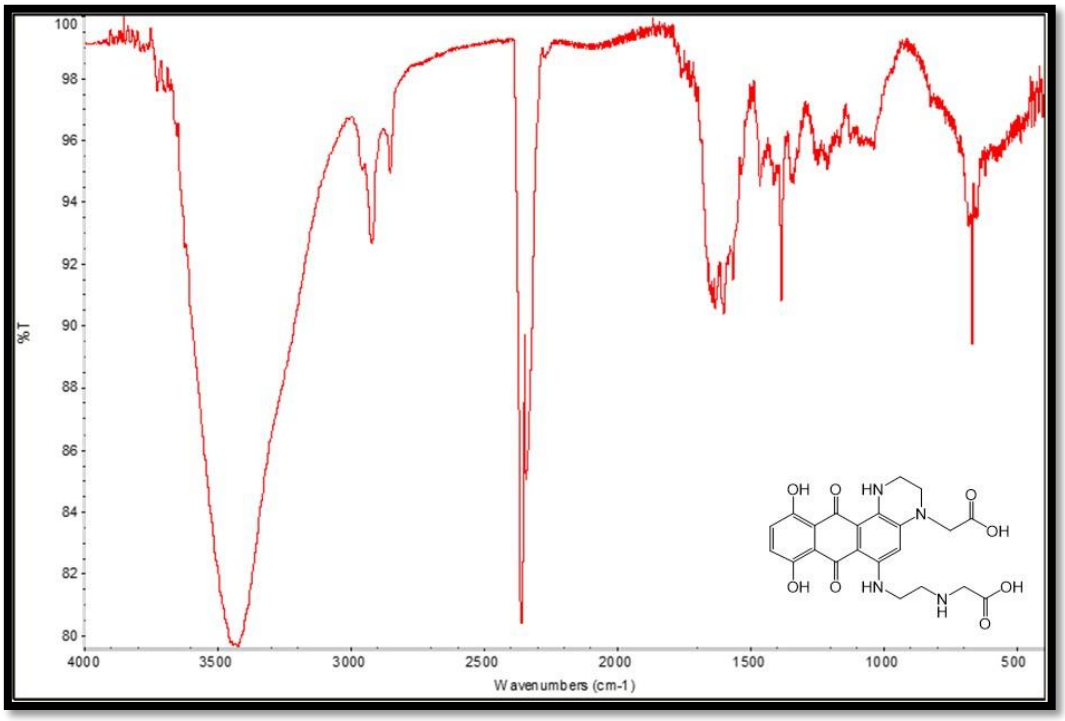

Figure 15. IR spectra of NAPHTdi.

The IR data of MTX and their derivatives NAPHT and NAPHTdi were similar and although indicated the presence of derivatives of MTX for NAPHT and NAPHTdi, spectra were not suggestive of the transformations occurred.

The ^{1}H NMR data of MTX, NAPHT, and NAPHTdi are presented in Table 5 and Figures 16, 17, and 18, respectively.

Table 5. ^{1}H NMR data¥ of MTX, NAPHT, and NAPHTdi.

δ_H					
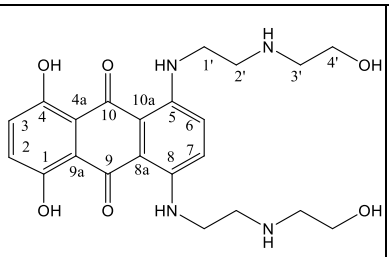 **MTX**		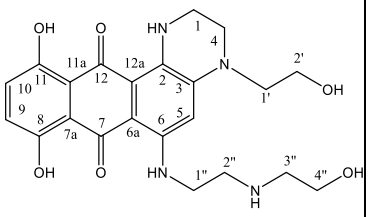 **NAPHT**		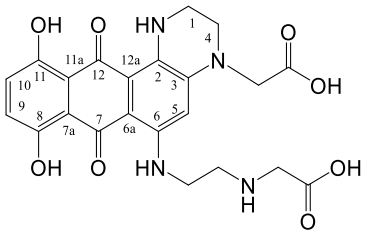 **NAPHTdi**	
1-OH	13.44,*s*, 2H	8-OH	14.36,*s*, 1H	8-OH	14.26, *s* ,1H
4-OH		11-OH	13.56,*s*, 1H	11-OH	13.55, *s*, 1H
5-NH	10.41, *brs*, 2H	2-NH	10.95, *s*, 1H	2-NH	10.91, *s*, 1H
8-NH		6-NH	11.34, *s*, 1H	6-NH	11.33, *s*, 1H
H-2	7.65, *s*, 2H	H-9	7.00 – 6.97, 2H	H-9	7.03 – 7.01, m, 2H
H-3		H-10		H-10	
H-6	7.19, *s*, 2H	H-5	6.19, *s*, 1H	H-5	6.23, *s*, 1H
H-7					
4'-OH	5.34, *brs*, 2H	4''-OH	4.96, *s*, 1H	4''-OH	4.90-4.83, m, 1H
4''-OH	5.34, *brs*, 2H	2'-OH	4.66, *s*, 1H	2'-OH	4.14-4.13, m, 1H
H-1'	3.89-3.87, *m*, 2H	H-1''	3.72, *m* (under H_2O)	H-1''	3.38, *m* (under H_2O)
H-1''		H-1		H-1	
H-2'	3.69-3.66, *m*, 4H	H-2''	3.63, *m* (under H_2O)	H-2''	3.18, *m*, (under H_2O)
H-2''		H-4		H-4	
H-3'		H-3''	2.89, *t*, 4H	H-3''	3.16, *m*, 4H
H-3''		H-1'		H-1'	
H-4'	3.07-3.05, *m*, 2H	H-2'	2.69, *t*, 4H	H-2'	
H-4''		H-4''		H-4''	

¥ Values in ppm (δH) relative to Me4Si as an internal reference. J values are in Hz. [singlet (*s*); triplet (*t*), multiplet (*m*)].

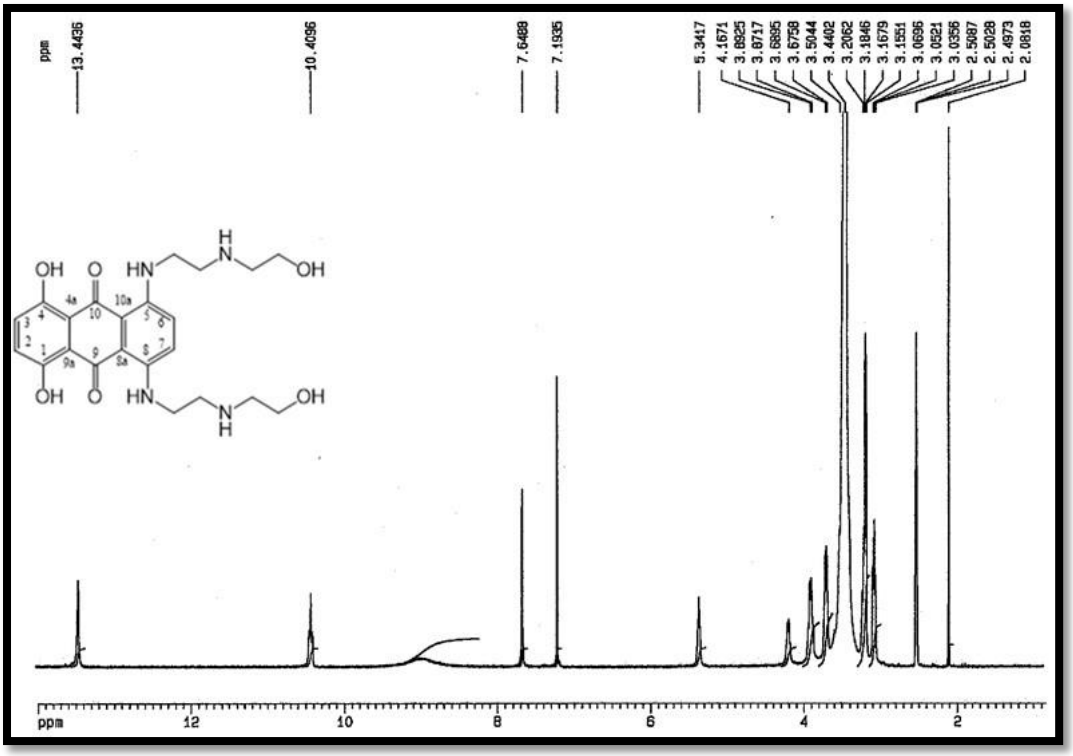

Figure 16. ^{1}H NMR spectra of MTX.

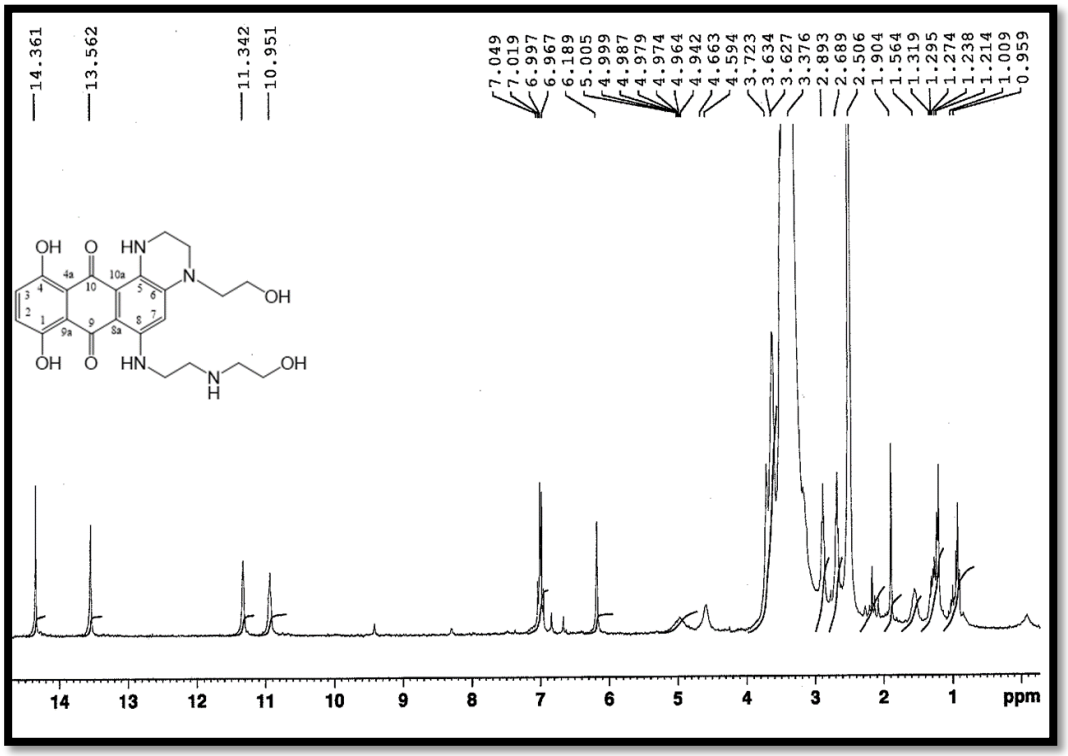

Figure 17. ^{1}H NMR spectra of NAPHT.

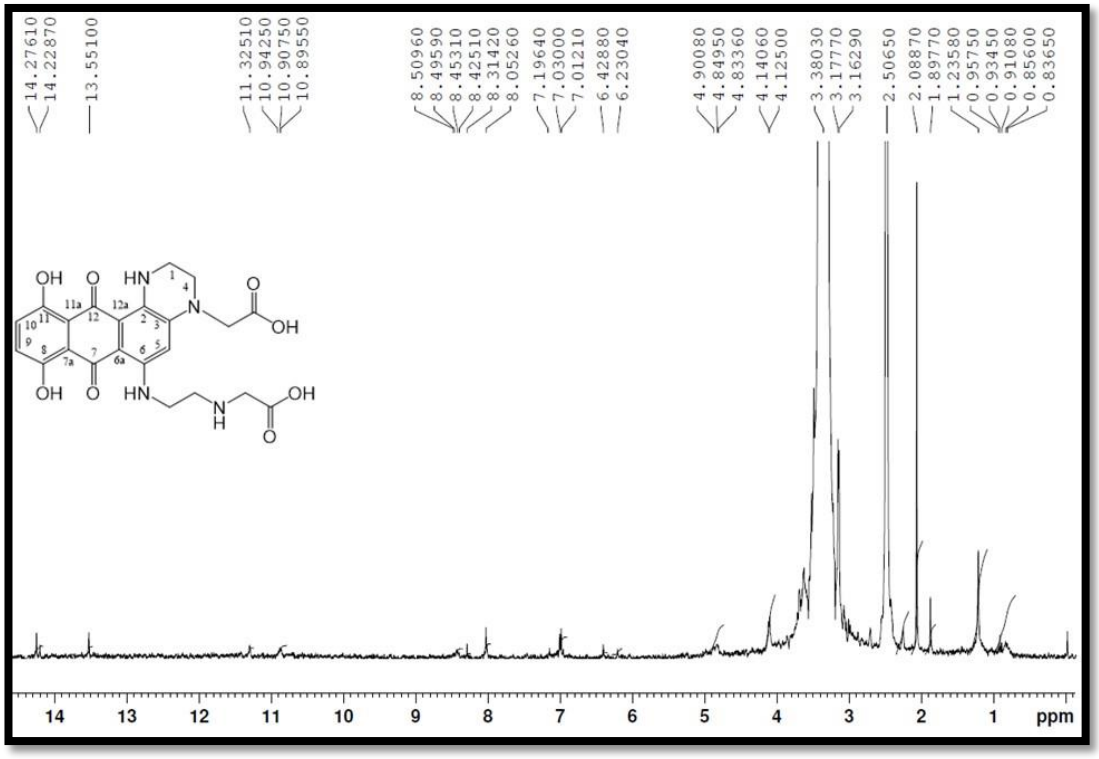

Figure 18. ^{1}H NMR spectra of NAPHTdi.

The multiplicity and coupling constants of the protons observed in the ^{1}H NMR spectrum of MTX showed the existence of two symmetrical 1, 4-disubstituted benzene rings, the signals of the protons of the hydroxyl and amine groups and of the aliphatic chain.

In turn, the ^{1}H NMR spectrum of NAPHT showed a different pattern of substitution in the aromatic ring while the proton signals of methylene groups, characteristic of the aliphatic chains, were maintained. The fusion of the piperazine ring with C-5/C-6 of the aromatic ring of the anthraquinone is evidenced by the lack of H-6 signal and the presence of a singlet corresponding to H-7 and of two aromatic protons, corresponding to H-2 and H-3. The proposed structure was in agreement with the result obtained from the HRMS.

The amount of NAPHTdi isolated allowed obtaining the ^{1}H spectrum, which revealed a similar pattern of substitution in the aromatic ring when compared to NAPHT while signals of deshielded protons were observed at 4.1 and 3.1 ppm for the methylene groups characteristic of the aliphatic chains for the proposed structure of NAPHTdi. The proposed structure was in agreement with the result obtained from the HRMS.

4.3. Differentiation alters cell division and microscopic characteristics of H9c2

The differentiation protocol was conducted with 1% FBS and RA for 7 days. The differentiation by 10 nM RA and 1% FBS by 7 days led to morphological changes making cells more resembled to the cardiac phenotype. There were substantial differences between undifferentiated cells and differentiated cells, which are illustrated in Figure 19. At panel 19B and D, two detailed Figures of both differentiated and undifferentiated H9c2 cells cultivated for 7 days in multi-well plates are presented. The differentiation protocol dramatically reduced cell division. In fact, cellular density was substantially higher in undifferentiated cells cultivated for 7 days with 10% FBS medium without RA. Also, while inhibition of cell division occurred, the cell bodies of differentiated cells became smaller and fusiform when compared to undifferentiated cells, which exhibit a large and flat cell body. Overall, differentiated cells showed to established a more organized network bearing a more cardiac-like morphology, as shown by phase-contrast morphology. The differentiation also resulted in a lower proliferation rate as verified by Hoechst 33258 staining.

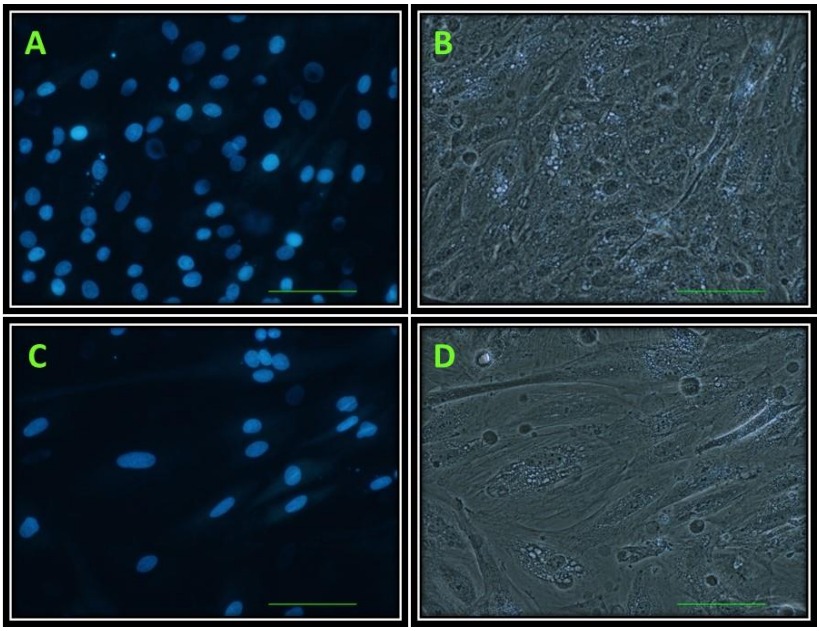

Figure 19. Fluorescence microscopy (Hoechst 33258 staining, A and C) and phase contrast microscopy images (B and D) of undifferentiated (A and B) and differentiated (C and D) H9c2 cells for 7 days. Images are representative of three independent experiments (scale bar 100 µm).

4.4. Toxicological evaluation of mitoxantrone

4.4.1. Microscopic evaluation of mitoxantrone-incubated H9c2 cells

Cells were morphologically assessed after 24h exposure to MTX. H9c2 cells were incubated with MTX (2 and 5 µM), as described in the Methods section. Phase-contrast microscopy and Hoescht staining were used. Phase-contrast microscopy, after 24h

incubation, revealed cell death, with intensifying features of cell death when increasing concentrations (Figure 20). In particular, H9c2 cell exposed with 5 μM of MTX showed signs of loss of membrane integrity and decrease in cell number (Figure 20C and 20F). No signs of nuclear alteration were found by Hoescht staining. At 48h, the cell injury was more increased in MTX-incubated cells (data not shown).

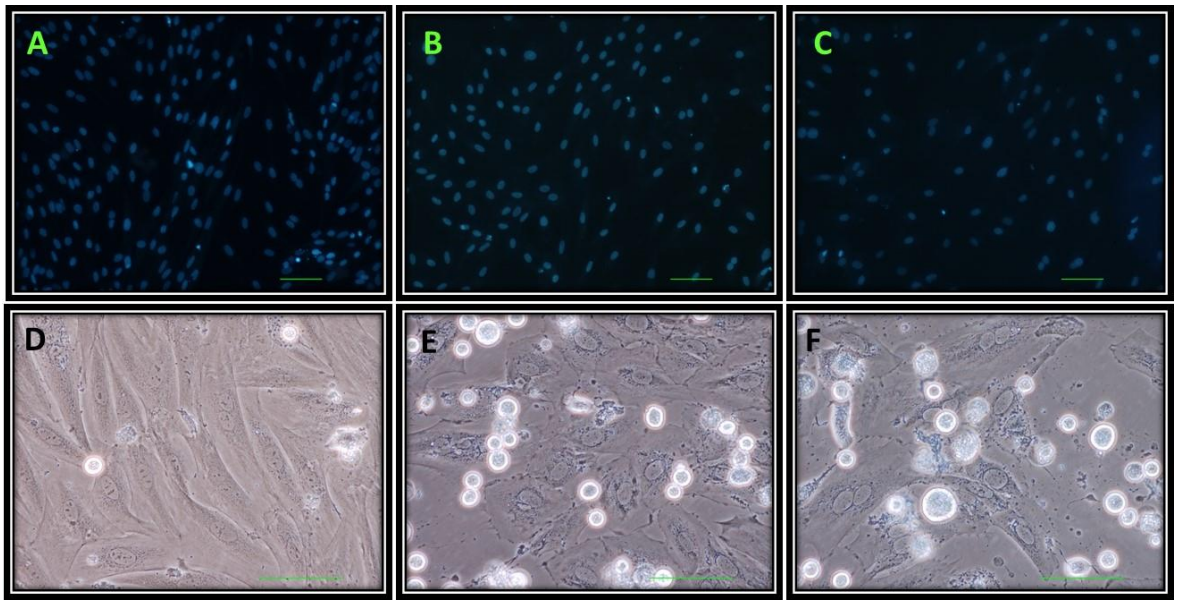

Figure 20. Fluorescence microscopy (Hoechst 33258 staining) (A, B, C), phase contrast microscopy (D, E, F) images of differentiated H9c2 cells after incubation with 2 and 5 μM of MTX for 24h. Control (A and D), MTX 2 μM (B and E), MTX 5 μM (C and F). Images are representative of three independent experiments (scale bar 100 μm).

Ethidium bromide/ acridine orange staining was also used for evaluate MTX effects on H9c2 cells. Through this method, living cells appear with a regular-sized green fluorescent nucleus, as shown in control H9c2 in Figure 21A. The number of cells largely decreased with increased MTX concentration, but cells present in the field remained with green nucleus, although with cytoplasmatic injury (Figure 21C).

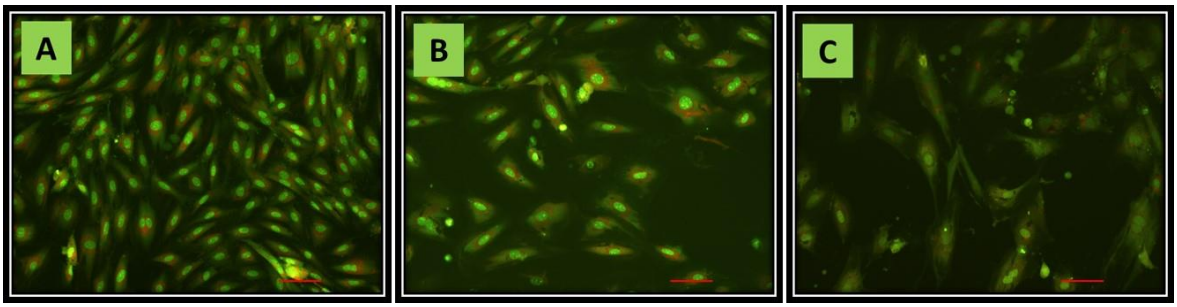

Figure 21. Ethidium bromide and acridine orange (A, B, C) images of differentiated H9c2 cells in control and in cells incubated with 2 and 5 µM of MTX for 24h. Control (A), MTX 2 µM (B), MTX 5 µM (C). Images are representative of three independent experiments (scale bar 100 µm).

Assessment of mitochondrial membrane potential in differentiated H9c2 cells incubated with 2 µM of MTX (B) and 5 µM of MTX (C) for 12h (Figure 22) was done. Lower levels of fluorescence resulting from MTX treatment were observed, suggesting the depolarization of mitochondrial membrane potential at 12h. This depolarization effect seems dose dependent (Figure 22C).

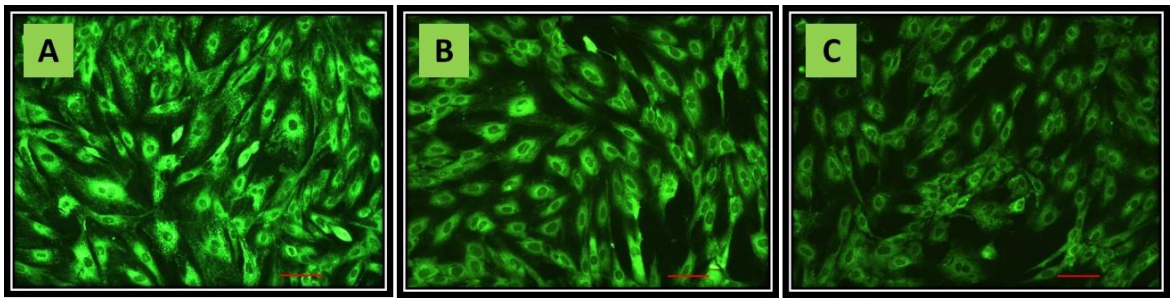

Figure 22. Mitochondrial transmembrane potential (A, B, C) images of differentiated H9c2 cells after incubation with 2 and 5 µM of MTX for 12h. Control (A), MTX 2 µM (B), MTX 5 µM (C). Images are representative of three independent experiments (scale bar 100 µm).

4.4.2. Mitoxantrone led to a time- and concentration-dependent mitochondrial dysfunction

The ability of MTX to interfere with MTT reduction was evaluated at 2 time-points (24 and 48h) and with several concentrations (0.01 to 5 µM). At 24h (Figure 23A), MTX at concentration 0.1 µM already caused significant cytotoxicity when compared to control cells, being the highest dose tested (5 µM) able to decrease the levels of MTT reduction to 85.99 ± 8.52%. At 48h, as can be seen in Figure 23B, the cytotoxicity elicited was even higher, when compared to control and the same concentrations in the earlier time point.

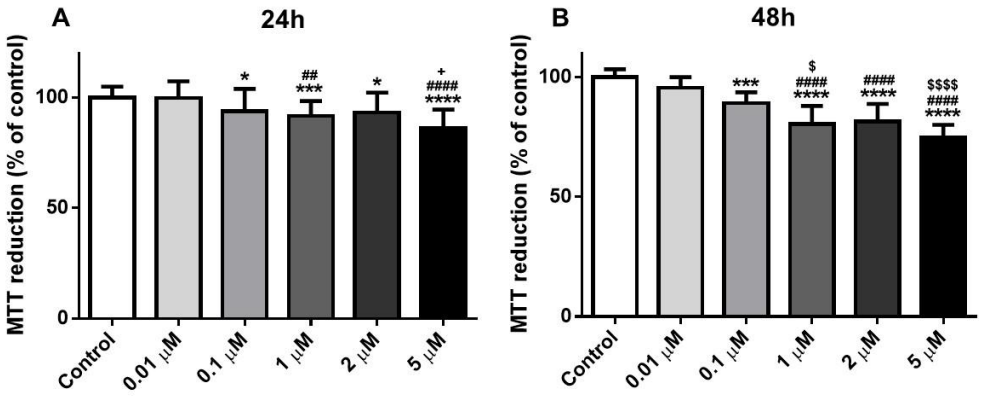

Figure 23. Mitochondrial dysfunction evaluated by MTT reduction assay in differentiated H9c2 cells incubated with 0.01, 0.1, 1, 2 and 5 μM of MTX for 24 (A) and 48h (B). Results are presented as mean ± SD of 5 independent experiments (total of 30 wells). Statistical analysis were performed using Kruskal–Wallis test, followed by the Dunn's *post hoc* test (*p < 0.05, ***p < 0.001, ****p < 0.0001 vs. control; ##p < 0.01, ####p < 0.0001 vs. 0.01 μM; $p < 0.05, $$$$p < 0.0001 vs. 0.1 μM; +p < 0.05 vs. 2 μM).

4.4.3. Mitoxantrone was only able to cause significant loss of membrane integrity at the highest concentrations tested

The ability of MTX to cause LDH leakage to the extracellular medium was tested at 2 time-points (24 and 48h) and with several concentrations (0.01 to 5 μM). At 24h (Figure 24A), only the higher concentrations of MTX (1, 2 and 5 μM) caused significant cellular membrane integrity loss when compared to control cells. In Figure 24B, the data obtained after the 48h incubation of H9c2 differentiated cells is observed. MTX, at 48h, caused a significant decrease in cellular toxicity, being observed that at 1 μM MTX the viability was 64.08 ± 8.26%, 2 μM MTX the viability was 43.47 ± 7.49% and at 5 μM the viability was 27.98 ± 9.92%.

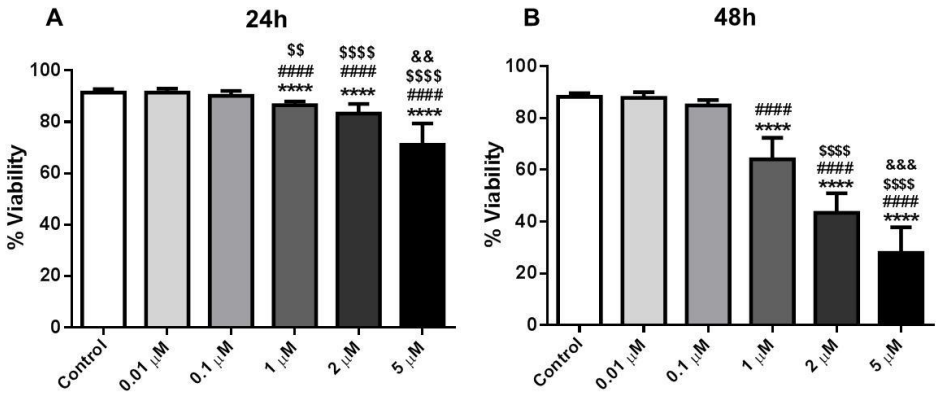

Figure 24. Cellular viability evaluated using the LDH leakage assay (% of extracellular LDH/total LDH) in differentiated H9c2 cells incubated with 0.01, 0.1, 1, 2 and 5 μM of MTX for 24 (A) and 48h (B). Results are presented as mean ± SD of 5 independent experiments (total of 30 wells). Statistical analysis was done using the Kruskal–Wallis test, followed by the Dunn's *post hoc* test (****p < 0.0001 vs. control; ####p < 0.0001 vs. 0.01 μM; $$p < 0.01, $$$$p < 0.0001 vs. 0.1 μM; &&p < 0.01, &&&p < 0.001 vs. 1 μM).

4.4.4. Mitoxantrone caused a significant lysosome uptake dysfunction in H9c2 differentiated cells

After 24 and 48h incubation with several concentrations of MTX (0.01 to 5 μM), the lysossomal uptake of NR was evaluated. At 24h (Figure 25A), the highest concentrations of MTX (1, 2 and 5 μM) caused a substantial impairment of lysossomal uptake of NR when compared to control cells. At 48h (Figure 25B), lysossomal functionality was even more impaired in MTX highest concentrations (1, 2 and 5 μM). At 48h, the H9c2 cells incubated MTX 1 μM had 58.98 ± 15.41%, 2 μM had 37.81 ± 7.34 %, and 5 μM 24.64 ± 4.07% NR uptake ability when compared to control cells (Figure 25B).

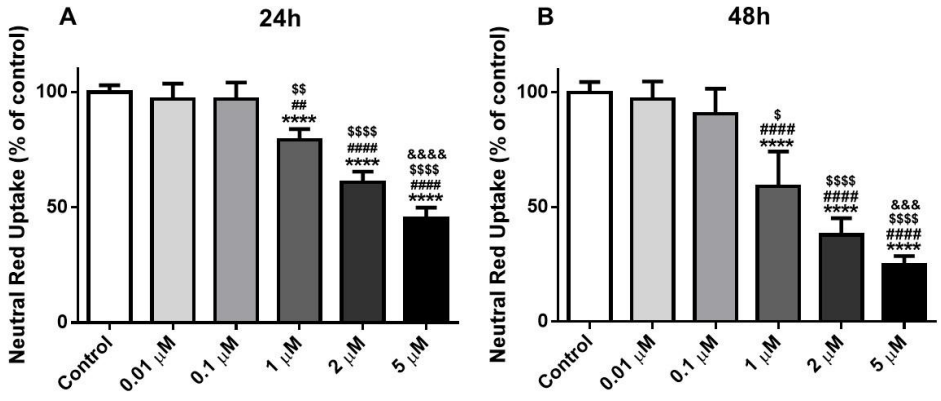

Figure 25. NR uptake (% of control) in differentiated H9c2 cells incubated with 0.01, 0.1, 1, 2 and 5 μM of MTX for 24 (A) and 48h (B). Results are presented as mean ± SD of 5 independent experiments (total of 30 wells). Statistical analysis was done using the Kruskal–Wallis test, followed by the Dunn's *post hoc* test (****p < 0.0001 vs. control; ##p < 0.01, ####p < 0.0001 vs. 0.01 μM; $$p$ < 0.05, $$$$$p$ < 0.01, $$$$$p$ < 0.0001 vs. 0.1 μM; &&&p < 0.001, &&&&p < 0.0001 vs. 1 μM).

4.4.5. Buthionine sulphoximine, an inhibitor of gamma-glutamylcysteine synthetase, had no effect on cellular death caused by mitoxantrone incubation in H9c2 cells

Buthionine sulphoximine, an inhibitor of gamma-glutamylcysteine synthetase, at 50 μM concentration, was pre-incubated in H9c2 cells, to access if the decrease of glutathione

synthesis caused any effect on the cytotoxicity caused by MTX. Buthionine sulphoximine did not cause any significant alteration on the cell death caused by the 48h incubation of 2 µM MTX (Figure 26). At 48h, 2 µM MTX had 53.95 ± 5.26% viability, whereas the condition 2 µM MTX plus buthionine sulphoximine had a viability of 50.96 ± 8.30% (Figure 26). The use of buthionine sulphoximine at 50 µM did not cause any significant change in cellular viability when compared to control cells.

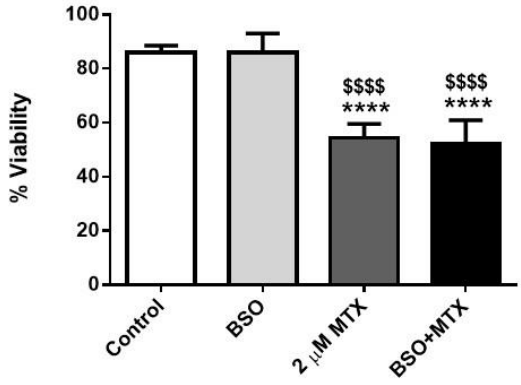

Figure 26. Cellular viability evaluated using the LDH leakage assay (% of extracellular LDH/total LDH) in differentiated H9c2 cells incubated with 2 µM of MTX and buthionine sulphoximine (BSO), an inhibitor of gamma-glutamylcysteine synthetase at 50 µM and BSO + MTX, for 48h. Results are presented as mean ± SD of 4 independent experiments (total of 20 wells). Statistical analysis was done using the Kruskal–Wallis test, followed by the Dunn's *post hoc* test (****$p < 0.0001$ vs. control; $^{\$\$\$\$}p < 0.0001$ vs. BSO 50 µM).

4.4.6. N-acetyl cysteine, a glutathione precursor and reactive species scavenger, was not able to revert the cell death caused by mitoxantrone incubation

N-acetyl cysteine, a glutathione precursor and reactive species scavenger (Avantaggiato et al., 2014), at 1 mM concentration, was used in H9c2 cells. The antioxidant, N-acetyl cysteine, did not cause any significant alteration on the cell death caused by the 48h incubation of 2 µM MTX (Figure 27). At 48h, 2 µM MTX had 52.20 ± 4.38% viability, whereas the condition 2 µM MTX plus N-acetyl cysteine had a viability of 47.47 ± 6.82% (Figure 27). The use of N-acetyl cysteine at 1 mM did not cause any significant change in cellular viability when compared to control cells.

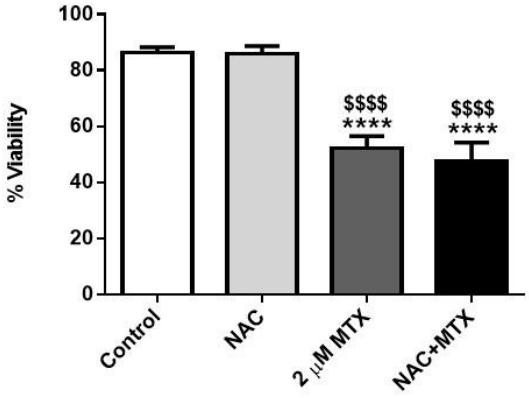

Figure 27. Cellular viability evaluated using the LDH leakage assay (% of extracellular LDH/total LDH) in differentiated H9c2 cells incubated with 2 μM of MTX and N-acetyl cysteine (NAC), an antioxidant and reactive species scavenger at 1 mM and NAC + MTX for 48h. Results are presented as mean ± SD of 4 independent experiments (total of 24 wells). Statistical analysis was done using the Kruskal–Wallis test, followed by the Dunn's *post hoc* test (****$p < 0.0001$ vs. control; $^{\$\$\$\$}p < 0.0001$ vs. NAC 1 mM).

4.4.7. L-carnitine, a mitochondrial enhancer was not able to revert cell death caused by mitoxantrone incubation

L-carnitine acts as a carrier for fatty acids across the inner mitochondrial membrane for subsequent β-oxidation (Zammit et al., 2009). L-carnitine did not cause any significant alteration on the cell death caused by the 48h incubation with 2 μM MTX (Figure 28). At 48h, 2 μM MTX had 53.29 ± 5.67% viability, whereas the condition 2 μM MTX plus L-carnitine had a viability of 52.83 ± 5.56% (Figure 28). The use of L-carnitine at 2 mg/mL did not cause any significant change in cellular viability when compared to control cells.

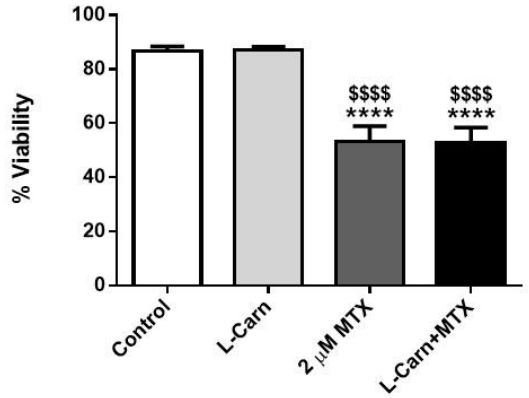

Figure 28. Cellular viability evaluated using the LDH leakage assay (% of extracellular LDH/total LDH) in differentiated H9c2 cells incubated with 2 µM of MTX, and L-Carnitine (L-Carn), a mitochondrial enhancer at 2 mg/mL and L-Carn + MTX for 48h. Results are presented as mean ± SD of 4 independent experiments (total of 24 wells). Statistical analysis was done by using the Kruskal–Wallis test, followed by the Dunn's *post hoc* test (*****p* < 0.0001 vs. control; $^{\$\$\$\$}p$ < 0.0001 vs. L-Carnitine 2 mg/mL.

4.4.8. 3-Methyladenine, an autophagy inhibitor, did not inhibit cell death caused by incubation with mitoxantrone

3-Methyladenine was used to assess if autophagy was involved on MTX cytotoxicity. 3-Methyladenine did not inhibit the cell death caused by the 48h incubation of 2 µM MTX (Figure 29). At 48h, 2 µM MTX had 49.40 ± 4.00% viability, whereas the condition 2 µM MTX plus 3-methyladenine had a viability of 48.30 ± 2.92% (Figure 29). The use of 3-methyladenine at 2.5 mM did not cause any significant change in cellular viability when compared to vehicle cells.

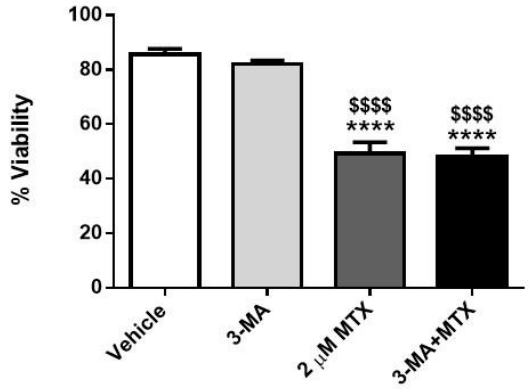

Figure 29. Cellular viability evaluated using the LDH leakage assay (% of extracellular LDH/total LDH) in differentiated H9c2 cells incubated with 2 µM of MTX, 3-methyladenine (3-MA) 2.5 mM and 3-MA + MTX for 48h. DMSO (final concentration of 0.1% v/v) was used as vehicle. Results are mean ± SD of 4 independent experiments (24 wells). Statistical analysis: Kruskal–Wallis test, followed by the Student–Newman–Keuls *post hoc* test (*****p* < 0.0001 vs. vehicle; $^{\$\$\$\$}p$ < 0.0001 vs. 3-MA 2.5 mM).

4.4.9. The 3-methyladenine, an autophagy inhibitor, led to a partial protection to the impairment caused in lysossomal uptake by mitoxantrone

3-Methyladenine is used to inhibit and study the mechanism of autophagy (lysosomal self-degradation) and apoptosis (Viola et al., 2012). After 24 and 48h incubation with 2 µM MTX, the lysossomal uptake of NR was evaluated. At 24h, 2 µM MTX had 56.14 ± 7.92%, whereas the condition 2 µM MTX plus 3-methyladenine had values of 65.95 ± 7.37% (Figure 30A). At 48h (Figure 30B), lysossomal function was even more impaired in the condition 2 µM MTX. At 48h, the H9c2 cells incubated MTX 2 µM had 22.76 ± 6.77%, and 2 µM MTX plus 3-methyladenine had 36.44 ± 9.06% NR ability uptake when compared to vehicle cells.

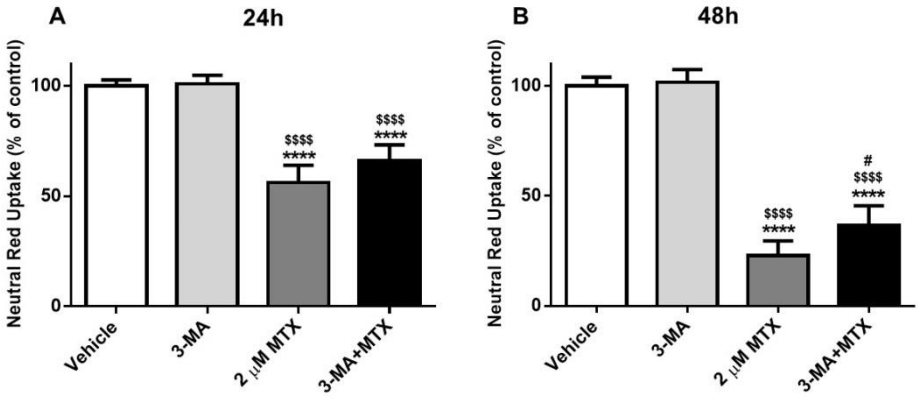

Figure 30. NR uptake (% of vehicle) in differentiated H9c2 cells incubated with 2 µM of MTX, 3-methyladenine (3-MA) 2.5 mM and 3-MA + MTX for 24 (A) and 48h (B). DMSO (final concentration of 0.1% v/v) was used as vehicle. Results are mean ± SD of 7 independent experiments (42 wells). Statistical analysis: Kruskal–Wallis test, followed by the Student–Newman–Keuls *post hoc* test (****p < 0.0001 vs. vehicle; $^{\$\$\$\$}p$ < 0.0001 vs. 3-MA 2.5 mM; $^{\#}p$ < 0.05 vs. 2 µM).

4.4.10. The caspase inhibitor, Ac-LETD-CHO, did not inhibit the cell death caused by mitoxantrone in H9c2 cells

Caspase inhibitor (100 µM) did not inhibit the cell death caused by the 48h incubation with 2 µM MTX (Figure 31A). At 48h, 2 µM MTX had 49.81 ± 3.43% viability, whereas the condition 2 µM MTX plus caspase inhibitor had a viability of 45.19 ± 12.63% (Figure 31A). The use of caspase inhibitor at 100 µM did not cause any significant change in cellular viability when compared to control cells.

At 200 µM concentration, the caspase inhibitor also did not protected H9c2 cells from the damage caused by MTX (Figure 31B). At 48h, 2 µM MTX had 44.35 ± 6.40% viability, whereas the condition 2 µM MTX plus caspase inhibitor (200 µM) had a viability of 44.74 ± 4.78% (Figure 31B). The use of caspase inhibitor at 200 µM did not cause any significant alteration on cellular viability when compared to control cells.

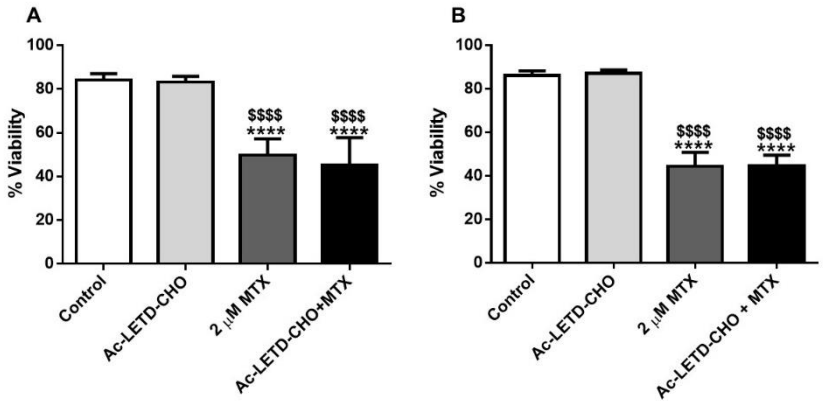

Figure 31. Cellular viability evaluated using the LDH leakage assay (% of extracellular LDH/total LDH) in differentiated H9c2 cells incubated with 2 µM of MTX, Ac-LETD-CHO 100 µM (A) or 200 µM (B) and Ac-LETD-CHO + MTX for 48h. Results are mean ± SD of 4 independent experiments (24 wells). Statistical analysis: Kruskal–Wallis test, followed by the Student–Newman–Keuls *post hoc* test (****$p < 0.0001$ vs. control; $^{\$\$\$\$}p < 0.0001$ vs. Ac-LETD-CHO).

4.4.11. Cycloheximide, a protein synthesis inhibitor, did not inhibit the cell death caused by incubation with mitoxantrone

Cycloheximide (10 µg/mL) did not prevent MTX-induced cytotoxicity in H9c2 cells. At the cellular level, cycloheximide blocks the translation of messenger RNA on cytosolic, 80S ribosomes, but does not inhibit organelle protein synthesis (Obrig et al., 1971). At 48h, 2 µM MTX had 86.95 ± 5.79%, MTT reduction whereas the condition 2 µM MTX plus cycloheximide had 88.04 ± 5.72% MTT reduction ability when compared to control cells (Figure 32). Cycloheximide by itself did not cause any cytotoxicity in the time-point and concentration tested.

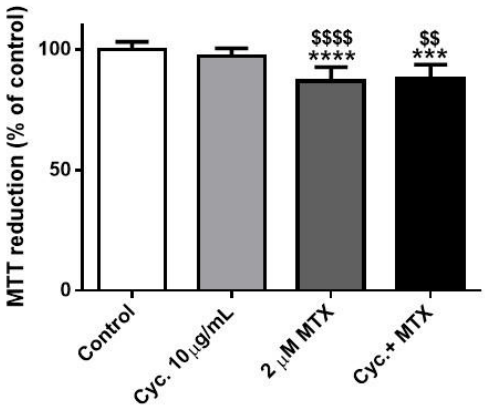

Figure 32. Mitochondrial dysfunction evaluated by MTT reduction assay in differentiated H9c2 cells incubated with 2 µM of MTX, cycloheximide (Cyc.) 10 µg/mL and Cyc. + MTX for 48h. Results are mean ± SD of 3 independent experiments (18 wells). Statistical analysis: Kruskal–Wallis test, followed by the Student–Newman–Keuls *post hoc* test (***$p < 0.001$; ****$p < 0.0001$ vs. control; $^{\$\$}p < 0.01$; $^{\$\$\$\$}p < 0.0001$ vs. cycloheximide 10 µg/mL).

4.4.12. 1-Aminobenzotriazole, a suicide CYP450 inhibitor, did not revert the cytotoxicity caused by mitoxantrone

1-Aminobenzotriazole inhibits CYP450 metabolism (Linder et al., 2009). 1-Aminobenzotriazole (0.5 mM) did not inhibit cell death caused by the 48h incubation of 2 µM MTX (Figure 33). At 48h, 2 µM MTX had 48.39 ± 6.49% viability, whereas the condition 2 µM MTX plus 1-aminobenzotriazole showed a viability of 46.69 ± 4.61% (Figure 33A). After 48h incubation, the lysossomal uptake of NR was evaluated. At 48h, the H9c2 cells incubated MTX 2 µM had 34.73 ± 4.69%, 2 µM MTX plus 1-aminobenzotriazole had 33.09 ± 5.72% NR ability when compared to control cells (Figure 33B). 1-Aminobenzotriazole by itself did not cause any cytotoxicity in the time-point and concentration tested.

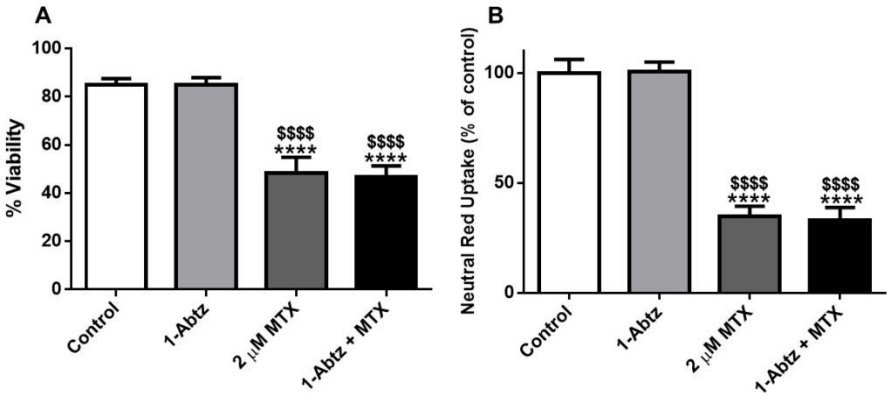

Figure 33. Cellular viability evaluated using the LDH leakage assay (% of extracellular LDH/total LDH) (A) in differentiated H9c2 cells incubated with 2 µM of MTX, 1-aminobenzotriazole (1-abtz) 0.5 mM and 1-abtz + MTX for 48h. NR uptake (% control) (B) in differentiated H9c2 cells incubated with 2 µM of MTX, 1-abtz and 1-abtz + MTX for 48h. Results are mean ± SD of 6 independent experiments (36 wells). Statistical analysis were performed using Anova test, followed by the Tukey's *post hoc* test (****$p < 0.0001$ vs. control; $^{\$\$\$\$}p < 0.0001$ vs. 1-abtz 0.5 mM).

4.4.13. Metyrapone, a competitive CYP450 inhibitor, did not inhibit the cytotoxicity caused by mitoxantrone in H9c2 cells

Metyrapone is a competitive CYP450 inhibitor (Sampath-Kumar et al., 1997) and it did not inhibit the cytotoxicity caused by the 48h incubation of 2 µM MTX (Figure 34). At

48h, the H9c2 cells incubated MTX 2 µM had 64.96 ± 5.88%, 2 µM MTX plus metyrapone had a MTT reduction of 58.81 ± 6.46% when compared to control cells (Figure 34A). After 48h incubation, the lysossomal uptake of NR was evaluated. At 48h, the H9c2 cells incubated MTX 2 µM had 37.08 ± 13.34%, 2 µM mitoxantrone plus metyrapone had 34.84 ± 19.54% NR ability when compared to control cells (Figure 34B).

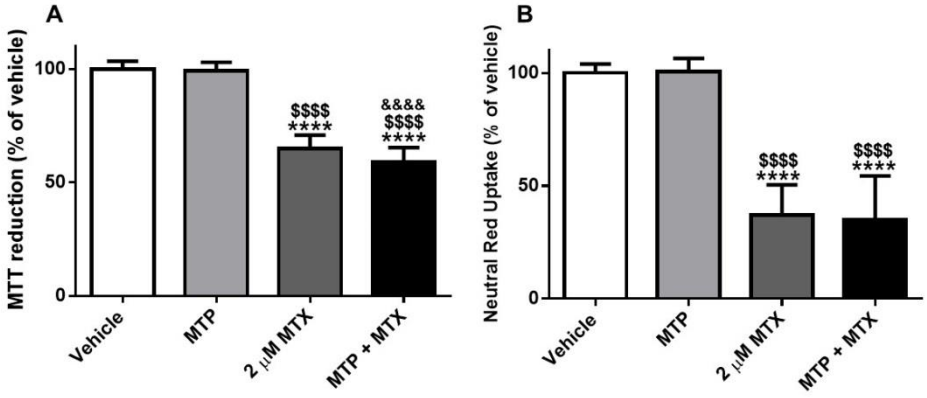

Figure 34. Mitochondrial dysfunction evaluated by MTT reduction assay (A) in differentiated H9c2 cells incubated with 2 µM of MTX, metyrapone (MTP) 0.5 mM and MTP + MTX for 48h. Results are presented as mean ± SD of 5 independent experiments (30 wells). Statistical analysis was performed using Anova test, followed by the Tukey's *post hoc* test (****p < 0.0001 vs. vehicle; $^{\$\$\$\$}$p < 0.0001 vs. MTP; $^{\&\&\&\&}$p < 0.0001 vs. 2 µM MTX. NR uptake (% of vehicle) (B) in differentiated H9c2 cells incubated with 2 µM of MTX, MTP and MTP + MTX for 48h. Results are mean ± SD of 4 independent experiments (24 wells). Statistical analysis: Kruskal–Wallis test, followed by the Student–Newman–Keuls *post hoc* test (****p < 0.0001 vs. vehicle; $^{\$\$\$\$}p$ < 0.0001 vs. MTP). DMSO (final concentration of 0.1% v/v) was used as vehicle.

4.4.14. Mitoxantrone was able to alter the ATP levels in H9c2 cells in a concentration-independent manner

To understand if MTX has effects in cellular energetics, intracellular ATP levels were measured in H9c2 cell exposed to MTX for 24h. ATP intracellular levels after MTX incubation were assessed through the bioluminescence assay. MTX increased the ATP levels in the time point tested, as shown in the Figure 35: after 24h incubation with MTX (2 and 5 µM), the ATP intracellular levels were about 41.10 ± 5.65 nmol/mg protein and 44.63 ± 8.80 nmol/mg protein, respectively, compared to 16.87 ± 1.54 nmol/mg protein for the control group.

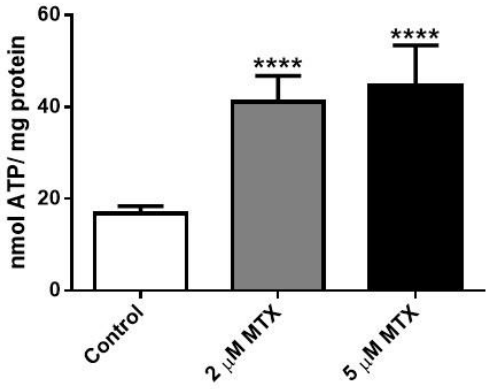

Figure 35. ATP levels in differentiated H9c2 cells incubated with 2 and 5 μM of MTX for 24h. Results, in nmol/mg protein, are presented as mean ± SD of 6 independent experiments. Statistical analysis was performed using Anova test, followed by the Tukey's *post hoc* test (****p < 0.0001 vs. control).

4.5. Toxicological evaluation of naphthoquinoxaline

4.5.1. Microscopic evaluation of naphthoquinoxaline incubated H9c2 cells

Cells were morphologically assessed after 24h exposure to NAPHT. H9c2 cells were incubated with NAPHT (2 and 5 μM), as described in the Methods section. Phase-contrast microscopy and Hoescht staining were used to describe the microscopic features associated with NAPHT-induced H9c2 cytotoxicity. Phase-contrast microscopy, after 24h incubation, revealed cell injury, with intensifying features with increasing concentrations, namely cytoplasmatic injury (Figure 36). The decrease in cell number was observed (Figure 36C and 36F), but the decrease was lower in comparison with the results of MTX. No apoptotic nucleus were observed. At 48h, the cell injury was increased in NAPHT-incubated cells (data not shown).

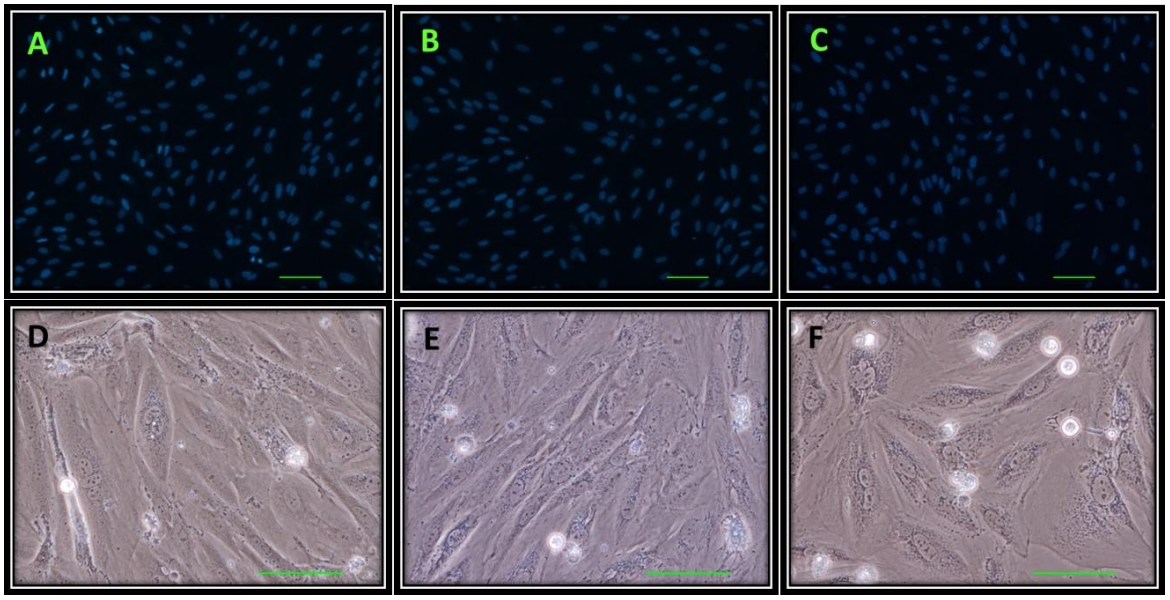

Figure 36. Fluorescence microscopy (Hoechst 33258 staining) (A, B, C), and phase contrast microscopy (D, E, F) images of differentiated H9c2 cells after incubation with 2 and 5 μM of NAPHT for 24h. DMSO (final concentration of 0.1% v/v) was used as vehicle (A and D), NAPHT 2 μM (B and E), and NAPHT 5 μM (C and F). Images are representative of three independent experiments (scale bar 100 μm).

Ethidium bromide/ acridine orange staining was also used for evaluate NAPHT effects on H9c2 cells. Through this method, living cells appear with a regular-sized green fluorescent nucleus, as shown in vehicle incubated H9c2 cells in Figure 37A. The cells incubated with NAPHT show with green nucleus, although with signs of cytoplasmatic injury (Figure 37B and C).

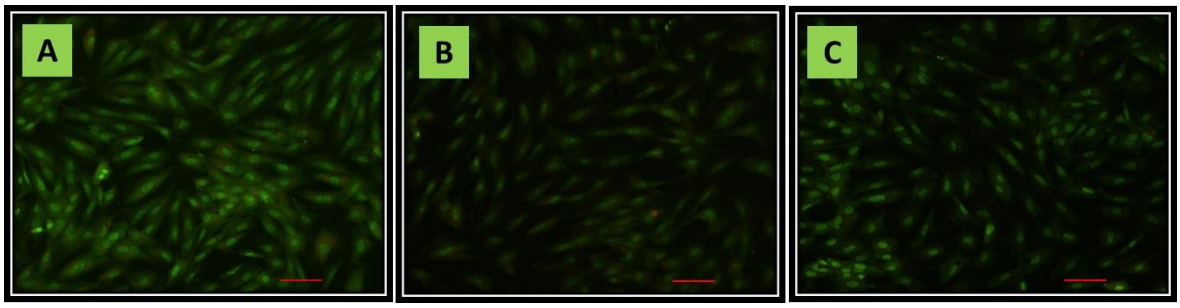

Figure 37. Ethidium bromide and acridine orange (A, B, C) images of differentiated H9c2 cells after incubation with 2 and 5 μM of NAPHT for 24h. DMSO (final concentration of 0.1% v/v) was used as vehicle (A), NAPHT 2 μM (B), NAPHT 5 μM (C). Images are representative of three independent experiments (scale bar 100 μm).

Assessment of mitochondrial membrane potential in differentiated H9c2 cells incubated with 2 µM of NAPHT (B) and 5 µM of NAPHT (C) for 12h (Figure 38) was also performed. Lower levels of fluorescence resulting from NAPHT treatment were observed, suggesting that the depolarization of mitochondrial membrane potential at 12h occurred after incubation with NAPHT. This depolarization effect seems to be dose dependent (Figure 38).

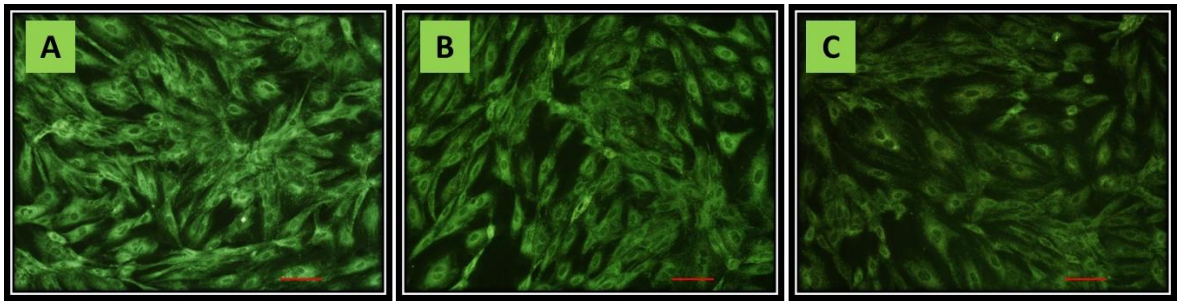

Figure 38. Images of mitochondrial transmembrane potential of differentiated H9c2 cells after incubation with 2 and 5 µM of NAPHT for 12h (A, B, C). DMSO (final concentration of 0.1% v/v) was used as vehicle (A), NAPHT 2 µM (B), NAPHT 5 µM (C). Images are representative of three independent experiments (scale bar 100 µm).

4.5.2. Naphthoquinoxaline caused a time- and concentration-dependent mitochondrial dysfunction

The ability of NAPHT to interfere with MTT reduction was evaluated at 2 time-points (24 and 48h) and with several concentrations (1 to 5 µM). At 24h (Figure 39A), NAPHT at concentration 2 and 5 µM caused cytotoxicity when compared to control cells. At 48h, (Figure 39A) NAPHT at all the concentrations tested caused significant cytotoxicity when compared to vehicle cells, being the highest concentration tested (5 µM) able to decrease the levels of MTT reduction to 82.49 ± 4.05% when compared to vehicle cells (100 ± 3.85%).

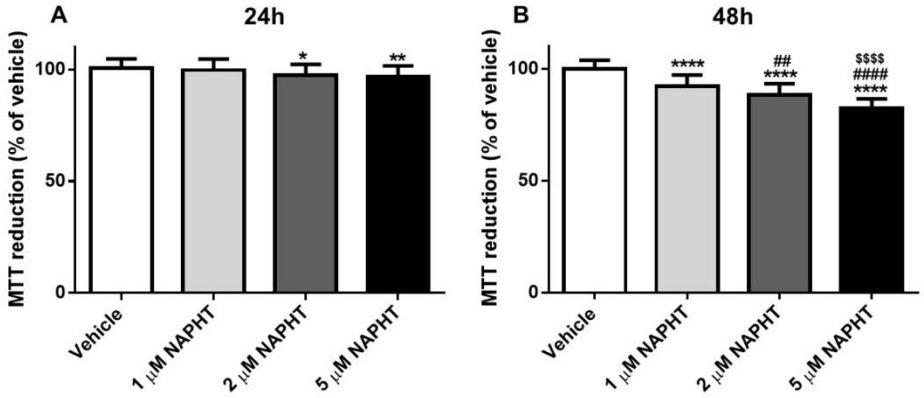

Figure 39. Mitochondrial dysfunction evaluated by MTT reduction in differentiated H9c2 cells incubated with 1, 2 and 5 µM of NAPHT for 24 (A) and 48h (B). DMSO (final concentration of 0.1% v/v) was used as vehicle. Results are presented as mean ± SD of 6 independent experiments (total of 35 - 36 wells). Statistical analysis were performed using the Anova test, followed by the Tukey's *post hoc* test (*p < 0.05, **p < 0.01, ***p < 0.001 vs. vehicle; $^{\#\#}$p < 0.01, $^{\#\#\#\#}$p < 0.0001 vs. 1 µM; $^{\$\$\$\$}$p < 0.0001 vs. 2 µM).

4.5.3. Naphthoquinoxaline was able to cause significant loss of membrane integrity

The ability of NAPHT to cause cell death was tested at 2 time-points (24 and 48h) and with several concentrations (1 to 5 µM). At 24h (Figure 40A), all the concentrations of NAPHT (1, 2 and 5 µM) tested caused significant cellular membrane integrity loss when compared to control cells. In Figure 40B, the data obtained after the 48h incubation of NAPHT in H9c2 differentiated cells is observed. NAPHT at 48h caused a significant decrease in cellular integrity, being observed that at 2 µM NAPHT the viability was 73.02 ± 2.86% and at 5 µM the viability was 52.07 ± 6.83%, when compared with vehicle cells (81.91 ± 1.89%).

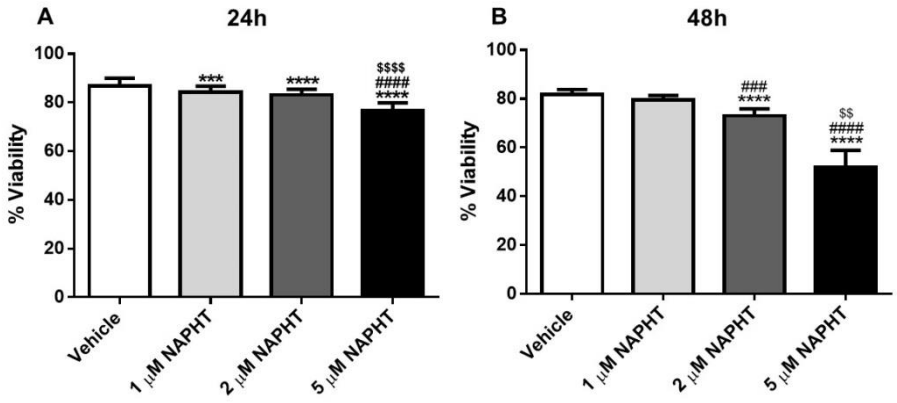

Figure 40. Cellular viability evaluated using the LDH leakage assay (% of extracellular LDH/total LDH) in differentiated H9c2 cells incubated with 1, 2 and 5 µM of NAPHT for 24 (A) and 48h (B). DMSO (final concentration of 0.1% v/v) was used as vehicle. Results are presented as mean ± SD of 6 independent experiments (total of 35 - 36 wells). Statistical analysis was performed at 24h using the Kruskal–Wallis test, followed by the Student–Newman–Keuls *post hoc* test. For 48h, the Anova test, followed by the Tukey's *post hoc* test, was used (***p < 0.001, ****p < 0.0001 vs. vehicle; $^{\#\#\#}$p < 0.001, $^{\#\#\#\#}$p < 0.0001 vs. 1 µM; $^{\$\$}$p < 0.01, $^{\$\$\$\$}$p < 0.0001 vs. 2 µM).

4.5.4. Naphthoquinoxaline caused a significant lysosome uptake dysfunction in H9c2 differentiated cells

After 24 and 48h incubation with several concentrations of NAPHT (1 to 5 µM), the lysossomal uptake of NR was evaluated. At 24h (Figure 41A), only the highest concentrations of NAPHT (2 and 5 µM) caused a substantial impairment of lysossomal uptake of NR when compared to control cells. At 48h (Figure 41B) the H9c2 cells incubated with NAPHT 2 µM had 88.82 ± 5.53% of NR uptake, while 5 µM showed values of 68.83 ± 6.28% NR incorporation when compared to vehicle cells (100.00 ± 6.18%).

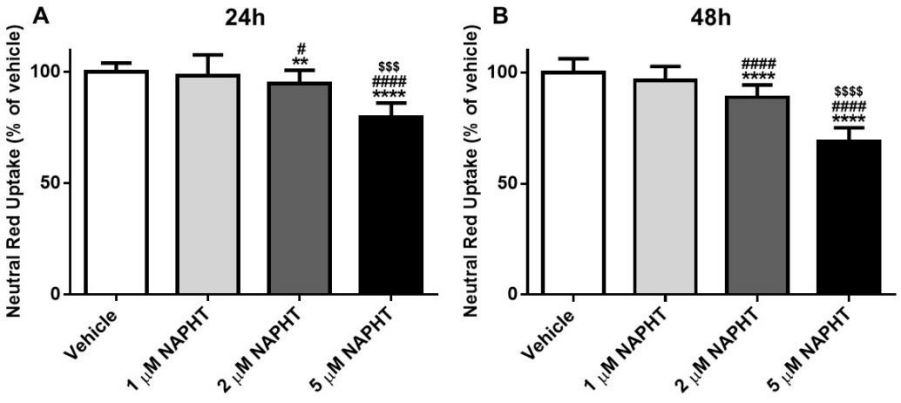

Figure 41. NR uptake (% of vehicle) in differentiated H9c2 cells incubated with 1, 2 and 5 µM of NAPHT for 24 (A) and 48h (B). DMSO (final concentration of 0.1% v/v) was used as vehicle. Results are presented as mean ± SD of 5 independent experiments (total of 30 wells). Statistical analysis was performed using the Anova test, followed by the Tukey's *post hoc* test for analysis at 24h and Kruskal–Wallis test, followed by the Student–Newman–Keuls *post hoc* test, for analysis at 48h (**p < 0.01, ****p < 0.0001 vs. vehicle; $^{\#}$p < 0.05, $^{\#\#\#\#}$p < 0.0001 vs. 1 µM; $^{\$\$}$p < 0.01, $^{\$\$\$\$}$p < 0.0001 vs. 2 µM).

4.5.5. N-acetyl cysteine incubation increased cell death caused by naphthoquinoxaline

N-acetyl cysteine, a glutathione precursor and reactive species scavenger (Avantaggiato et al., 2014), at 1 mM concentration was used in H9c2 cells. N-acetyl cysteine increased cell death caused by 2 µM NAPHT (Figure 42). At 48h, 2 µM NAPHT had 74.09 ± 2.50% viability, whereas in the condition 2 µM NAPHT plus N-acetyl cysteine the viability observed was 68.16 ± 3.26% (Figure 42). The use of N-acetyl cysteine at 1 mM did not cause significant change in cellular viability when compared to vehicle cells.

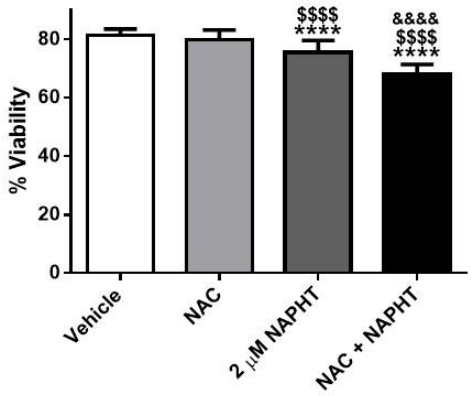

Figure 42. Cellular viability at 48h evaluated using the LDH leakage assay (% of extracellular LDH/total LDH) in differentiated H9c2 cells incubated with 2 µM of NAPHT and N-acetyl cysteine (NAC), an antioxidant, at 1 mM. DMSO (final concentration of 0.1% v/v) was used as vehicle. Results are presented as mean ± SD of 4 independent experiments (total of 24 wells). Statistical analysis was performed using the Anova test, followed by the Tukey's *post hoc* test (****$p < 0.0001$ vs. vehicle; $^{\$\$\$\$}p < 0.0001$ vs. NAC; $^{\&\&\&\&}p < 0.0001$ vs. 2 µM NAPHT).

4.5.6. 3-Methyladenine, an autophagy inhibitor, caused a partial protection to the damage caused by naphthoquinoxaline

After 48h incubation with 2 µM NAPHT, the lysossomal uptake of NR was evaluated. At 48h, 2 µM NAPHT showed values of 88.26 ± 6.93%, whereas the condition 2 µM NAPHT plus 3-methyladenine had the values of 94.24 ± 7.91% (Figure 43). Thus, 3-methyladenine caused a partial protection to the effects caused by NAPHT.

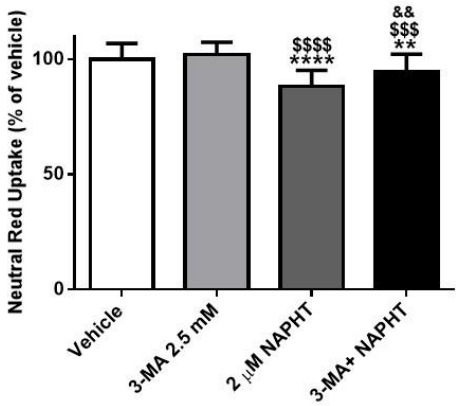

Figure 43. NR uptake (% of vehicle) in differentiated H9c2 cells incubated with 2 µM of NAPHT, 3-methyladenine (3-MA) 2.5 mM and 3-MA + NAPHT for 48h. DMSO (final concentration of 0.1% v/v) was used as vehicle. Results are mean ± SD of 5 independent experiments (30 wells). Statistical analysis was performed using the Anova test, followed by the Tukey's *post hoc* test (**p <

0.01, ****p < 0.0001 vs. vehicle; $$$p < 0.001, $$$$p < 0.0001 vs. 3-MA 2.5 mM; &&p < 0.01 vs. 2 µM NAPHT).

4.5.7. Naphthoquinoxaline did not cause any significant alteration on ATP levels at an early time-point

To understand if NAPHT has effects in cellular energetics, intracellular ATP levels were measured in H9c2 cell exposed to NAPHT for 24h. In the NAPHT tested concentration, and time point (24h), no significance changes were detected, as shown in the Figure 44. After the 24h incubation with NAPHT (2 and 5 µM), the ATP intracellular levels were about 14.94 ± 4.38 nmol/mg protein and 16.74 ± 4.21 nmol/mg protein, respectively, compared to 14.24 ± 3.48 nmol/mg protein for the vehicle group.

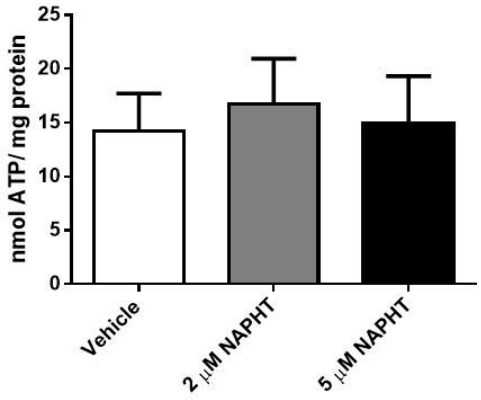

Figure 44. ATP levels in differentiated H9c2 cells incubated with 2 and 5 µM NAPHT for 24h. DMSO (final concentration of 0.1% v/v) was used as vehicle. Results, in nmol/mg protein are presented as mean ± SD of 6 independent experiments.

5.
DISCUSSION AND CONCLUSIONS

5. Discussion and conclusions

Xenobiotics that cause heart damage may have a part of their toxicity resulting from metabolization. This chemical change is mainly catalysed by enzymes, and usually favours the increase of hydrophilicity of parental xenobiotics. The majority of the metabolism in the body occurs in the liver, and the metabolites formed can reach the heart due to the distribution via blood stream. Moreover, the heart also has metabolizing enzymes, therefore *in loco* it generates metabolites that may cause cardiac toxicity (Wormhoudt et al., 1999). Several anticancer drugs can lead to cardiotoxicity. Some drugs, like DOX and cyclophosphamide, are shown to be cardiotoxic through their metabolites (Costa et al., 2013). Other anticancer drugs are scarcely studied regarding the cardiotoxicity of their metabolites.

5.1. Synthesis and purification of the mitoxantrone metabolite naphthoquinoxaline

The full characterization of the metabolic profile and the elucidation of the metabolites structure in new chemical entities are often not completed during clinical development or even after the drugs' introduction into the market (Fura et al., 2004). It is also often difficult to predict *a priori* whether after metabolization a certain compound could form a toxic or pharmacologically active metabolite. The degree of contribution of active metabolites to the overall observed therapeutic or toxic effects needs further study, but the rapid chemical synthesis of metabolites by traditional methods is often challenging (Fura et al., 2004).

In this thesis, the synthesis of MTX metabolites was accomplished by the HRP catalysed H_2O_2 oxidation (Figure 10). Several derivatives were observed by chromatographic analysis of the crude product and two purified derivatives were isolated and identified as NAPHT, an already reported metabolite of MTX, and a newly isolated derivative, NAPHTdi. The enzymatically catalysed oxidation of MTX by HRP/H_2O_2 has already been demonstrated in other works (Reszka et al., 1986, Kolodziejczyk et al., 1988, Bruck and Bruck, 2011). In those works, the isolation of the metabolite NAPTH was achieved and it was partially characterized by ^{13}C NMR and liquid chromatography-mass spectrometry. Herein, the isolation and structure characterization of NAPHT was accomplished and additionally the isolation of a possible oxidation product of MTX, NAPHTdi, was achieved for the first time.

In the study by Blanz *et al*., NAPHT metabolite was isolated by preparative HPLC from the urine of a patient and it was characterized by tandem mass spectrometry and UV-visible spectroscopy (Blanz et al., 1991b). Moreover, two studies in cell systems suggest that NAPHT may contribute to the cytotoxic activity of MTX (Duthie and Grant, 1989, Mewes et al., 1993).

The proposed mechanism for the formation of NAPHT and NAPHTdi (seen in Figure 45) (Blanz et al., 1991b) established the reaction to proceed via a two-electron oxidation of the phenylenediamine substructure I to the formation of the highly reactive quinone II. The nonprotonated form IV of the equilibrium reacts by an intramolecular attack of the basic amino group of the side chain with the electrophilic centre at C-6 of MTX radical cation. Subsequent oxidation of the cyclized radical V led to the formation of NAPHT. As the reaction progressed, further oxidation of the NAPHT side-chains occurred, yielding the dicarboxylic acid derivative NAPHTdi.

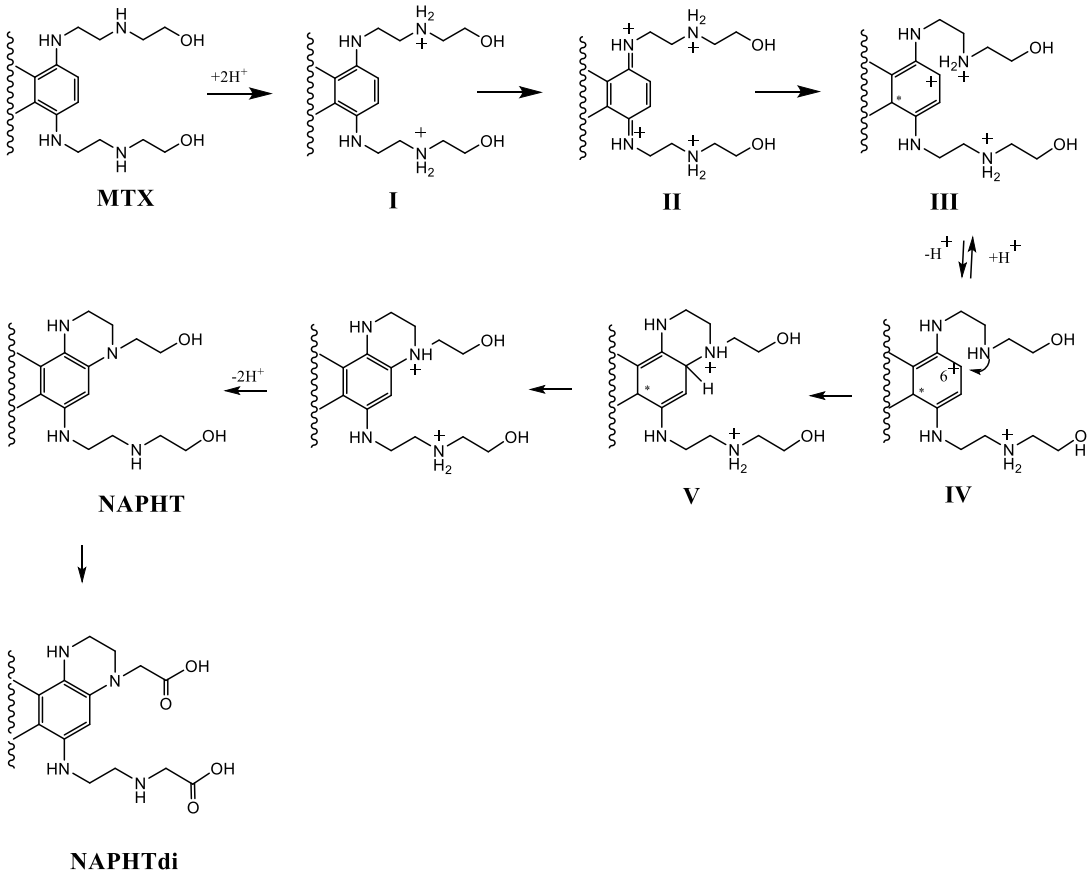

Figure 45. Proposed mechanism for the formation of NAPHT and NAPHTdi after the oxidation of MTX. Adapted from Blanz *et al*., 1991b.

The NAPHT and other metabolites resulting from oxidation of MTX are not normally purified after synthesis. For example, in the study of Bruck *et al*., the crude product of the HRP/H_2O_2 catalysed oxidation was used for the steady-state spectrokinetic and HPLC-MS analysis without further purification (Bruck and Bruck, 2011). Herein, with the purification methods used allowed to obtain a high purity NAPHT metabolite that allowed further toxicological evaluation. Nevertheless, the amount of NAPHTdi obtained did not allow further *in vitro* studies and the unequivocal structure characterization. ^{13}C NMR analysis should be considered in a future work for its full chemical characterization. This compound has already been previously proposed by UV analysis to be formed with the HRP catalysed H_2O_2 oxidation (Bruck and Harvey, 2003). In this thesis, NAPHTdi was first time isolated and characterized.

5.2. Decreased foetal bovine serum and the addition of retinoic acid to H9c2 cells caused cell differentiation

The H9c2 myoblast cell line, originated from rat ventricular tissue, has been used *in vitro* as a model for skeletal and cardiac muscle due to the morphological features and electrical/hormonal signalling properties of these cells (Kimes and Brandt, 1976, Hescheler et al., 1991).

H9c2 cells show electrophysiological and biochemical properties of both skeletal and cardiac tissues, including depolarization in response to acetylcholine (Kimes and Brandt, 1976), and rapid activation of calcium currents through L-type channels (Hescheler et al., 1991, Mejia-Alvarez et al., 1994, Wang et al., 1999). An interesting feature of this cell line is its ability to differentiate from mono-nucleated myoblasts to myotubes upon reduction of serum concentration (Hescheler et al., 1991). With myotube formation the expression of myogenic transcription factors (Chun et al., 2000) and calcium channel proteins also occurs (Menard et al., 1999).

Despite the wide use of the H9c2 cell line in the undifferentiated state, a cardiac-like phenotype can be obtained after differentiation in a low FBS (1%) and 10 nM RA - supplemented media. Because the adult heart tissue is composed mainly by differentiated cardiomyocytes, toxicological studies can have different outcomes depending on the developmental state of the biological model used (Branco et al., 2011). In the study by Menard *et al.,* the cells were cultured in DMEM supplemented with 1% foetal calf serum (replaced every 2 days) and RA (Menard et al., 1999). RA-treated cells exhibited morphological changes with rather large and rounded cells. The treatment of H9c2 cells with RA maintained their cardiac phenotype and inhibited myogenic differentiation of those

cells (Menard et al., 1999). In the study by Branco *et al.,* they investigated whether RA-driven cell differentiation results in the increase of specific markers for cardiac cells (Branco et al., 2011). Higher protein content of phosphorylated-troponin I, cardiac troponin T and ventricular myosin light chain were observed when H9c2 cells were differentiated in a low serum media supplemented with RA, confirming that this treatment drives H9c2 cells to a cardiac-like phenotype (Branco et al., 2011).

In the study by Ruiz *et al*., they observed morphological alterations in H9c2 cells, after the induction of differentiation by serum reduction and RA supplementation. The results obtained confirm that H9c2 myoblasts fuse and form multinucleated cells (Ruiz et al., 2012). The differentiation process initiates a cell cycle arrest, which decreases cellular proliferation and alters their morphological features (Menard et al., 1999, Branco et al., 2011), as we found with our results. Cellular proliferation depends on the existence of growth factors in the culture media, hence it is expected that the reduction in the concentration of those factors will induce cell growth arrest, whereas the addition of RA drives the differentiation towards a cardiac phenotype (Menard et al., 1999, Branco et al., 2011, Pereira et al., 2011, Ruiz et al., 2012).

In our work, the differentiation protocol was conducted with RA 10 nM and 1% FBS for 7 days. There were substantial differences between undifferentiated cells and differentiated cells, which are illustrated in Figure 19. The differentiation protocol dramatically reduced cell division as in study the Branco *et al.* and in the study the Ruiz *et al.* (Branco et al., 2011, Ruiz et al., 2012). In fact, cellular density was substantially higher in undifferentiated cells maintained for 7 days as seen with Hoescht 33258 staining. Also, while accompanying inhibition of cell division, the cell bodies of differentiated cells became smaller and fusiform when compared to undifferentiated cells, which exhibit a large and flat cell body (Figure 19). This differentiation model becomes a more reliable cardiac model leading to a better extrapolation of results.

5.3. Cytotoxicity effects of mitoxantrone in differentiated H9c2 cells

Cytotoxicity assays are widely used as *in vitro* toxicology studies. The LDH leakage assay, the NR and the MTT assays are the most common assays employed for the detection of cytotoxicity following exposure to potentially toxic substances (Fotakis and Timbrell, 2006). The LDH leakage assay is based on the measurement of LDH activity in the extracellular medium. The loss of intracellular LDH and its release into the culture medium is an indicator of irreversible cell death due to cell membrane damage. The MTT assay is another assay often used to determine cytotoxicity. MTT is a water soluble tetrazolium salt, which is converted to an insoluble purple formazan by the cleavage of the

tetrazolium ring mainly by succinate dehydrogenase within the mitochondria (Fotakis and Timbrell, 2006, Costa et al., 2009). The formazan product formed within the cells is impermeable to the cell membranes and therefore it accumulates in healthy cells. The NR assay is also used to measure cytotoxicity. Living cells take up the NR, which is mainly concentrated within the lysosomes of cells (Fotakis and Timbrell, 2006).

In this thesis, the three cytotoxicity assays were employed to assess MTX toxicity *in vitro*. The results obtained complemented themselves and allowed a better characterization of the mechanisms involved, because of the different nature of each assay. After the differentiation protocol, cells were incubated with MTX (0.01 µM to 5 µM) for two time-points (24 and 48h), where the cytotoxicity tests (LDH assay, MTT assay and the NR uptake assays) were performed. The MTX cytotoxicity was demonstrated at different concentrations and time points, through the decline in the cell viability observed in the LDH leakage assay (Figure 24), the decrease in the MTT reduction activity (Figure 23) and through a significant impairment of NR lysossomal uptake (Figure 25). The lowest MTX concentrations (0.01 and 0.1 µM) did not cause cytotoxicity in H9c2 cells. However, for the highest concentrations (1, 2, and 5 µM), cytotoxicity was time- and concentration-dependent in all assays, being the NR assay more sensitive for the MTX toxic effects in H9c2 differentiated cells.

In the work by Rossato and co-workers, they tested seven MTX concentrations (10 and 100 nM, and 1, 5, 10, 50 and 100 µM) and four time points were selected (24, 48, 72, and 96h), using the undifferentiated H9c2 cells as cellular model. Rossato *et al.* observed that MTX-induced cytotoxicity was time- and concentration-dependent in the LDH leakage assay and MTT reduction assay (Rossato et al., 2013b). When comparing our results with the results obtained in the study mentioned above, we observed that at 24h, in the study by Rossato, 1 µM MTX did not led to a significant cell death, whereas in our study the same concentration caused significant decrease in cells' viability (64.08 ± 8.26%). In the present thesis, the concentration of 5 µM after the 48h incubation also induced a higher cell death (27.98 ± 9.92%) when compared to the mentioned work. The differentiated H9c2 cells seem more sensitive to the MTX effects than the undifferentiated H9c2 cells used in the study by Rossato *et al*. In fact, despite the lower cellular division in differentiated cells, MTX appears to be more toxic in the cells with the cardiac phenotype, thus revealing that MTX does not act only on cellular division. In the MTT reduction test, herein a significant cytotoxicity was observed, however lower than in the study of Rossato *et al*. (Rossato et al., 2013b). In this thesis, the concentration of 0.1 µM after a 24h incubation already caused significant cytotoxicity (93.74 ± 10.22%) when compared to control cells (100.00 ± 4.99%), being the highest dose tested (5 µM) able to decrease the levels of MTT reduction to 85.99 ± 8.52% when compared to control cells. At 48h, the cytotoxicity elicited was even higher, when

compared to control cells and the earlier time point. In the work by Rossato *et al.,* either at 24 as after the 48h incubation, the MTT reduction was significantly lower in 1 and 5 µM MTX-incubated H9c2 undifferentiated cells (Rossato et al., 2013b) than in the results of this thesis. These differences are possibly the result of the differentiation. Our cells are differentiated having lower proliferation rate, whereas in the work by Rossato and co-workers the cells are rapidly dividing. The values obtained in the MTT reduction assay are the result of a ratio to control cells and the control wells of undifferentiated cells have higher metabolization ability. In the study by Rossato and colleagues, the results suggested that mitochondrial effects anticipate cellular membrane rupture for MTX toxicity, because they observed that the toxic effects occurred earlier in the MTT reduction assay than in the LDH leakage assay in all times tested (Rossato et al., 2013b). In the present work, the MTT test also seems to be very sensitive to exposure of low concentrations of MTX and earlier time points.

To the best of our knowledge, there are no studies in the literature for the NR assay in H9c2 cell incubated with MTX. This assay was for the first performed for MTX and is the most sensitive for the MTX toxic effects in H9c2 differentiated cells.

5.4. Evaluation of several pharmacological active molecules towards the cytotoxic effects of mitoxantrone

Several pharmacological active molecules were used to elucidate the mechanisms involved in MTX-induced cardiotoxicity, namely N-acetyl cysteine, buthionine sulphoximine, cycloheximide, and L-carnitine.

Reactive oxygen species are created during the process of mitochondrial oxidative energy generation, among other processes (Costa et al., 2011). Cellular damage occurs when reactive oxygen species production exceeds the detoxifying ability of antioxidant enzymes or cofactors. N-acetyl cysteine has antioxidant proprieties and is the precursor of the amino acid cysteine, which is one of the three components of glutathione (gamma-glutamyl-cysteinyl-glycine), the major antioxidant of the body that works in both intra and extracellular compartments (Avantaggiato et al., 2014). Buthionine sulphoximine induces oxidative stress by irreversibly inhibiting gamma-glutamylcysteine synthetase, an essential enzyme for the synthesis of glutathione (Reliene and Schiestl, 2006).

In our study in differentiated H9c2 cells, the pre-incubation with the radical scavenger N-acetyl cysteine (1 mM) (Figure 27) or with the inhibitor of gamma-glutamylcysteine synthetase, buthionine sulphoximine (50 µM), (Figure 26) did not alter any of the cytotoxic effects observed with the MTX (2 µM) incubation for 48h in the LDH assay.

The lack of protective effects of N-acetyl cysteine or of increased toxicity by buthionine sulphoximine in the present study may result in the fact that other mechanisms involved in MTX toxicity exert a major role when compared to oxidative stress or glutathione pathways. Rossato *et al.* tested N-acetyl cysteine (1 mM) in other experimental conditions: undifferentiated cells H9c2 were incubated with 100 nM and 1 μM MTX for 96h, being the MTT reduction test used for the evaluation. Consistently, the pre-incubation with the radical scavenger N-acetyl cysteine did not prevent any of the cytotoxic effects observed with the MTX incubation for 96h in the MTT reduction test (Rossato et al., 2013b). Ferreira *et al.* pre-treated SH-SY5Y differentiated cells with buthionine sulphoximine (25 μM) before adding 3, 4- methylenedioxymethamphetamine or metabolites (100, 200, 400 and 800 μM), for 24 and 48h, also using the MTT reduction test (Ferreira et al., 2013). In the study by Ferreira *et al*., they observed that the buthionine sulphoximine (25 μM) after 48h of exposure was not cytotoxic as evaluated by the MTT test and by the cellular protein content, but N-methyl-α-methyldopamine incubation in buthionine sulphoximine pre-treated cells for 48h increased the toxicity of this 3, 4- methylenedioxymethamphetamine metabolite (Ferreira et al., 2013). The authors verified in SH-SY5Y cells that the glutathione pathways were involved in the toxicity of that methylenedioxymethamphetamine metabolite (Ferreira et al., 2013). To the best of our knowledge, there are no studies with differentiated H9c2 cells and MTX with buthionine sulphoximine or N-acetyl cysteine.

Our study in differentiated H9c2 cells showed that with mitochondrial enhancer L-carnitine (2 mg/mL) was not able to prevent any of the cytotoxic effects observed with the MTX (2 μM) incubation for 48h in the LDH assay (Figure 28). L-carnitine is considered a mitochondrial enhancer by improving the mitochondrial β-oxidation of fatty acids, the *trans*-esterification/excretion of acyl-coenzyme A esters, the oxidation of α-ketoacids, and by the removal of toxic acyl carnitine ester from the mitochondria (Zammit et al., 2009). The work of Rossato *et al*. evidenced the early MTX-induced energetic crisis as a possible key factor in the cell injury, however Rossato *et al.* showed that L-carnitine (1 mM) did not prevent any of the cytotoxic effects observed with the MTX (100 nM and 1 μM) incubation for 96h in the MTT reduction test in undifferentiated cells H9c2 (Rossato et al., 2013b).

Our study in differentiated H9c2 cells, the pre-incubation with cycloheximide (10 μg/mL) did not prevent any of the cytotoxic effects observed with the MTX (2 μM) incubation for 48h in the LDH assay (Figure 32). Protein synthesis is involved in many processes of programmed and non-programmed cell death (Martins et al., 2013), but it does not seem to have a major role in these experimental conditions.

5.5. Mechanisms of cell death induced by mitoxantrone

Cell death has been generally subdivided into several categories: apoptosis (type I), autophagy (type II), and necrosis (type III) (Lockshin and Zakeri, 2004). Cell death can be classified according to their morphological appearance (apoptosis, necrosis, autophagy), criteria based on enzymes (with or without the involvement of nucleases or different classes of proteases, such as caspases, cathepsins and glutaminases), functional aspects (programmed or accidental, physiological or pathological) or immunological characteristics (immunogenic or non-immunogenic) (Galluzzi et al., 2007). In multicellular organisms, cells that are no longer needed or that are a threat to the organism are destroyed by a tightly regulated cell suicide process known as programmed cell death, or apoptosis (Alberts et al., 2002). Apoptosis is characterized by chromatin condensation, DNA fragmentation, and possible activation and not activation of caspases (Klionsky, 2007). Caspases play a central role in the transduction of death receptors apoptotic signals. There are two types of caspases: initiator caspases, caspase 2, 8, 9, and 10, and effector caspases, caspase 3, 6, and 7 (Denault et al., 2007).

There are two distinct molecular signalling pathways that lead to cell death by apoptosis, the intrinsic pathway or mitochondrial and the extrinsic pathway or via the death receptor (de Bruin and Medema, 2008). Mitochondrial changes, including variations in mitochondrial membrane potential, can be key events during drug-induced apoptosis. The permeabilization the mitochondrial membrane induces the formation of pores through which small molecules are released from their intermembrane space (de Bruin and Medema, 2008).

Autophagy is now recognized as an important process involved in different human pathologies, such as neurodegenerative diseases, aging, and cancer (Klionsky, 2007, Rubinsztein et al., 2007). Autophagy is characterized by the formation of autophagic vacuoles in the cytoplasm of cells that are dying (Galluzzi et al., 2007) and is a general term for the degradation of cytoplasmatic components within lysosomes (Mizushima, 2007).

Necrosis is a type of cell death where the cell rapidly loses the integrity of its membrane, venting the intracellular contents (Galluzzi et al., 2007). Unlike apoptosis, necrosis has been considered as an uncontrolled cell death, leading to irreversible cell damage. Necrosis involves dramatic changes in the mitochondria, including mitochondrial depolarization, ATP depletion, generation of reactive oxygen species, loss of calcium homeostasis and causes vacuolation, loss of membrane integrity, cell swelling followed by complete lysis without vesicle formation and disintegration of organelles (de Bruin and Medema, 2008).

Mechanisms of cell death induced by MTX and reported in the literature are: apoptosis at lower concentrations (below 20 pg/mL) and necrosis at higher concentrations (exceed 20 ng/mL) (Neuhaus et al., 2006). Signals of apoptosis were already described

after 24 and 48h of MTX (1.60 µM) incubation in the undifferentiated H9c2 cells (Kluza et al., 2004). Moreover, Rossato *et al*. showed that in undifferentiated H9c2 cells, the incubation of 100 nM and 1 µM MTX, for 24h, caused an increase in caspase-3 activity (Rossato et al., 2013b).

To explore the role of apoptosis, the cells H9c2 were incubated in the presence of a caspase 8 and 9 inhibitor (100 and 200 µM), as described in the Methods section. The caspase inhibitor (caspase 8 and 9, at 100 or 200 µM) did not prevent cytotoxicity. Microscopic evaluation, Hoechst and ethidium bromide/acridine orange staining showed no signs of apoptosis, namely condensed and pyknotic nuclei. But that does not eliminate the possibility that in shorter incubation times, apoptosis may occur. Apoptosis is characterized by plasma membrane and mitochondrial alterations, dilation of the endoplasmic reticulum, fatty degeneration and nuclear changes (Kumar, 2010). Mitochondrial changes, including variations in mitochondrial membrane potential, are the key events during drug-induced apoptosis. In fact, in this thesis, lower levels of mitochondrial potential membrane resulting from MTX treatment were observed, suggesting the depolarization of mitochondrial membrane potential at 12h. This depolarization effect seems to be dose dependent (Figure 22). Rossato *et al.* showed that MTX (100 nM and 1 µM) caused hyperpolarization of the mitochondrial membrane potential after 24, 48, and 96h of MTX incubation in undifferentiated H9c2 cells (Rossato et al., 2013b). The method used by Rossato to evaluate mitochondrial potential membrane was flow cytometry analysis. The mitochondrial hyperpolarization drives more calcium into the mitochondria matrix and impaired electron chain mitochondrial activity (Rossato et al., 2013b). In our study, the method used to evaluate membrane potential and incubation-time and -concentration were different. The main signs of apoptosis in MTX-treated H9c2 cells are rapid release of the mitochondrial proteins apoptosis-inducing factor and cytochrome c into the cytosol (Kluza et al., 2004). Kluza *et al*. observed that MTX-treated H9c2 cells (1.60 µM) for 24h caused a decreased in mitochondrial transmembrane potential by cytofluorometric analysis (Kluza et al., 2004).

In this thesis, the loss of mitochondrial potential membrane may be an early event in the apoptotic process. However, this loss of mitochondrial potential membrane (decrease levels of fluorescence resulting from MTX treatment) may not be an early requirement for apoptosis, but may be a consequence of early apoptotic-signalling pathway.

To explore the role of autophagy in the cytotoxicity induced by MTX (2 µM), differentiated H9c2 cells were incubated in the presence of an autophagy inhibitor, 3-methyladenine (2.5 mM). The NR test was the most sensitive test for MTX cytotoxicity which could indicate that lysossomal damage could be a triggering factor for MTX-induced damage (Figure 25). The autophagy inhibitor (3-methyladenine) partially protected against MTX-induced cytotoxicity. The use of 3-methyladenine was performed with MTX for the first

time (Figure 30). The 3-methyladenine led to a partial protection in the NR test (Figure 30), which was not observed in the LDH assay (Figure 29), thus demonstrating that other mechanisms may be involved in MTX-membrane damage.

5.6. Evaluation of ATP levels and mitochondrial transmembrane potential of mitoxantrone

To understand if MTX has any effects on cellular energetics, intracellular ATP levels were assessed through the bioluminescence test. In our study, levels of ATP increased with incubation of MTX at 24h in differentiated H9c2 cells (Figure 35). In other models results are different. Recently, Rossato *et al*. showed that MTX (100 nM and 1 μM) caused an important energetic imbalance evidenced by decreased ATP levels and hyperpolarization of the mitochondrial membrane potential (as referred in 5.5) after 24, 48, and 96h of MTX incubation in undifferentiated H9c2 cells (Rossato et al., 2013b). In the study of Shipp *et al*., they determined the sensitivity of cultured rat heart cells to MTX treatment. Those cells were treated with several drug concentrations (0.05 to 5 μg/mL) for 3h and then medium was replaced. ATP levels were measured 72h after initial exposure and a concentration-dependent decline in ATP levels was observed. ATP suppression was maximal at 72h for all MTX concentrations tested; at that time point, there was also a substantial loss of spontaneous synchronous contraction in the cultures (Shipp et al., 1993).

In vivo, male Wistar rats treated with 3 cycles of 2.5 mg/kg MTX at day 0, 10, and 20 and euthanized on day 48, showed ATP decreases. That ATP decrease was shown to be related to mitochondrial disruption (Rossato et al., 2014). Therefore, ATP levels seem to be affected by MTX. In our study with MTX an increase in the levels of ATP was reported, which seem to be an adaptive response to MTX-incubation. Longer incubation time should be tested in our model to assess if it is an adaptive response.

5.7. The role of the cytochrome metabolism on mitoxantrone

So far the following enzymes were detected in the heart: CYP450, NADPH cytochrome reductase, dihydropyrimidine dehydrogenase, epoxide hydrolase, DT-diaphorase, glutathione S-transferase and UDP-glucuronosyltransferases, among others.

CYP450 is a superfamily of enzymes that are found in all living organisms. They are mixed function mono-oxygenases, which are involved in the oxidative metabolism of a wide range of xenobiotics and endogenous compounds (Elbekai and El-Kadi, 2006). Several CYP450 have been identified in human (Delozier et al., 2007) and animal heart tissues

(Imaoka et al., 2005) as well as different *in vitro* models such as primary rat cardiomyocytes (Thum and Borlak, 2000), immortalized H9c2 cells (Zordoky and El-Kadi, 2007), and recently in the atrial HL-1 cell line (Elshenawy et al., 2013).

Cardiac expression of CYP450 subfamilies identified in mammals includes: CYP1A, CYP1B, CYP2A, CYP2B, CYP2D, CYP2E, CYP2J, CYP2R, CYP2S, CYP2U, CYP4A, CYP4B, CYP4F and CYP11B (Chaudhary et al., 2009).

Herein, CYP450 inhibitors, namely metyrapone and 1-aminobenzotriazole, were also used to evaluate the role of the CYP450 metabolism on MTX cytotoxicity, since the oxidoreductive metabolism of MTX has a significant role on its antitumor effects and recent data suggest that MTX metabolism can be related to its cardiotoxicity (Blanz et al., 1991b, Bruck and Bruck, 2011, Rossato et al., 2013a). MTX has particular effectiveness in tumours with high contents of peroxidases (Blanz et al., 1991b, Bruck and Bruck, 2011). Duthie *et al.* showed that metyrapone is able to prevent the cytotoxic effect of MTX in human liver derived HepG2 hepatoma cells, thereby giving further evidence for the participation of the CYP450-dependent mixed function oxidase systems on MTX toxicity as referred above (Duthie and Grant, 1989). Similar results (metyrapone prevent the cytotoxic effect of MTX) were obtained with a rat hepatocytes model (Mewes et al., 1993) and with human breast cancer cells (Li et al., 1995) incubated with MTX and CYP450 inhibitors.

In the study by Rossato *et al*. the influence of CYP450- and CYP2E1-mediated metabolism for the cytotoxicity of MTX was assessed after 96h incubation with MTX (100 nM and 1 μM) in H9c2 undifferentiated cells. The co-incubation of MTX with CYP450 and CYP2E1 inhibitors partially prevented the cytotoxicity caused by the drug, thus highlighting that the metabolism of MTX is relevant for its undesirable effects in that model. They proved that the bioactivation of MTX mediated through CYP450 and namely through CYP2E1 metabolism occurs *in loco* in the cardiomyoblasts and exerts a significant role in the cellular damage promoted by MTX (Rossato et al., 2013a). Moreover, they demonstrated that the cytotoxicity caused by MTX after S9 hepatic fractions metabolization was significantly higher than that observed in the H9c2 cells incubated with MTX without S9 metabolization (Rossato et al., 2013a).

In this thesis, metyrapone and 1-aminobenzotriazole did not prevent of the MTX cytotoxicity observed in differentiated H9c2 cells at 48h. The two inhibitors used have different mechanisms. 1-Aminobenzotriazole is suicide nonspecific inhibitor. It is a metabolism-based inactivator of CYP450 by the mechanism of N-alkylation of heme moiety. 1-Aminobenzotriazole has been implicated in the inhibition of CYP1A, 2A, 2B, 2C, 2E, 3A, 4A, and 4B in various organs of different species (Linder et al., 2009). Metyrapone is a competitive inhibitor of CYP450-mediated ω/ω-1 hydroxylase activity (Asakura and Shichi,

1992), and it is mainly an inhibitor of CYP11B1 (11-β-hydroxylase), but it also inhibits CYP11B2 (Sampath-Kumar et al., 1997) and CYP3A4 (Park et al., 2005).

Rossato *et al.* described protection with CYP450 inhibitors at 96h in MTT assay (Rossato et al., 2013a), whereas in our work the time point was 48h. Thus, longer time point may be required for MTX metabolization to form significant amounts of toxic metabolites. On the other hand, to the best our knowledge, there are no studies regarding enzyme expression in differentiated H9c2 cells and the CYP450 expression can be altered by cellular differentiation. In undifferentiated H9c2 cells, there is only few knowledge about CYP isoenzymes (Zordoky and El-Kadi, 2007). In the study by Zordoky and El-Kadi, they showed that CYP1A1 and 1B1, CYP2B1, CYP2B2, CYP2E1, CYP2J3, CYP2C11, 2C13 and 2C23 were expressed in H9c2 cells. They concluded that multiple CYP genes are expressed in H9c2 cells at comparable level to those expressed in the heart or cardiomyocytes (Zordoky and El-Kadi, 2007). However, at this point no study has been made to clarify if differentiation alters CYP450 expression, and therefore different metabolites can be formed.

5.8. Incubation naphthoquinoxaline in differentiated H9c2 cells

In this thesis, MTT (Figure 39), LDH (Figure 40), and NR (Figure 41) assays were done at 24h and 48h and with different NAPHT concentrations. For NAPHT incubation (1, 2, and 5 µM) cytotoxicity was time- and concentration-dependent in all assays, being LDH the most sensitive test. At 48h, all the concentrations tested caused significant cytotoxicity when compared to vehicle cells, being the highest concentration tested (5 µM) able to decrease the levels of MTT reduction to values that reached 82.49 ± 4.05%. All the concentrations of NAPHT of 1, 2, and 5 µM tested for 24h, caused significant cellular membrane integrity loss when compared to vehicle cells. NAPHT at 48h caused a significant decrease in cellular integrity, being observed that at 2 µM NAPHT the viability was 73.02 ± 2.86% and at 5 µM the viability was 52.07 ± 6.83%, when compared with vehicle cells (81.91 ± 1.89%). NAPHT at 2 and 5 µM caused a substantial impairment of lysossomal uptake of NR when compared to vehicle cells. At 48h, in the NR assay, the H9c2 cells incubated with NAPHT 2 µM (88.82 ± 5.53%) and 5 µM (68.83 ± 6.28%) showed a significant lysosome uptake dysfunction when compared to vehicle cells (100.00 ± 6.18%).

Two pharmacological active molecules were tested to elucidate the mechanisms involved in NAPHT-induced cardiotoxicity, namely 3-methyladenine (an autophagy inhibitor) and N-acetyl cysteine (a glutathione precursor and reactive species scavenger). 3-Methyladenine caused a partial protection to the damage caused in lysossomal uptake

by NAPHT (Figure 43). NAPHT caused cardiotoxicity in micromolar concentration being autophagy involved. On the other hand, N-acetyl cysteine increased cell death caused by 2 µM NAPHT (Figure 42). This result may suggest a preconditioning stage that early reactive species formation can elicit and that N-acetyl cysteine may avoid (Ferreira et al., 2013). This mechanism needs further investigation.

Phase contrast microscopy and several staining's (Figure 36-38) were used to evaluate cytotoxicity of NAPHT. Phase microscopy allowed to observe that NAPHT caused cell damage at 24 or 48h incubation. Assessment of mitochondrial membrane potential in differentiated H9c2 cells incubated with 2 and 5 µM NAPHT for 12h showed significant effects: there was an evident decrease in mitochondrial potential seen in fluorescent microscopy (Figure 38). To understand if NAPHT had effects in cellular energetics, intracellular ATP levels were measured in H9c2 cell after a 24h incubation. In the NAPHT tested concentrations, no significance changes were detected (Figure 44). The work by Shipp *et al.* demonstrated that the metabolite NAPHT had a higher potential on ATP depletion than MTX in neonatal rat heart cells and, importantly, that the bioenergetics impairment hugely depends on iron availability (Shipp et al., 1993). The work by Shipp a co-workers is the only work available so far regarding to NAPHT cytotoxicity and used a different model and methodology than the work herein performed.

5.9. Toxicological comparison between mitoxantrone and naphthoquinoxaline

For the highest concentrations of MTX (1, 2, and 5 µM) cytotoxicity was time- and concentration-dependent in all assays, being the NR assay more sensitive for the MTX toxic effects in H9c2 differentiated cells. On the other hand, for NAPHT (1, 2, and 5 µM) cytotoxicity was time- and concentration-dependent in all assays, being LDH the most sensitive test. MTX and NAPHT caused a time- and concentration-dependent cytotoxicity, although with different sensitivity towards the assays used. 3-Methyladenine caused a partial protection to the damage caused in lysossomal uptake by both NAPHT and MTX, suggesting that for both molecules autophagy has an important role. N-acetyl cysteine increased cell death caused by 2 µM NAPHT, whereas N-acetyl cysteine did not cause any alteration in the cytotoxicity observed after MTX incubation. Both molecules caused a decreased of mitochondrial membrane potential in differentiated H9c2 cells incubated in similar conditions (time and concentration).

Regarding ATP levels, drugs had different effects, since NAPHT had no effects and MTX caused a significant increase in MTX incubated cells, suggesting an adaptive response towards MTX in H9c2 cells.

MTX and NAPHT share several mechanisms, but differ in other aspects that should be further investigated, mainly because the data on NAPHT are very scarce.

5.10. Final conclusions

Based on the results presented in this study, we propose the following main conclusions:

- With the enzymatic oxidation of MTX, several derivatives could be observed by HPLC and two purified derivatives were isolated and identified as NAPHT and NAPHTdi.
- MTX and NAPHT caused a time- and concentration-dependent cytotoxicity, although with different sensitivity towards the assays used.
- MTX and NAPHT caused cardiotoxicity at micromolar concentration being autophagy involved.
- MTX and NAPHT caused a decreased of mitochondrial membrane potential in differentiated H9c2 cells incubated in similar conditions.
- ATP levels were affected in a different manner in MTX- and NAPHT-incubated H9c2 cells.
- Thus, both drugs seem to impair cellular pathways in a dissimilar manner, although both cause early mitochondrial depolarization.

6.
REFERENCES

6. References

Adão R, Keulenaer G, Leite-Moreira A, Brás-Silva C (2013) Cardiotoxicidade associada à terapêutica oncológica: mecanismos fisiopatológicos e estratégias de prevenção. Rev Port Cardiol 32:395-409.

Alberts B, Johnson A, Lewis J, Raff M, Roberts K, P. W (2002) Molecular Biology of the Cell. Garland Science New York, 4th ed. pp.73.

Alberts DS, Bachur NR, Holtzman JL (1971) The pharmacokinetics of daunomycin in man. Clin Pharmacol Ther 12:96-104.

Alberts DS, Peng YM, Leigh S, Davis TP, Woodward DL (1985) Disposition of mitoxantrone in cancer patients. Cancer Res 45:1879-1884.

Alexander J, Dainiak N, Berger HJ, Goldman L, Johnstone D, Reduto L, Duffy T, Schwartz P, Gottschalk A, Zaret BL (1979) Serial assessment of doxorubicin cardiotoxicity with quantitative radionuclide angiocardiography. N Engl J Med 300:278-283.

Almeida VL, Leitão A, Reina LCB, Montanari CA, Donnici CL (2005) Câncer e agentes antineoplásicos ciclo-celular específicos e ciclo-celular não específicos que interagem com o DNA: Uma introdução: Quim. Nova 28:118-129.

Appelbaum F, Strauchen JA, Graw RG, Jr., Savage DD, Kent KM, Ferrans VJ, Herzig GP (1976) Acute lethal carditis caused by high-dose combination chemotherapy. A unique clinical and pathological entity. Lancet 1:58-62.

Arcamone F, Cassinelli G, Fantini G, Grein A, Orezzi P, Pol C, Spalla C (1969) Adriamycin, 14-hydroxydaunomycin, a new antitumor antibiotic from S. peucetius var. caesius. Biotechnol Bioeng 11:1101-1110.

Aronson JK, Dukes MNG, Meyler L (2006) Anthracyclines and related compounds. In: Meyler's Side Effects of Drugs: The International Encyclopedia of Adverse Drug Reactions and Interactions (Aronson, J. K., ed), pp 245-255 Amsterdam, Holland: Elsevier.

Asakura T, Shichi H (1992) Cytochrome P450-mediated prostaglandin omega/omega-1 hydroxylase activities in porcine ciliary body epithelial cells. Exp Eye Res 55:377-384.

Avantaggiato A, Bertuzzi G, Vitiello U, Iannucci G, Pasin M, Pascali M, Cervelli V, Carinci F (2014) Role of Antioxidants in Dermal Aging: An In Vitro Study by q-RT-PCR. Aesthetic Plast Surg DOI 10.1007/s00266-00014-00380-00269.

Avasarala JR, Cross AH, Clifford DB, Singer BA, Siegel BA, Abbey EE (2003) Rapid onset mitoxantrone-induced cardiotoxicity in secondary progressive multiple sclerosis. Mult Scler 9:59-62.

Ayash LJ, Wright JE, Tretyakov O, Gonin R, Elias A, Wheeler C, Eder JP, Rosowsky A, Antman K, Frei E, 3rd (1992) Cyclophosphamide pharmacokinetics: correlation with cardiac toxicity and tumor response. J Clin Oncol 10:995-1000.

Bachur NR, Gee M (1971) Daunorubicin metabolism by rat tissue preparations. J Pharmacol Exp Ther 177:567-572.

Bailey SM, Lewis AD, Patterson LH, Fisher GR, Knox RJ, Workman P (2001) Involvement of NADPH: cytochrome P450 reductase in the activation of indoloquinone EO9 to free radical and DNA damaging species. Biochem Pharmacol 62:461-468.

Bartoszek A, Wolf CR (1992) Enhancement of doxorubicin toxicity following activation by NADPH cytochrome P450 reductase. Biochem Pharmacol 43:1449-1457.

Batra VK, Morrison JA, Woodward DL, Siverd NS, Yacobi A (1986) Pharmacokinetics of mitoxantrone in man and laboratory animals. Drug Metab Rev 17:311-329.

Behnia K, Boroujerdi M (1999) Inhibition of aldo-keto reductases by phenobarbital alters metabolism, pharmacokinetics and toxicity of doxorubicin in rats. J Pharm Pharmacol 51:1275-1282.

Benjamin RS, Chawla SP, Ewer MS, Carrasco CH, Mackay B, Holmes F (1985) Evaluation of mitoxantrone cardiac toxicity by nuclear angiography and endomyocardial biopsy: an update. Invest New Drugs 3:117-121.

Bertazzoli C, Bellini O, Magrini U, Tosana MG (1979) Quantitative experimental evaluation of adriamycin cardiotoxicity in the mouse. Cancer Treat Rep 63:1877-1883.

Billingham ME, Mason JW, Bristow MR, Daniels JR (1978) Anthracycline cardiomyopathy monitored by morphologic changes. Cancer Treat Rep 62:865-872.

Blanz J, Mewes K, Ehninger G, Proksch B, Greger B, Waidelich D, Zeller KP (1991a) Isolation and structure elucidation of urinary metabolites of mitoxantrone. Cancer Res 51:3427-3433.

Blanz J, Mewes K, Ehninger G, Proksch B, Waidelich D, Greger B, Zeller KP (1991b) Evidence for oxidative activation of mitoxantrone in human, pig, and rat. Drug Metab Dispos 19:871-880.

Bonadonna G, Monfardini S (1969) Cardiac toxicity of daunorubicin. Lancet 1:837.

Bonadonna G, Monfardini S, De Lena M, Fossati-Bellani F, Beretta G (1970) Phase I and preliminary phase II evaluation of adriamycin (NSC 123127). Cancer Res 30:2572-2582.

Boucek RJ, Olson RD, Brenner DE, Ogunbunmi EM, Inui M, Fleischer S (1987) The major metabolite of doxorubicin is a potent inhibitor of membrane-associated ion pumps. A correlative study of cardiac muscle with isolated membrane fractions. J Biol Chem 262:15851-15856.

Bowden GT, Roberts R, Alberts DS, Peng YM, Garcia D (1985) Comparative molecular pharmacology in leukemic L1210 cells of the anthracene anticancer drugs mitoxantrone and bisantrene. Cancer Res 45:4915-4920.

Branco AF, Pereira SL, Moreira AC, Holy J, Sardao VA, Oliveira PJ (2011) Isoproterenol cytotoxicity is dependent on the differentiation state of the cardiomyoblast H9c2 cell line. Cardiovasc Toxicol 11:191-203.

Braverman AC, Antin JH, Plappert MT, Cook EF, Lee RT (1991) Cyclophosphamide cardiotoxicity in bone marrow transplantation: a prospective evaluation of new dosing regimens. J Clin Oncol 9:1215-1223.

Bruce WR, Lin H (1969) An empirical cellular approach to the improvement of cancer chemotherapy. Cancer Res 29:2308-2313.

Bruck TB, Bruck DW (2011) Oxidative metabolism of the anti-cancer agent mitoxantrone by horseradish, lacto-and lignin peroxidase. Biochimie 93:217-226.

Bruck TB, Harvey PJ (2003) Oxidation of mitoxantrone by lactoperoxidase. Biochim Biophys Acta 1649:154-163.

Buzdar AU, Marcus C, Smith TL, Blumenschein GR (1985) Early and delayed clinical cardiotoxicity of doxorubicin. Cancer 55:2761-2765.

Capela JP, da Costa Araujo S, Costa VM, Ruscher K, Fernandes E, Bastos ML, Dirnagl U, Meisel A, Carvalho F (2013) The neurotoxicity of hallucinogenic amphetamines in primary cultures of hippocampal neurons. Neurotoxicology 34:254-263.

Capela JP, Meisel A, Abreu AR, Branco PS, Ferreira LM, Lobo AM, Remiao F, Bastos ML, Carvalho F (2006) Neurotoxicity of Ecstasy metabolites in rat cortical neurons, and influence of hyperthermia. J Pharmacol Exp Ther 316:53-61.

Cazin B, Gorin NC, Laporte JP, Gallet B, Douay L, Lopez M, Najman A, Duhamel G (1986) Cardiac complications after bone marrow transplantation. A report on a series of 63 consecutive transplantations. Cancer 57:2061-2069.

Chabner BA, Bertino J, Cleary J, Ortiz T, Lane A, Supko JG (2012) Agentes citotóxicos. In: As bases Farmacológicas da Terapêutica de Goodman e Gilman (Hill, M., ed), pp 1357-1359: Laurence L. Brunton, Bruce A. Chabner e Björn C.

Chaudhary KR, Batchu SN, Seubert JM (2009) Cytochrome P450 enzymes and the heart. IUBMB life 61:954-960.

Chiccarelli FS, Morrison JA, Cosulich DB, Perkinson NA, Ridge DN, Sum FW, Murdock KC, Woodward DL, Arnold ET (1986) Identification of human urinary mitoxantrone metabolites. Cancer Res 46:4858-4861.

Chun YK, Kim J, Kwon S, Choi SH, Hong F, Moon K, Kim JM, Choi SL, Kim BS, Ha J, Kim SS (2000) Phosphatidylinositol 3-kinase stimulates muscle differentiation by activating p38 mitogen-activated protein kinase. Biochem Biophys Res Commun 276:502-507.

Coleman RE, Maisey MN, Knight RK, Rubens RD (1984) Mitoxantrone in advanced breast cancer--a phase II study with special attention to cardiotoxicity. Eur J Cancer Clin Oncol 20:771-776.

Colombo A, Cardinale D (2013) Using cardiac biomarkers and treating cardiotoxicity in cancer. Future Cardiol 9:105–118.

Coltman CA, Jr., McDaniel TM, Balcerzak SP, Morrison FS, Von Hoff DD (1983) Mitoxantrone hydrochloride (NSC-310739) in lymphoma. A Southwest Oncology Group study. Invest New Drugs 1:65-70.

Costa VM, Carvalho F, Bastos ML, Carvalho RA, Carvalho M, Remiao F (2011) Contribution of catecholamine reactive intermediates and oxidative stress to the pathologic features of heart diseases. Curr Med Chem 18:2272-2314.

Costa VM, Carvalho F, Duarte JA, Bastos Mde L, Remiao F (2013) The heart as a target for xenobiotic toxicity: the cardiac susceptibility to oxidative stress. Chem Res Toxicol 26:1285-1311.

Costa VM, Silva R, Ferreira LM, Branco PS, Carvalho F, Bastos ML, Carvalho RA, Carvalho M, Remiao F (2007) Oxidation process of adrenaline in freshly isolated rat cardiomyocytes: formation of adrenochrome, quinoproteins, and GSH adduct. Chem Res Toxicol 20:1183-1191.

Costa VM, Silva R, Tavares LC, Vitorino R, Amado F, Carvalho F, Bastos Mde L, Carvalho M, Carvalho RA, Remiao F (2009) Adrenaline and reactive oxygen species elicit proteome and energetic metabolism modifications in freshly isolated rat cardiomyocytes. Toxicology 260:84-96.

Cowen RL, Patterson AV, Telfer BA, Airley RE, Hobbs S, Phillips RM, Jaffar M, Stratford IJ, Williams KJ (2003) Viral delivery of P450 reductase recapitulates the ability of constitutive overexpression of reductase enzymes to potentiate the activity of mitomycin C in human breast cancer xenografts. Mol Cancer Ther 2:901-909.

Crossley RJ (1984) Clinical safety and tolerance of mitoxantrone. Semin Oncol 11:54-58.

Cummings J, Bartoszek A, Smyth JF (1991) Determination of covalent binding to intact DNA, RNA, and oligonucleotides by intercalating anticancer drugs using high-performance liquid chromatography. Studies with doxorubicin and NADPH cytochrome P-450 reductase. Anal Biochem 194:146-155.

Cusack BJ, Mushlin PS, Voulelis LD, Li X, Boucek RJ, Jr., Olson RD (1993) Daunorubicin-induced cardiac injury in the rabbit: a role for daunorubicinol? Toxicol Appl Pharmacol 118:177-185.

de Bruin EC, Medema JP (2008) Apoptosis and non-apoptotic deaths in cancer development and treatment response. Cancer Treat Rev 34:737-749.

de Graaf H, Dolsma WV, Willemse PH, van der Graaf WT, Sleijfer DT, de Vries EG, Mulder NH (1997) Cardiotoxicity from intensive chemotherapy combined with radiotherapy in breast cancer. Br J Cancer 76:943-945.

Delozier TC, Kissling GE, Coulter SJ, Dai D, Foley JF, Bradbury JA, Murphy E, Steenbergen C, Zeldin DC, Goldstein JA (2007) Detection of human CYP2C8, CYP2C9, and CYP2J2 in cardiovascular tissues. Drug Metab Dispos 35:682-688.

Denault JB, Eckelman BP, Shin H, Pop C, Salvesen GS (2007) Caspase 3 attenuates XIAP (X-linked inhibitor of apoptosis protein)-mediated inhibition of caspase 9. Biochem J 405:11-19.

Di Marco A, Boretti G, Rusconi A (1967) [Metabolic transformation of daunomycin by tissue extracts]. Farmaco Sci 22:535-542.

Di Marco A, Gaetani M, Scarpinato B (1969) Adriamycin (NSC-123,127): a new antibiotic with antitumor activity. Cancer Chemother Rep 53:33-37.

Doroshow JH, Davies KJ (1986) Redox cycling of anthracyclines by cardiac mitochondria. II. Formation of superoxide anion, hydrogen peroxide, and hydroxyl radical. J Biol Chem 261:3068-3074.

Doroshow JH, Locker GY, Myers CE (1980) Enzymatic defenses of the mouse heart against reactive oxygen metabolites: alterations produced by doxorubicin. J Clin Invest 65:128-135.

Dorr RT, Lagel K (1994) Effect of sulfhydryl compounds and glutathione depletion on rat heart myocyte toxicity induced by 4-hydroperoxycyclophosphamide and acrolein in vitro. Chem Biol Interact 93:117-128.

Durr FE, Wallace RE, Citarella RV (1983) Molecular and biochemical pharmacology of mitoxantrone. Cancer Treat Rev 10 Suppl B:3-11.

Duthie SJ, Grant MH (1989) The role of reductive and oxidative metabolism in the toxicity of mitoxantrone, adriamycin and menadione in human liver derived Hep G2 hepatoma cells. Br J Cancer 60:566-571.

Ehninger G, Proksch B, Heinzel G, Schiller E, Weible KH, Woodward DL (1985) The pharmacokinetics and metabolism of mitoxantrone in man. Invest New Drugs 3:109-116.

Ehninger G, Schuler U, Proksch B, Zeller KP, Blanz J (1990) Pharmacokinetics and metabolism of mitoxantrone. A review. Clin Pharmacokinet 18:365-380.

Eksborg S, Strandler HS, Edsmyr F, Naslund I, Tahvanainen P (1985) Pharmacokinetic study of i.v. infusions of adriamycin. Eur J Clin Pharmacol 28:205-212.

Elbekai RH, El-Kadi AO (2006) Cytochrome P450 enzymes: central players in cardiovascular health and disease. Pharmacol Ther 112:564-587.

Elshenawy OH, Anwar-Mohamed A, Abdelhamid G, El-Kadi AO (2013) Murine atrial HL-1 cell line is a reliable model to study drug metabolizing enzymes in the heart. Vascul Pharmacol 58:326-333.

Espinosa E, Raposo CG (2010) Classification of Anticancer Drugs Based on Therapeutic Targets. In Macromolecular Anticancer Therapeutics (L.H. Reddy e P. Couvreur eds) vol. 29 (Springer, ed), pp 515–523 New York.

Estorch M, Carrio I, Martinez-Duncker D, Berna L, Torres G, Alonso C, Ojeda B (1993) Myocyte cell damage after administration of doxorubicin or mitoxantrone in breast cancer patients assessed by indium 111 antimyosin monoclonal antibody studies. J Clin Oncol 11:1264-1268.

Ewer MS, Suter TM (2010) Diagnostic Aspects of Cardiovascular Toxicity of Antitumor Drugs. In: Cardiotoxicity of Non-Cardiovascular Drugs (Minotti, G., ed), pp 201-221: Wiley.

Faivre S, Djelloul S, Raymond E (2006) New paradigms in anticancer therapy: targeting multiple signaling pathways with kinase inhibitors. Semin Oncol 33:407-420.

Ferlay J, Steliarova-Foucher E, Lortet-Tieulent J, Rosso S, Coebergh JW, Comber H, Forman D, Bray F (2013) Cancer incidence and mortality patterns in Europe: Estimates for 40 countries in 2012. Eur J Cancer 49:1374-1403.

Ferreira PS, Nogueira TB, Costa VM, Branco PS, Ferreira LM, Fernandes E, Bastos ML, Meisel A, Carvalho F, Capela JP (2013) Neurotoxicity of "ecstasy" and its metabolites in human dopaminergic differentiated SH-SY5Y cells. Toxicol Lett 216:159-170.

Fidler JM, DeJoy SQ, Gibbons JJ, Jr. (1986) Selective immunomodulation by the antineoplastic agent mitoxantrone. I. Suppression of B lymphocyte function. J Immunol 137:727-732.

Forrest GL, Gonzalez B, Tseng W, Li X, Mann J (2000) Human carbonyl reductase overexpression in the heart advances the development of doxorubicin-induced cardiotoxicity in transgenic mice. Cancer Res 60:5158-5164.

Fotakis G, Timbrell JA (2006) In vitro cytotoxicity assays: comparison of LDH, neutral red, MTT and protein assay in hepatoma cell lines following exposure to cadmium chloride. Toxicol Lett 160:171-177.

Fox EJ (2004) Mechanism of action of mitoxantrone. Neurology 63:S15-18.

Fox ME, Smith PJ (1990) Long-term inhibition of DNA synthesis and the persistence of trapped topoisomerase II complexes in determining the toxicity of the antitumor DNA intercalators mAMSA and mitoxantrone. Cancer Res 50:5813-5818.

Freitas M, Costa VM, Ribeiro D, Couto D, Porto G, Carvalho F, Fernandes E (2013) Acetaminophen prevents oxidative burst and delays apoptosis in human neutrophils. Toxicol Lett 219:170-177.

Friedman HS, Colvin OM, Aisaka K, Popp J, Bossen EH, Reimer KA, Powell JB, Hilton J, Gross SS, Levi R, et al. (1990) Glutathione protects cardiac and skeletal muscle from cyclophosphamide-induced toxicity. Cancer Res 50:2455-2462.

Friesen C, Herr I, Krammer PH, Debatin KM (1996) Involvement of the CD95 (APO-1/FAS) receptor/ligand system in drug-induced apoptosis in leukemia cells. Nat Med 2:574-577.

Fura A, Shu YZ, Zhu M, Hanson RL, Roongta V, Humphreys WG (2004) Discovering drugs through biological transformation: role of pharmacologically active metabolites in drug discovery. J Med Chem 47:4339-4351.

Galluzzi L, Maiuri MC, Vitale I, Zischka H, Castedo M, Zitvogel L, Kroemer G (2007) Cell death modalities: classification and pathophysiological implications. Cell Death Differ 14:1237-1243.

Gambliel HA, Burke BE, Cusack BJ, Walsh GM, Zhang YL, Mushlin PS, Olson RD (2002) Doxorubicin and C-13 deoxydoxorubicin effects on ryanodine receptor gene expression. Biochem Biophys Res Commun 291:433-438.

Geisberg C, Pentassuglia L, Sawyer DB (2012) Cardiac side effects of anticancer treatments: new mechanistic insights. Curr Heart Fail Rep 9:211-218.

Gewirtz DA (1999) A critical evaluation of the mechanisms of action proposed for the antitumor effects of the anthracycline antibiotics adriamycin and daunorubicin. Biochem Pharmacol 57:727-741.

Gewirtz DA, Yanovich S (1986) Metabolism of the anthracycline antibiotic daunorubicin to daunorubicinol and deoxydaunorubicinol aglycone in hepatocytes isolated from the rat and the rabbit. Biochem Pharmacol 35:4059-4064.

Goldberg MA, Antin JH, Guinan EC, Rappeport JM (1986) Cyclophosphamide cardiotoxicity: an analysis of dosing as a risk factor. Blood 68:1114-1118.

Gottdiener JS, Appelbaum FR, Ferrans VJ, Deisseroth A, Ziegler J (1981) Cardiotoxicity associated with high-dose cyclophosphamide therapy. Arch Intern Med 141:758-763.

Gupta MK, Neelakantan TV, Sanghamitra M, Tyagi RK, Dinda A, Maulik S, Mukhopadhyay CK, Goswami SK (2006) An assessment of the role of reactive oxygen species and redox signaling in norepinephrine-induced apoptosis and hypertrophy of H9c2 cardiac myoblasts. Antioxid Redox Signal 8:1081-1093.

Hajihassan Z, Rabbani-Chadegani A (2011) Interaction of mitoxantrone, as an anticancer drug, with chromatin proteins, core histones and H1, in solution. Int J Biol Macromol 48:87-92.

Halliwell B, Gutteridge J (2007) Free Radicals in Biology and Medicine. Oxford University: London, U.K. 4th ed. 1-28.

Heibein AD, Guo B, Sprowl JA, Maclean DA, Parissenti AM (2012) Role of aldo-keto reductases and other doxorubicin pharmacokinetic genes in doxorubicin resistance, DNA binding, and subcellular localization. BMC cancer 12:381.

Henderson IC, Allegra JC, Woodcock T, Wolff S, Bryan S, Cartwright K, Dukart G, Henry D (1989) Randomized clinical trial comparing mitoxantrone with doxorubicin in previously treated patients with metastatic breast cancer. J Clin Oncol 7:560-571.

Hescheler J, Meyer R, Plant S, Krautwurst D, Rosenthal W, Schultz G (1991) Morphological, biochemical, and electrophysiological characterization of a clonal cell (H9c2) line from rat heart. Circ Res 69:1476-1486.

Huber SA (1990) Doxorubicin-induced alterations in cultured myocardial cells stimulate cytolytic T lymphocyte responses. Am J Pathol 137:449-456.

Imaoka S, Hashizume T, Funae Y (2005) Localization of rat cytochrome P450 in various tissues and comparison of arachidonic acid metabolism by rat P450 with that by human P450 orthologs. Drug Metab Pharmacokinet 20:478-484.

Infarmed (2004) ENDOXAN 2 g Pó para solução para perfusão - Resumo das características do medicamento.

Infarmed (2011) DaunoXome 2 mg/ml, concentrado para solução para perfusão - Resumo das características do medicamento.

Ismahil MA, Hamid T, Haberzettl P, Gu Y, Chandrasekar B, Srivastava S, Bhatnagar A, Prabhu SD (2011) Chronic oral exposure to the aldehyde pollutant acrolein induces dilated cardiomyopathy. Am J Physiol Heart Circ Physiol 301:H2050-2060.

Iwamoto RH, Lim P, Bhacca NS (1968) The structure of daunomycin. Tetrahedron Lett 3891-3894.

Johnson AM, Haynes WD, Leppard PJ, McDonald PJ, Neoh SH (1983) Ultrastructural and biochemical studies on the immunohistochemistry of Toxoplasma gondii antigens using monoclonal antibodies. Histochemistry 77:209-215.

Johnson RK, Zee-Cheng RK, Lee WW, Acton EM, Henry DW, Cheng CC (1979) Experimental antitumor activity of aminoanthraquinones. Cancer Treat Rep 63:425-439.

Kalyanaraman B, Joseph J, Kalivendi S, Wang S, Konorev E, Kotamraju S (2002) Doxorubicin-induced apoptosis: implications in cardiotoxicity. Mol Cell Biochem 234-235:119-124.

Kharasch ED, Novak RF (1983) Bis(alkylamino)anthracenedione antineoplastic agent metabolic activation by NADPH-cytochrome P-450 reductase and NADH dehydrogenase: diminished activity relative to anthracyclines. Arch Biochem Biophys 224:682-694.

Kimes BW, Brandt BL (1976) Properties of a clonal muscle cell line from rat heart. Exp Cell Res 98:367-381.

Klionsky DJ (2007) Autophagy: from phenomenology to molecular understanding in less than a decade. Nat Rev Mol Cell Biol 8:931-937.

Kluza J, Marchetti P, Gallego MA, Lancel S, Fournier C, Loyens A, Beauvillain JC, Bailly C (2004) Mitochondrial proliferation during apoptosis induced by anticancer agents: effects of doxorubicin and mitoxantrone on cancer and cardiac cells. Oncogene 23:7018-7030.

Kolodziejczyk P, Reszka K, Lown JW (1988) Enzymatic oxidative activation and transformation of the antitumor agent mitoxantrone. Free Radic Biol Med 5:13-25.

Kotamraju S, Chitambar CR, Kalivendi SV, Joseph J, Kalyanaraman B (2002) Transferrin receptor-dependent iron uptake is responsible for doxorubicin-mediated apoptosis in endothelial cells: role of oxidant-induced iron signaling in apoptosis. J Biol Chem 277:17179-17187.

Kumar V, Abbas, A. K., Fausto, N., Aster, J. (2010) Cell Injury, Cell Death, and Adaptations In: Robbins and Cotran Pathologic Basis of Disease, pp 1-30: Saunders Elsevier.

Kushner BH, Cheung NK (1991) Cyclophosphamide and the heart. J Clin Oncol 9:529-530.

Lenzhofer R, Magometschnigg D, Dudczak R, Cerni C, Bolebruch C, Moser K (1983) Indication of reduced doxorubicin-induced cardiac toxicity by additional treatment with antioxidative substances. Experientia 39:62-64.

Levine ES, Friedman HS, Griffith OW, Colvin OM, Raynor JH, Lieberman M (1993) Cardiac cell toxicity induced by 4-hydroperoxycyclophosphamide is modulated by glutathione. Cardiovasc Res 27:1248-1253.

Li SJ, Rodgers EH, Grant MH (1995) The activity of xenobiotic enzymes and the cytotoxicity of mitoxantrone in MCF 7 human breast cancer cells treated with inducing agents. Chem Biol Interact 97:101-118.

Licata S, Saponiero A, Mordente A, Minotti G (2000) Doxorubicin metabolism and toxicity in human myocardium: role of cytoplasmic deglycosidation and carbonyl reduction. Chem Res Toxicol 13:414-420.

Linder CD, Renaud NA, Hutzler JM (2009) Is 1-aminobenzotriazole an appropriate in vitro tool as a nonspecific cytochrome P450 inactivator? Drug Metab Dispos 37:10-13.

Liu LF (1989) DNA topoisomerase poisons as antitumor drugs. Annu Rev Biochem 58:351-375.

Lockshin RA, Zakeri Z (2004) Apoptosis, autophagy, and more. Int J Biochem Cell Biol 36:2405-2419.

Loveless H, Arena E, Felsted RL, Bachur NR (1978) Comparative mammalian metabolism of adriamycin and daunorubicin. Cancer Res 38:593-598.

Lown JW, Morgan AR, Yen SF, Wang YH, Wilson WD (1985) Characteristics of the binding of the anticancer agents mitoxantrone and ametantrone and related structures to deoxyribonucleic acids. Biochemistry 24:4028-4035.

Marmont AM, Damasio E, Rossi F (1969) Cardiac toxicity of daunorubicin. Lancet 1:837-838.

Martins JB, Bastos ML, Carvalho F, Capela JP (2013) Differential Effects of Methyl-4-Phenylpyridinium Ion, Rotenone, and Paraquat on Differentiated SH-SY5Y Cells. J Toxicol 2013:347312.

Mejia-Alvarez R, Tomaselli GF, Marban E (1994) Simultaneous expression of cardiac and skeletal muscle isoforms of the L-type Ca2+ channel in a rat heart muscle cell line. J Physiol 478 (Pt 2):315-329.

Menard C, Pupier S, Mornet D, Kitzmann M, Nargeot J, Lory P (1999) Modulation of L-type calcium channel expression during retinoic acid-induced differentiation of H9c2 cardiac cells. J Biol Chem 274:29063-29070.

Menna P, Paz OG, Chello M, Covino E, Salvatorelli E, Minotti G (2012) Anthracycline cardiotoxicity. Expert Opin Drug Saf 11 Suppl 1:S21-36.

Menna P, Salvatorelli E, Minotti G (2008) Cardiotoxicity of antitumor drugs. Chem Res Toxicol 21:978-989.

Mewes K, Blanz J, Ehninger G, Gebhardt R, Zeller KP (1993) Cytochrome P-450-induced cytotoxicity of mitoxantrone by formation of electrophilic intermediates. Cancer Res 53:5135-5142.

Minotti G, Cavaliere AF, Mordente A, Rossi M, Schiavello R, Zamparelli R, Possati G (1995) Secondary alcohol metabolites mediate iron delocalization in cytosolic fractions of myocardial biopsies exposed to anticancer anthracyclines. Novel linkage between anthracycline metabolism and iron-induced cardiotoxicity. J Clin Invest 95:1595-1605.

Minotti G, Mancuso C, Frustaci A, Mordente A, Santini SA, Calafiore AM, Liberi G, Gentiloni N (1996) Paradoxical inhibition of cardiac lipid peroxidation in cancer patients treated with doxorubicin. Pharmacologic and molecular reappraisal of anthracycline cardiotoxicity. J Clin Invest 98:650-661.

Minotti G, Menna P, Salvatorelli E, Cairo G, Gianni L (2004a) Anthracyclines: molecular advances and pharmacologic developments in antitumor activity and cardiotoxicity. Pharmacol Rev 56:185-229.

Minotti G, Recalcati S, Menna P, Salvatorelli E, Corna G, Cairo G (2004b) Doxorubicin cardiotoxicity and the control of iron metabolism: quinone-dependent and independent mechanisms. Methods Enzymol 378:340-361.

Minotti G, Recalcati S, Mordente A, Liberi G, Calafiore AM, Mancuso C, Preziosi P, Cairo G (1998) The secondary alcohol metabolite of doxorubicin irreversibly inactivates aconitase/iron regulatory protein-1 in cytosolic fractions from human myocardium. FASEB J 12:541-552.

Minotti G, Ronchi R, Salvatorelli E, Menna P, Cairo G (2001) Doxorubicin irreversibly inactivates iron regulatory proteins 1 and 2 in cardiomyocytes: evidence for distinct metabolic pathways and implications for iron-mediated cardiotoxicity of antitumor therapy. Cancer Res 61:8422-8428.

Minow RA, Gottlieb JA (1975) Adriamycin cardiotoxicity. Ann Intern Med 82:855-856.

Mizushima N (2007) Autophagy: process and function. Genes Dev 21:2861-2873.

Monsuez J, Charniot J, Vignat N, Artigou J (2010) Cardiac side-effects of cancer chemotherapy. Int J Cardiol 144:3-15.

Mortensen ME, Cecalupo AJ, Lo WD, Egorin MJ, Batley R (1992) Inadvertent intrathecal injection of daunorubicin with fatal outcome. Med Pediatr Oncol 20:249-253.

Mukherjee S, Banerjee SK, Maulik M, Dinda AK, Talwar KK, Maulik SK (2003) Protection against acute adriamycin-induced cardiotoxicity by garlic: role of endogenous antioxidants and inhibition of TNF-alpha expression. BMC pharmacology 3:16.

Murdock KC, Child RG, Fabio PF, Angier RB, Wallace RE, Durr FE, Citarella RV (1979) Antitumor agents. 1. 1,4-Bis[(aminoalkyl)amino]-9,10-anthracenediones. J Med Chem 22:1024-1030.

Nakamura S, Aoki M, Mori A, Nakahara T, Sakamoto K, Ishii K (2010) [Analysis of cardiac toxicity caused by cyclophosphamide in the H9c2 cell line and isolated and perfused rat hearts]. Gan To Kagaku Ryoho 37:677-680.

Neidle (1978) Topics in Antibiotic Chemistry. vol. Vol.2 pp 261-271 New York: Wiley.

Neilan TG, Blake SL, Ichinose F, Raher MJ, Buys ES, Jassal DS, Furutani E, Perez-Sanz TM, Graveline A, Janssens SP, Picard MH, Scherrer-Crosbie M, Bloch KD (2007) Disruption of nitric oxide synthase 3 protects against the cardiac injury, dysfunction, and mortality induced by doxorubicin. Circulation 116:506-514.

Neri B, Cini-Neri G (1986) Inhibition of endogenous respiration in rat heart slices as a measure of mitoxantrone cardiac toxicity. Oncology 43:264-267.

Neuhaus O, Kieseier BC, Hartung HP (2006) Therapeutic role of mitoxantrone in multiple sclerosis. Pharmacol Ther 109:198-209.

Nguyen B, Gutierrez PL (1990) Mechanism(s) for the metabolism of mitoxantrone: electron spin resonance and electrochemical studies. Chem Biol Interact 74:139-162.

Novak RF, Kharasch ED, Frank P, Runge-Morris M (eds.) (1988) In: Anthracycline and Anthracenedione-based anticancer agents. New York: Elsevier.

O'Connell TX, Berenbaum MC (1974) Cardiac and pulmonary effects of high doses of cyclophosphamide and isophosphamide. Cancer Res 34:1586-1591.

Obrig TG, Culp WJ, McKeehan WL, Hardesty B (1971) The mechanism by which cycloheximide and related glutarimide antibiotics inhibit peptide synthesis on reticulocyte ribosomes. J Biol Chem 246:174-181.

Octavia Y, Tocchetti CG, Gabrielson KL, Janssens S, Crijns HJ, Moens AL (2012) Doxorubicin-induced cardiomyopathy: from molecular mechanisms to therapeutic strategies. J Mol Cell Cardiol 52:1213-1225.

Olson LE, Bedja D, Alvey SJ, Cardounel AJ, Gabrielson KL, Reeves RH (2003) Protection from Doxorubicin-Induced Cardiac Toxicity in Mice with a Null Allele of Carbonyl Reductase 1. Cancer Res 63:6602-6606.

Olson RD, Li X, Palade P, Shadle SE, Mushlin PS, Gambliel HA, Fill M, Boucek Jr RJ, Cusack BJ (2000) Sarcoplasmic Reticulum Calcium Release Is Stimulated and Inhibited by Daunorubicin and Daunorubicinol. Toxicol Appl Pharmacol 169:168-176.

Olson RD, Mushlin PS, Brenner DE, Fleischer S, Cusack BJ, Chang BK, Boucek RJ, Jr. (1988) Doxorubicin cardiotoxicity may be caused by its metabolite, doxorubicinol. Proc Natl Acad Sci U S A 85:3585-3589.

Paciucci PA, Ohnuma T, Cuttner J, Silver RT, Holland JF (1983) Mitoxantrone in patients with acute leukemia in relapse. Cancer Res 43:3919-3922.

Pai VB, Nahata MC (2000) Cardiotoxicity of chemotherapeutic agents: incidence, treatment and prevention. Drug Saf 22:263-302.

Panousis C, Kettle AJ, Phillips DR (1997) Neutrophil-mediated activation of mitoxantrone to metabolites which form adducts with DNA. Cancer Lett 113:173-178.

Park H, Lee S, Suh J (2005) Structural and dynamical basis of broad substrate specificity, catalytic mechanism, and inhibition of cytochrome P450 3A4. J Am Chem Soc 127:13634-13642.

Patel KJ, Tredan O, Tannock IF (2013) Distribution of the anticancer drugs doxorubicin, mitoxantrone and topotecan in tumors and normal tissues. Cancer Chemother Pharmacol 72:127-138.

Patterson AV, Barham HM, Chinje EC, Adams GE, Harris AL, Stratford IJ (1995) Importance of P450 reductase activity in determining sensitivity of breast tumour cells to the bioreductive drug, tirapazamine (SR 4233). Br J Cancer 72:1144-1150.

Paul F, Dorr J, Wurfel J, Vogel HP, Zipp F (2009) Early mitoxantrone-induced cardiotoxicity in secondary progressive multiple sclerosis. BMJ Case Rep 10.1136/bcr.1106.2009.2004.

Pereira SL, Ramalho-Santos J, Branco AF, Sardao VA, Oliveira PJ, Carvalho RA (2011) Metabolic remodeling during H9c2 myoblast differentiation: relevance for in vitro toxicity studies. Cardiovasc Toxicol 11:180-190.

Perkins WE, Schroeder RL, Carrano RA, Imondi AR (1984) Myocardial effects of mitoxantrone and doxorubicin in the mouse and guinea pig. Cancer Treat Rep 68:841-847.

Platel D, Bonoron-Adele S, Robert J (2001) Role of daunorubicinol in daunorubicin-induced cardiotoxicity as evaluated with the model of isolated perfused rat heart. Pharmacol Toxicol 88:250-254.

Platel D, Pouna P, Bonoron-Adele S, Robert J (2000) Preclinical evaluation of the cardiotoxicity of taxane-anthracycline combinations using the model of isolated perfused rat heart. Toxicol Appl Pharmacol 163:135-140.

Pratt CB, Vietti TJ, Etcubanas E, Sexauer C, Krance RA, Mahoney DH, Patterson RB (1986) Novantrone for childhood malignant solid tumors. A pediatric oncology group phase II study. Invest New Drugs 4:43-48.

Rajagopalan S, Politi PM, Sinha BK, Myers CE (1988) Adriamycin-induced free radical formation in the perfused rat heart: implications for cardiotoxicity. Cancer Res 48:4766-4769.

Reliene R, Schiestl RH (2006) Glutathione depletion by buthionine sulfoximine induces DNA deletions in mice. Carcinogenesis 27:240-244.

Reszka K, Kolodziejczyk P, Lown JW (1986) Horseradish peroxidase-catalyzed oxidation of mitoxantrone: spectrophotometric and electron paramagnetic resonance studies. J Free Radic Biol Med 2:25-32.

Reszka KJ, Chignell CF (1996) Acid-catalyzed oxidation of the anticancer agent mitoxantrone by nitrite ions. Mol Pharmacol 50:1612-1618.

Richard B, Fabre G, De Sousa G, Fabre I, Rahmani R, Cano JP (1991) Interspecies variability in mitoxantrone metabolism using primary cultures of hepatocytes isolated from rat, rabbit and humans. Biochem Pharmacol 41:255-262.

Robert J, Gianni L (1993) Pharmacokinetics and metabolism of anthracyclines. Cancer Surv 17:219-252.

Roche FV (2002) Cancer and Chemotherapy. In: Foye's Principles of Medicinal Chemistry (David A. Williams, W. O. F., Thomas L. Lemke, ed), pp 1147-1191: Lippincott Williams & Wilkins.

Rossato LG, Costa VM, Dallegrave E, Arbo M, Silva R, Ferreira R, Amado F, Dinis-Oliveira RJ, Duarte JA, Bastos ML, Palmeira C, Remião F (2014) Mitochondrial cumulative damage induced by mitoxantrone: late onset cardiac energetic impairment. Cardiovasc Toxicol 14:30-40.

Rossato LG, Costa VM, de Pinho PG, Arbo MD, de Freitas V, Vilain L, Bastos ML, Palmeira C, Remiao F (2013a) The metabolic profile of mitoxantrone and its relation with mitoxantrone-induced cardiotoxicity. Arch Toxicol 87:1809–1820.

Rossato LG, Costa VM, Vilas-Boas V, Bastos ML, Rolo A, Palmeira C, Remiao F (2013b) Therapeutic concentrations of mitoxantrone elicit energetic imbalance in H9c2 cells as an earlier event. Cardiovasc Toxicol 13:413-425.

Rubinsztein DC, Gestwicki JE, Murphy LO, Klionsky DJ (2007) Potential therapeutic applications of autophagy. Nat Rev Drug Discov 6:304-312.

Ruddon RW (2007) Cancer Biology. New York: Oxford University Press, 4ª ed., 3-14.

Ruiz M, Courilleau D, Jullian JC, Fortin D, Ventura-Clapier R, Blondeau JP, Garnier A (2012) A cardiac-specific robotized cellular assay identified families of human ligands as inducers of PGC-1alpha expression and mitochondrial biogenesis. PloS one 7:e46753.

Rusconi A, Di Fronzo G, Di Marco A (1968) Distribution of tritiated daunomycin (NSC-82151) in normal rats. Cancer Chemother Rep 52:331-335.

Sá M, Gomes R, Silva N (2009) Cardiotoxicidade e quimioterapia. Rev Bras Clin Med 7:326-330.

Sampath-Kumar R, Yu M, Khalil MW, Yang K (1997) Metyrapone is a competitive inhibitor of 11beta-hydroxysteroid dehydrogenase type 1 reductase. J Steroid Biochem Mol Biol 62:195-199.

Sawyer DB, Fukazawa R, Arstall MA, Kelly RA (1999) Daunorubicin-induced apoptosis in rat cardiac myocytes is inhibited by dexrazoxane. Circ Res 84:257-265.

Schabel FM, Jr., Corbett TH, Griswold DP, Jr., Laster WR, Jr., Trader MW (1983) Therapeutic activity of mitoxantrone and ametantrone against murine tumors. Cancer Treat Rev 10 Suppl B:13-21.

Scott LJ, Figgitt DP (2004) Mitoxantrone: a review of its use in multiple sclerosis. CNS drugs 18:379-396.

Seiter K (2005) Toxicity of the topoisomerase II inhibitors. Expert Opin Drug Saf 4:219-234.

Senkus E, Jassem J (2011) Cardiovascular effects of systemic cancer treatment. Cancer Treat Rev 37:300-311.

Serrano J, Palmeira CM, Kuehl DW, Wallace KB (1999) Cardioselective and cumulative oxidation of mitochondrial DNA following subchronic doxorubicin administration. Biochim Biophys Acta 1411:201-205.

Shi J, Shen HM (2008) Critical role of Bid and Bax in indirubin-3'-monoxime-induced apoptosis in human cancer cells. Biochem Pharmacol 75:1729-1742.

Shi Q, Yang X, Greenhaw J, Salminen WF (2011a) Hepatic cytochrome P450s attenuate the cytotoxicity induced by leflunomide and its active metabolite A77 1726 in primary cultured rat hepatocytes. Toxicol Sci 122:579-586.

Shi Y, Moon M, Dawood S, McManus B, Liu PP (2011b) Mechanisms and management of doxorubicin cardiotoxicity. Herz 36:296-305.

Shipp NG, Dorr RT, Alberts DS, Dawson BV, Hendrix M (1993) Characterization of experimental mitoxantrone cardiotoxicity and its partial inhibition by ICRF-187 in cultured neonatal rat heart cells. Cancer Res 53:550-556.

Sikora K, Advani S, Koroltchouk V, Magrath I, Levy L, Pinedo H, Schwartsmann G, Tattersall M, Yan S (1999) Essential drugs for cancer therapy: a World Health Organization consultation. Ann Oncol 10:385-390.

Simunek T, Sterba M, Popelova O, Adamcova M, Hrdina R, Gersl V (2009) Anthracycline-induced cardiotoxicity: overview of studies examining the roles of oxidative stress and free cellular iron. Pharmacol Rep 61:154-171.

Singal PK, Iliskovic N (1998) Doxorubicin-induced cardiomyopathy. N Engl J Med 339:900-905.

Sinha BK, Motten AG, Hanck KW (1983) The electrochemical reduction of 1,4-bis-(2-[(2-hydroxyethyl)-amino] ethylamino)-anthracenedione and daunomycin: biochemical significance in superoxide formation. Chem Biol Interact 43:371-377.

Siveski-Iliskovic N, Hill M, Chow DA, Singal PK (1995) Probucol protects against adriamycin cardiomyopathy without interfering with its antitumor effect. Circulation 91:10-15.

Skladanowski A, Konopa J (1994) Interstrand DNA crosslinking induced by anthracyclines in tumour cells. Biochem Pharmacol 47:2269-2278.

Slavin RE, Millan JC, Mullins GM (1975) Pathology of high dose intermittent cyclophosphamide therapy. Hum Pathol 6:693-709.

Smith IE (1983) Mitoxantrone (novantrone): a review of experimental and early clinical studies. Cancer Treat Rev 10:103-115.

Smyth JF, Macpherson JS, Warrington PS, Leonard RC, Wolf CR (1986) The clinical pharmacology of mitozantrone. Cancer Chemother Pharmacol 17:149-152.

Soares AS, Costa VM, Diniz C, Fresco P (2013) Potentiation of cytotoxicity of paclitaxel in combination with Cl-IB-MECA in human C32 metastatic melanoma cells: A new possible therapeutic strategy for melanoma. Biomed Pharmacother 67:777-789.

Soares AS, Costa VM, Diniz C, Fresco P (2014) Combination of ClIBMECA with paclitaxel is a highly effective cytotoxic therapy causing mTORdependent autophagy and mitotic catastrophe on human melanoma cells. J Cancer Res Clin Oncol 140:921-935.

Sokolove PM (1988) Mitochondrial sulfhydryl group modification by adriamycin aglycones. FEBS Letters 234:199-202.

Sokolove PM (1991) Oxidation of mitochondrial pyridine nucleotides by aglycone derivatives of adriamycin. Arch Biochem Biophys 284:292-297.

Sokolove PM (1994) Interactions of adriamycin aglycones with mitochondria may mediate adriamycin cardiotoxicity. Int J Biochem 26:1341-1350.

Sokolove PM, Shinaberry RG (1988) Na+-independent release of Ca2+ from rat heart mitochondria. Induction by adriamycin aglycone. Biochem Pharmacol 37:803-812.

Stewart DJ, Green RM, Mikhael NZ, Montpetit V, Thibault M, Maroun JA (1986) Human autopsy tissue concentrations of mitoxantrone. Cancer Treat Rep 70:1255-1261.

Stewart DJ, Grewaal D, Green RM, Mikhael N, Goel R, Montpetit VA, Redmond MD (1993) Concentrations of doxorubicin and its metabolites in human autopsy heart and other tissues. Anticancer Res 13:1945-1952.

Stuart-Harris RC, Bozek T, Pavlidis NA, Smith IE (1984) Mitoxantrone: an active new agent in the treatment of advanced breast cancer. Cancer Chemother Pharmacol 12:1-4.

Swain SM, Whaley FS, Ewer MS (2003) Congestive heart failure in patients treated with doxorubicin: a retrospective analysis of three trials. Cancer 97:2869-2879.

Takanashi S, Bachur NR (1975) Daunorubicin metabolites in human urine. J Pharmacol Exp Ther 195:41-49.

Takanashi S, Bachur NR (1976) Adriamycin metabolism in man. Evidence from urinary metabolites. Drug Metab Dispos 4:79-87.

Takemura G, Fujiwara H (2007) Doxorubicin-induced cardiomyopathy from the cardiotoxic mechanisms to management. Prog Cardiovasc Dis 49:330-352.

Tan C, Tasaka H, Yu KP, Murphy ML, Karnofsky DA (1967) Daunomycin, an antitumor antibiotic, in the treatment of neoplastic disease. Clinical evaluation with special reference to childhood leukemia. Cancer 20:333-353.

Thomas X, Le QH, Fiere D (2002) Anthracycline-related toxicity requiring cardiac transplantation in long-term disease-free survivors with acute promyelocytic leukemia. Ann Hematol 81:504-507.

Thum T, Borlak J (2000) Cytochrome P450 mono-oxygenase gene expression and protein activity in cultures of adult cardiomyocytes of the rat. Br J Pharmacol 130:1745-1752.

Todaro MC, Oreto L, Qamar R, Paterick TE, Carerj S, Khandheria BK (2013) Cardioncology: state of the heart. Int J Cardiol 168:680-687.

Todorova V, Vanderpool D, Blossom S, Nwokedi E, Hennings L, Mrak R, Klimberg VS (2009) Oral glutamine protects against cyclophosphamide-induced cardiotoxicity in experimental rats through increase of cardiac glutathione. Nutrition 25:812-817.

Torres VM, Simic VD (2012) Doxorubicin-Induced Oxidative Injury of Cardiomyocytes - Do We Have Right Strategies for Prevention? In: Cardiotoxicity of Oncologic Treatments (Fiuza, M., ed): InTech.

Trillet V, Lakhal M, Lang J, Perrin-Fayolle E, Timour Chah Q, Fiere D, Faucon G (1985) Cellular pharmacokinetics of daunorubicin: uptake by leukaemic cells in vivo and fate. Eur J Clin Pharmacol 29:127-129.

Twelves CJ, Dobbs NA, Gillies HC, James CA, Rubens RD, Harper PG (1998) Doxorubicin pharmacokinetics: the effect of abnormal liver biochemistry tests. Cancer Chemother Pharmacol 42:229-234.

Uchegbu IF, Double JA, Turton JA, Florence AT (1995) Distribution, metabolism and tumoricidal activity of doxorubicin administered in sorbitan monostearate (Span 60) niosomes in the mouse. Pharm Res 12:1019-1024.

Unverferth DV, Unverferth BJ, Balcerzak SP, Bashore TA, Neidhart JA (1983) Cardiac evaluation of mitoxantrone. Cancer Treat Rep 67:343-350.

Valen G, Yan ZQ, Hansson GK (2001) Nuclear factor kappa-B and the heart. J Am Coll Cardiol 38:307-314.

Vasquez-Vivar J, Martasek P, Hogg N, Masters BS, Pritchard KA, Jr., Kalyanaraman B (1997) Endothelial nitric oxide synthase-dependent superoxide generation from adriamycin. Biochemistry 36:11293-11297.

Viola G, Bortolozzi R, Hamel E, Moro S, Brun P, Castagliuolo I, Ferlin MG, Basso G (2012) MG-2477, a new tubulin inhibitor, induces autophagy through inhibition of the Akt/mTOR pathway and delayed apoptosis in A549 cells. Biochem Pharmacol 83:16-26.

Volkova M, Palmeri M, Russell KS, Russell RR (2011) Activation of the aryl hydrocarbon receptor by doxorubicin mediates cytoprotective effects in the heart. Cardiovasc Res 90:305-314.

Von Hoff DD, Layard MW, Basa P, Davis HL, Jr., Von Hoff AL, Rozencweig M, Muggia FM (1979) Risk factors for doxorubicin-induced congestive heart failure. Ann Intern Med 91:710-717.

Wang L, Sun Y, Asahi M, Otsu K (2011) Acrolein, an Environmental Toxin, Induces Cardiomyocyte Apoptosis via Elevated Intracellular Calcium and Free Radicals. Cell Biochem Biophys 61:131-136.

Wang W, Watanabe M, Nakamura T, Kudo Y, Ochi R (1999) Properties and expression of Ca2+-activated K+ channels in H9c2 cells derived from rat ventricle. Am J Physiol 276:H1559-1566.

Wolf CR, Macpherson JS, Smyth JF (1986) Evidence for the metabolism of mitozantrone by microsomal glutathione transferases and 3-methylcholanthrene-inducible glucuronosyl transferases. Biochem Pharmacol 35:1577-1581.

Wormhoudt LW, Commandeur JN, Vermeulen NP (1999) Genetic polymorphisms of human N-acetyltransferase, cytochrome P450, glutathione-S-transferase, and epoxide hydrolase enzymes: relevance to xenobiotic metabolism and toxicity. Crit Rev Toxicol 29:59-124.

Xu X, Persson HL, Richardson DR (2005) Molecular pharmacology of the interaction of anthracyclines with iron. Mol Pharmacol 68:261-271.

Yap HY, Esparza L, Blumenschein GR, Hortobagyi GN, Bodey GP (1983) Combination chemotherapy with cyclophosphamide, mitoxantrone and 5-fluorouracil in patients with metastatic breast cancer. Cancer Treat Rev 10 Suppl B:53-55.

Zammit VA, Ramsay RR, Bonomini M, Arduini A (2009) Carnitine, mitochondrial function and therapy. Adv Drug Deliv Rev 61:1353-1362.

Zbinden G, Beilstein AK (1982) Comparison of cardiotoxicity of two anthracenediones and doxorubicin in rats. Toxicol Lett 11:289-297.

Zhang J, Herman EH, Ferrans VJ (1993) Dendritic cells in the hearts of spontaneously hypertensive rats treated with doxorubicin with or without ICRF-187. Am J Pathol 142:1916-1926.

Zhou S, Starkov A, Froberg MK, Leino RL, Wallace KB (2001) Cumulative and irreversible cardiac mitochondrial dysfunction induced by doxorubicin. Cancer Res 61:771-777.

Zordoky BN, El-Kadi AO (2007) H9c2 cell line is a valuable in vitro model to study the drug metabolizing enzymes in the heart. J Pharmacol Toxicol Methods 56:317-322.